Fisher, John (1986) *Design development and evaluation of an improved pericardial bioprosthetic heart valve.*

PhD thesis

DESIGN DEVELOPMENT AND EVALUATION OF AN IMPROVED PERICARDIAL BIOPROSTHETIC HEART VALVE

Volumes I and II

VOLUME II

John Fisher BSc MIMechE CENG

Degree of Doctor of Philosophy

University of Glasgow

Department of Cardiac Surgery
and
Department of Clinical Physics and BioEngineering

Faculty of Medicine

September 1986

LIST OF TABLES AND ILLUSTRATIONS

VOLUME II

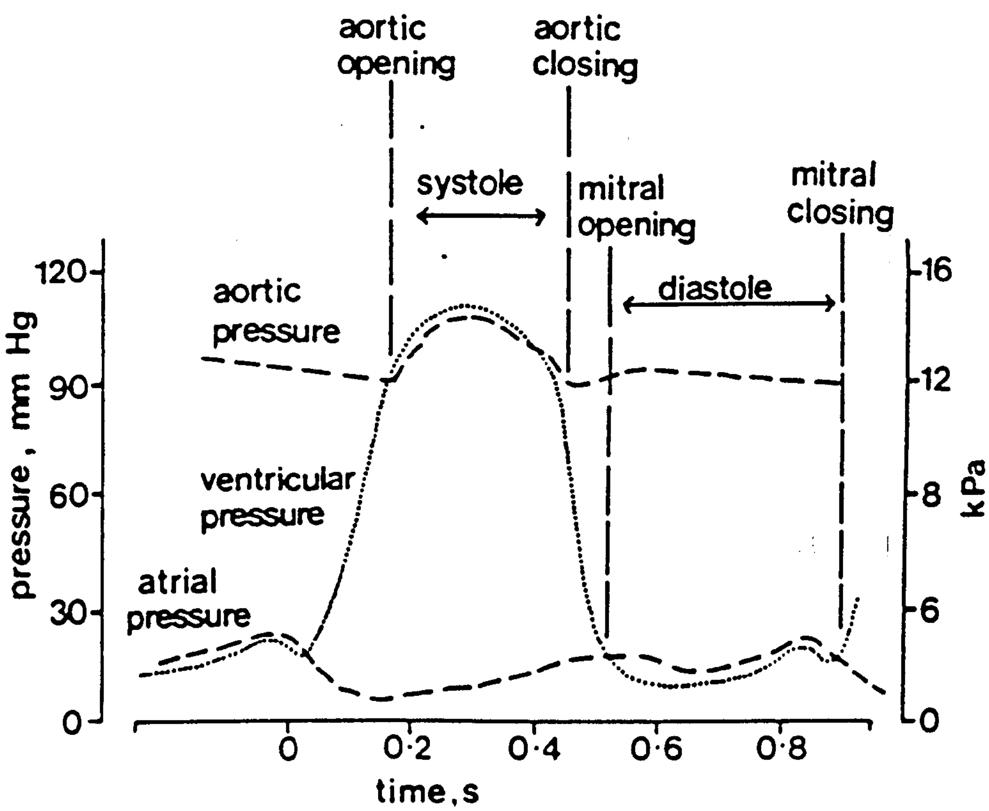

Figure 1.1 Typical pressure signals for the left heart showing the opening and closing of the valves.

Figure 1.2 Starr-Edwards ball and cage valve

Figure 1.3 Bjork-Shiley tilting disc valve

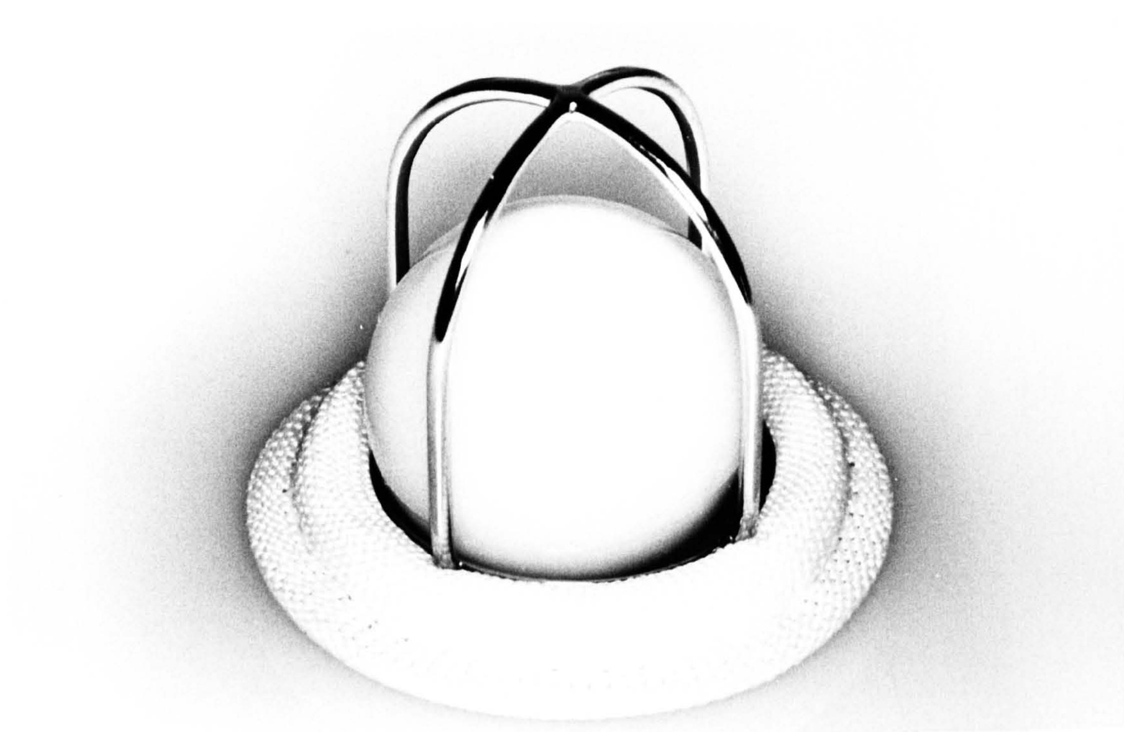

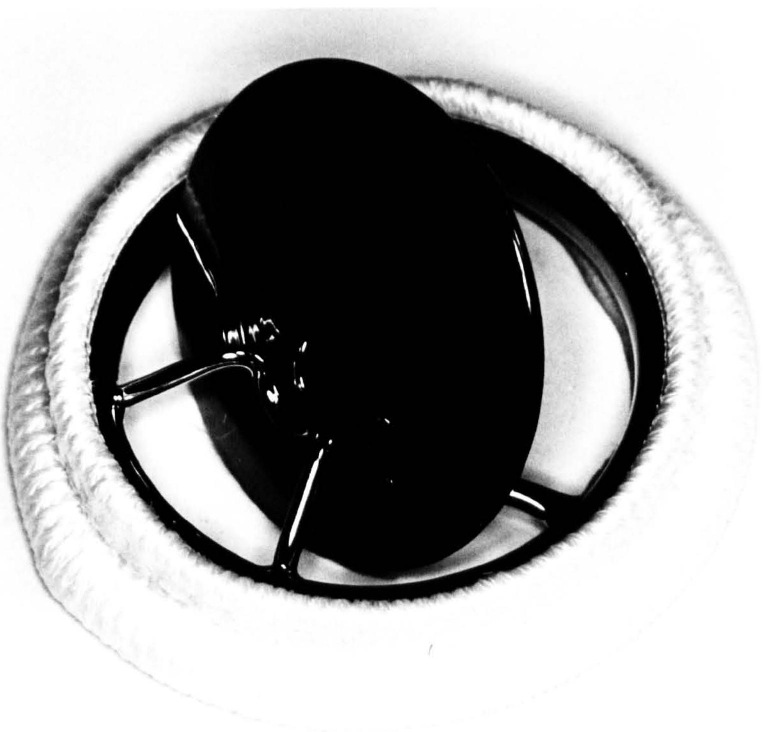

Figure 1.4 Duromedics bileaflet valve

Figure 1.5 Hancock porcine valve

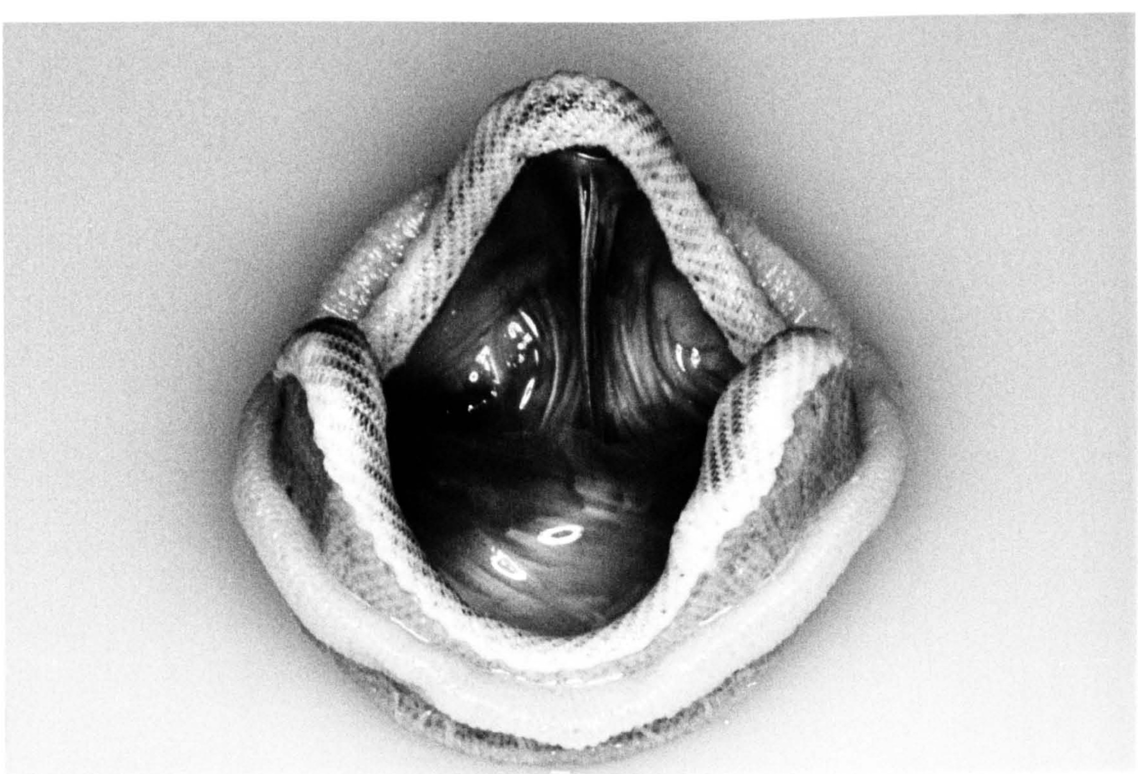

Figure 1.6 Ionescu-Shiley pericardial valve

Figure 1.7 Hancock porcine valve explanted after eight years with a hole in one leaflet

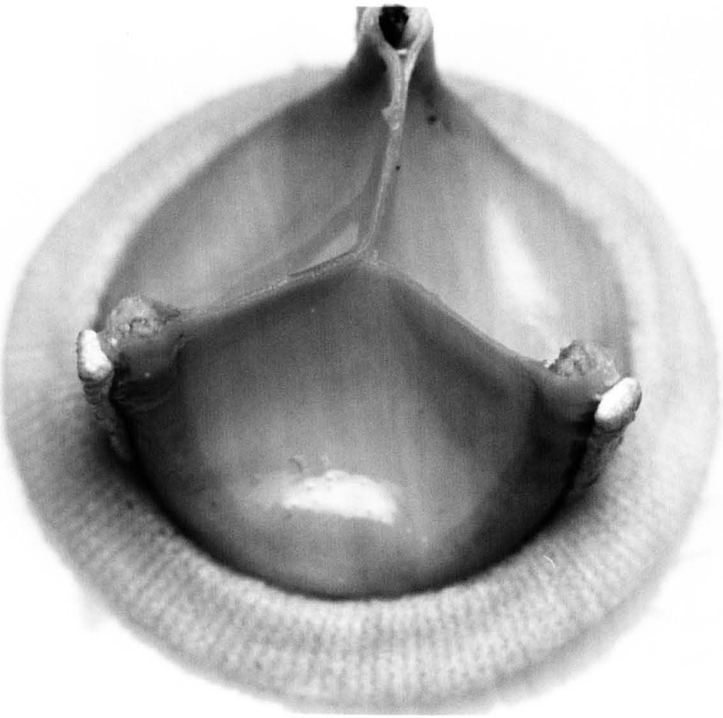

Figure 1.8 Carpentier-Edwards porcine valve explanted after five years with a tear at the commissures

Figure 1.9 Ionescu-Shiley standard valve explanted after four years with a tear at the top of a post

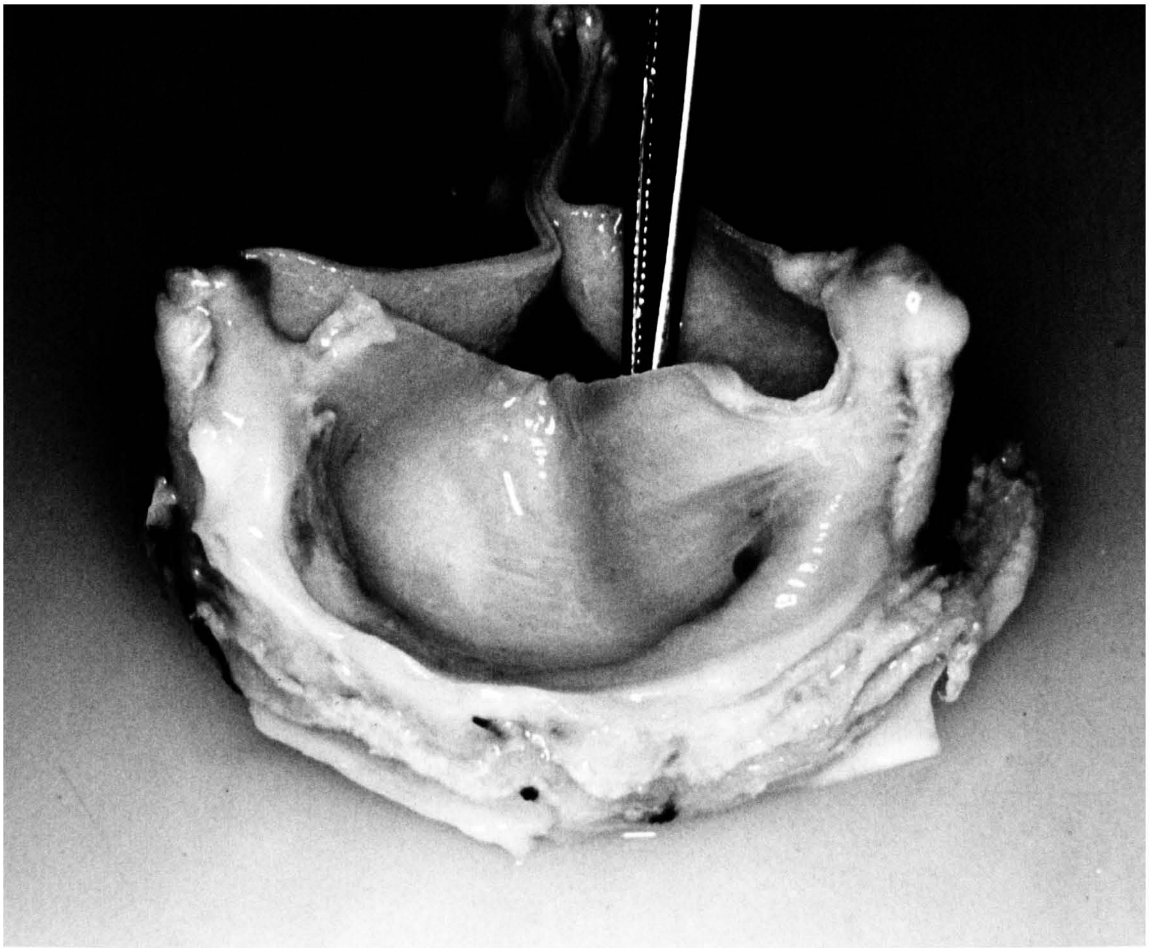

Figure 1.10 Carpentier-Edwards valve explanted after six years with severe calcification.

Figure 1.11 Six explanted Ionescu-Shiley Low Profile valves explanted with torn or damaged leaflets

A

B

C

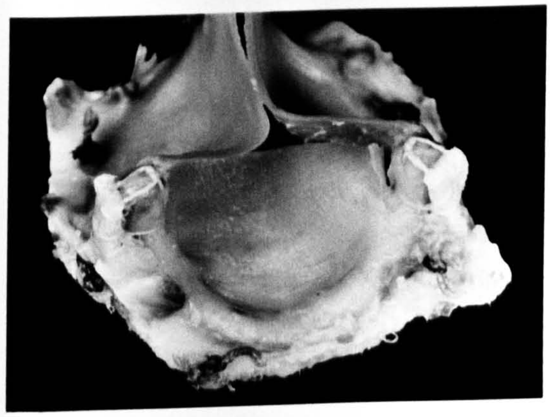

D

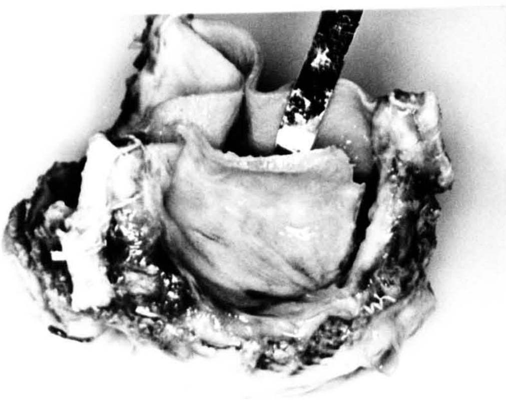

E

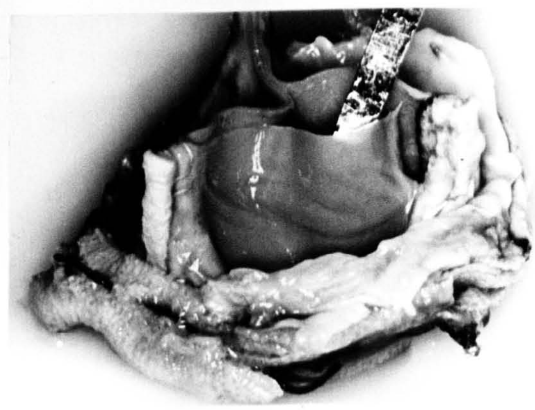

F

Figure 1.12 Two explanted Hancock pericardial valves with torn leaflets

G

H

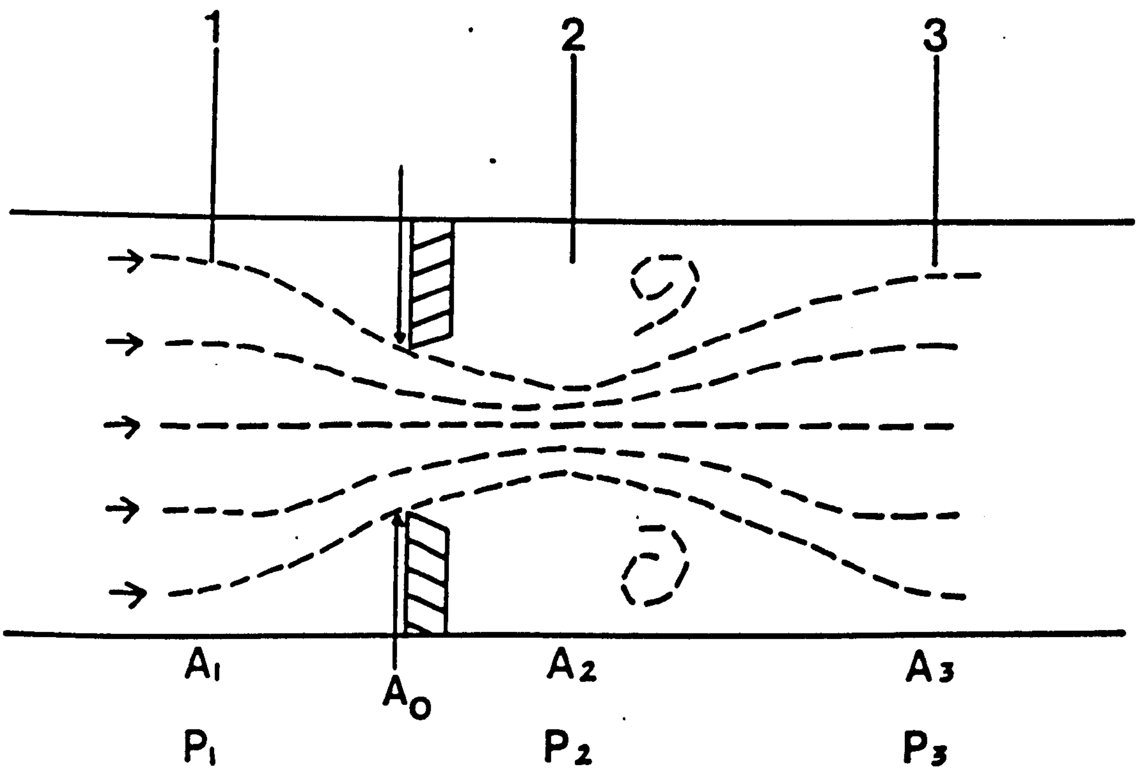

Figure 2.1 Diagram of the flow through an orifice plate in a cylindrical pipe.

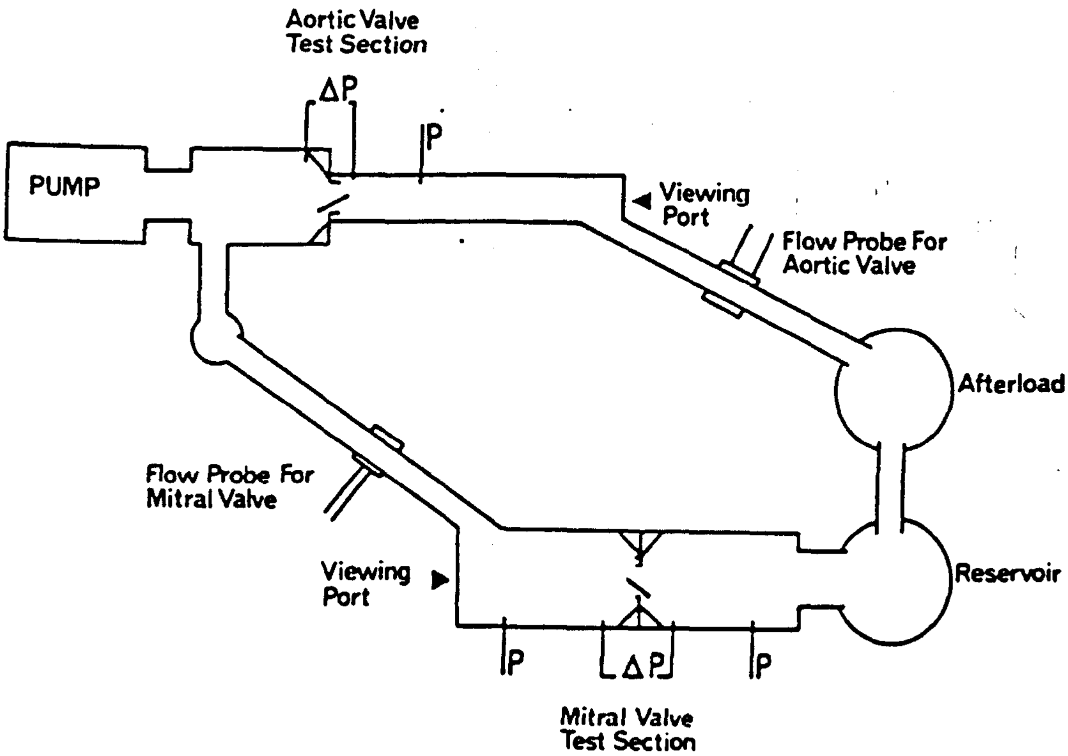

Figure 2.2 Diagram of the pulsatile flow test apparatus, ΔP and P show the position of the pressure transducers.

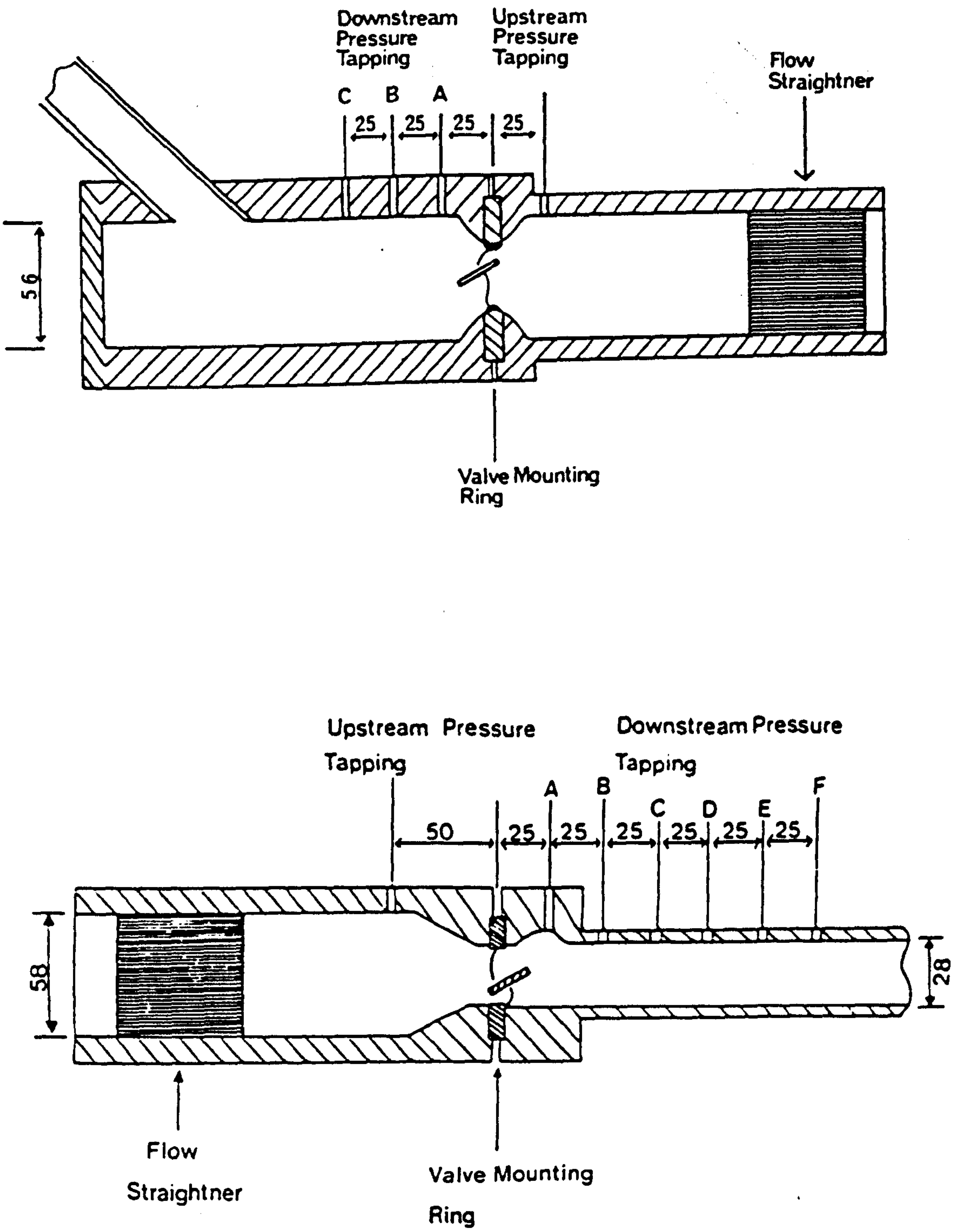

Figure 2.3 Diagrams of the mitral valve test section (top) and the aortic valve test section (below) showing the position of the pressure measurement points.

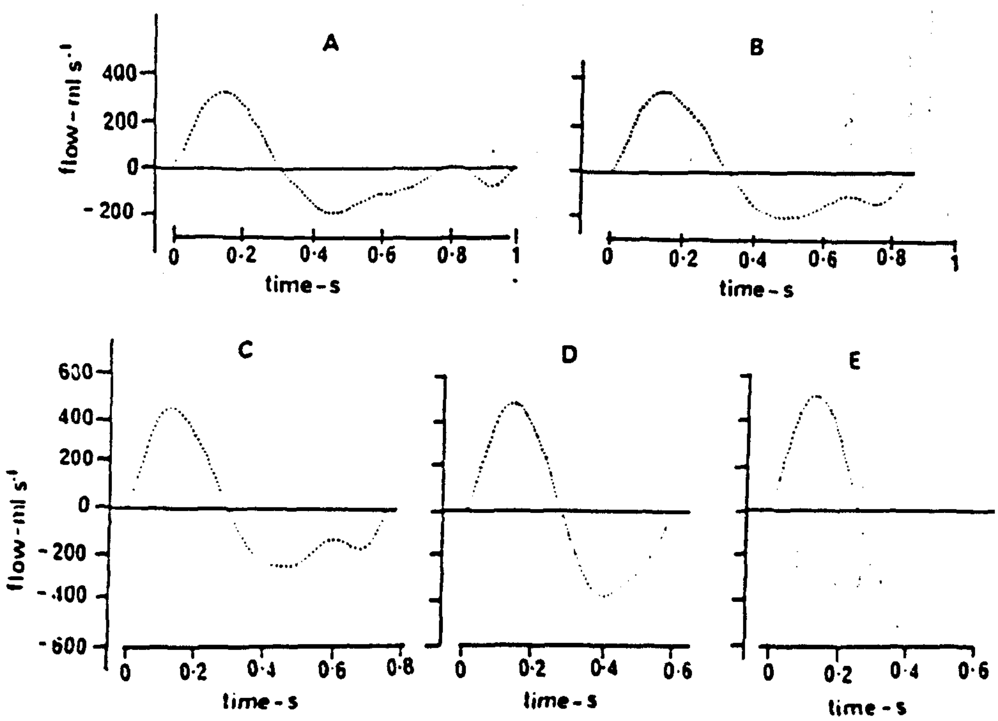

Figure 2.4 Flow time waveforms produced by the pump (+ve flow is systole). Standard test conditions.

Waveform A, stroke volume 60 ml, rate 60 min^{-1}

Waveform B, stroke volume 70 ml, rate 70 min^{-1}

Waveform C, stroke volume 80 ml, rate 80 min^{-1}

Waveform D, stroke volume 80 ml, rate 100 min^{-1}

Waveform E, stroke volume 80 ml, rate 120 min^{-1}

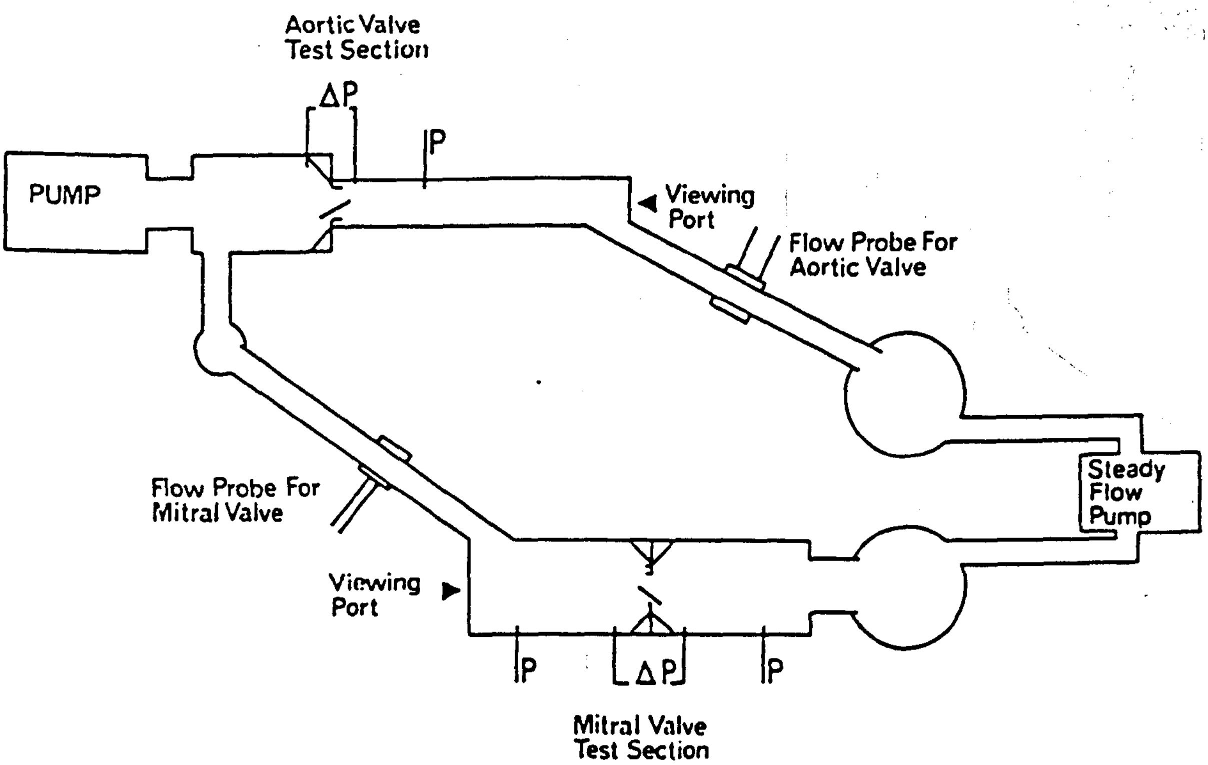

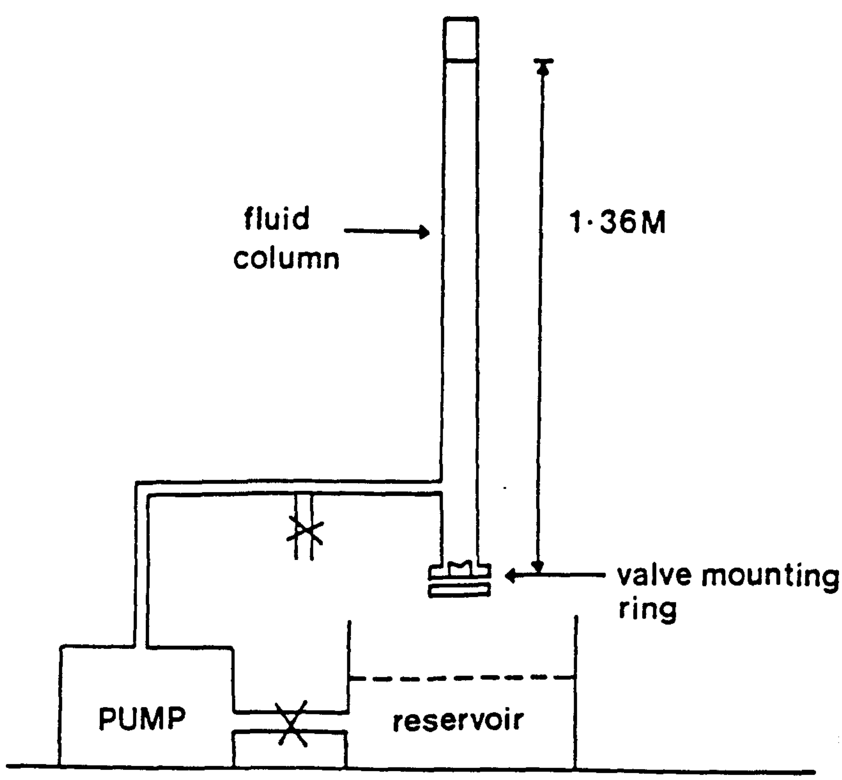

Figure 2.5 Diagrams of the test apparatus used for the steady flow tests (above) and static column tests (below).

Figure 2.6 Rowan Ash accelerated fatigue tester

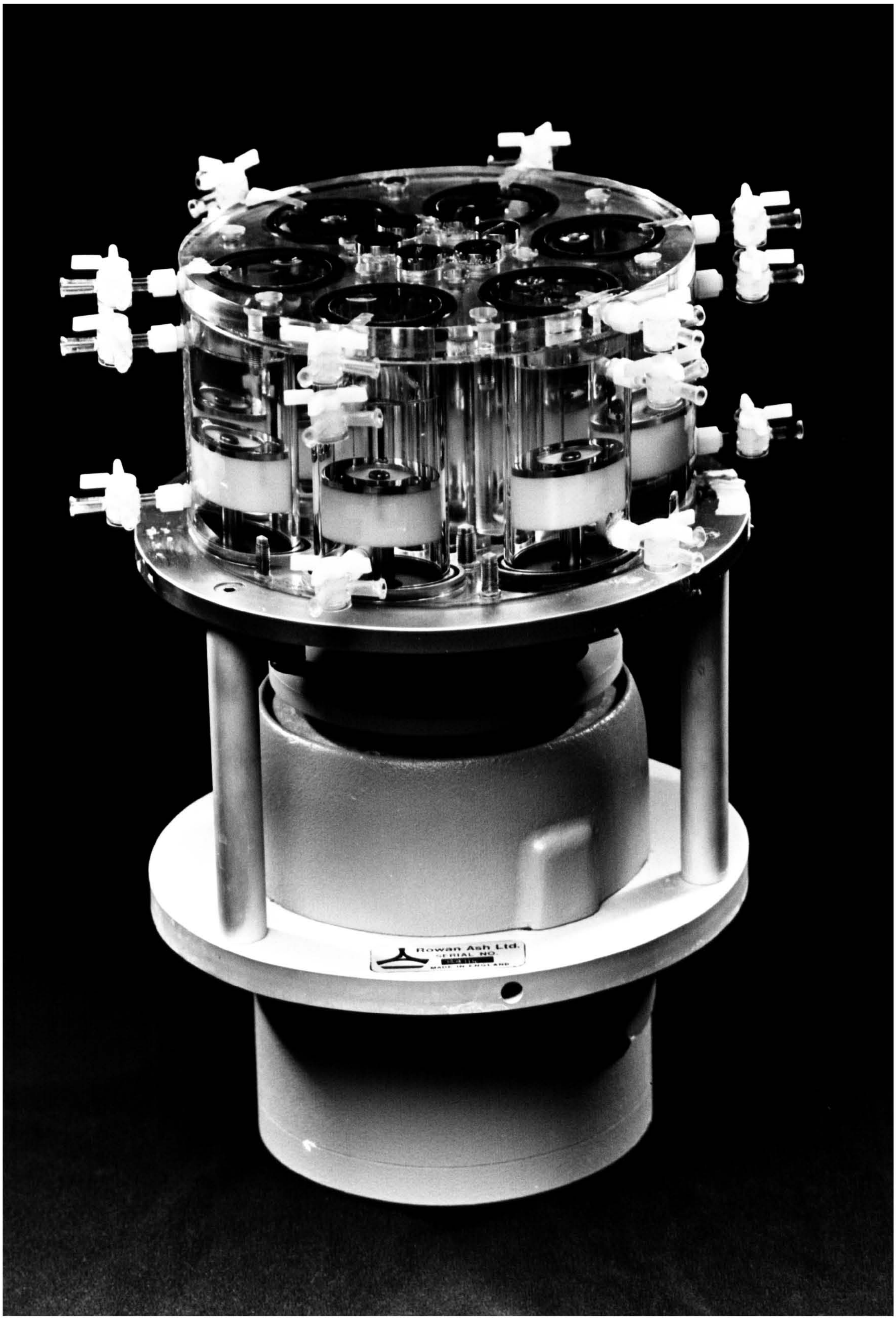
Rowan Ash Ltd.
SERIAL NO
MADE IN ENGLAND

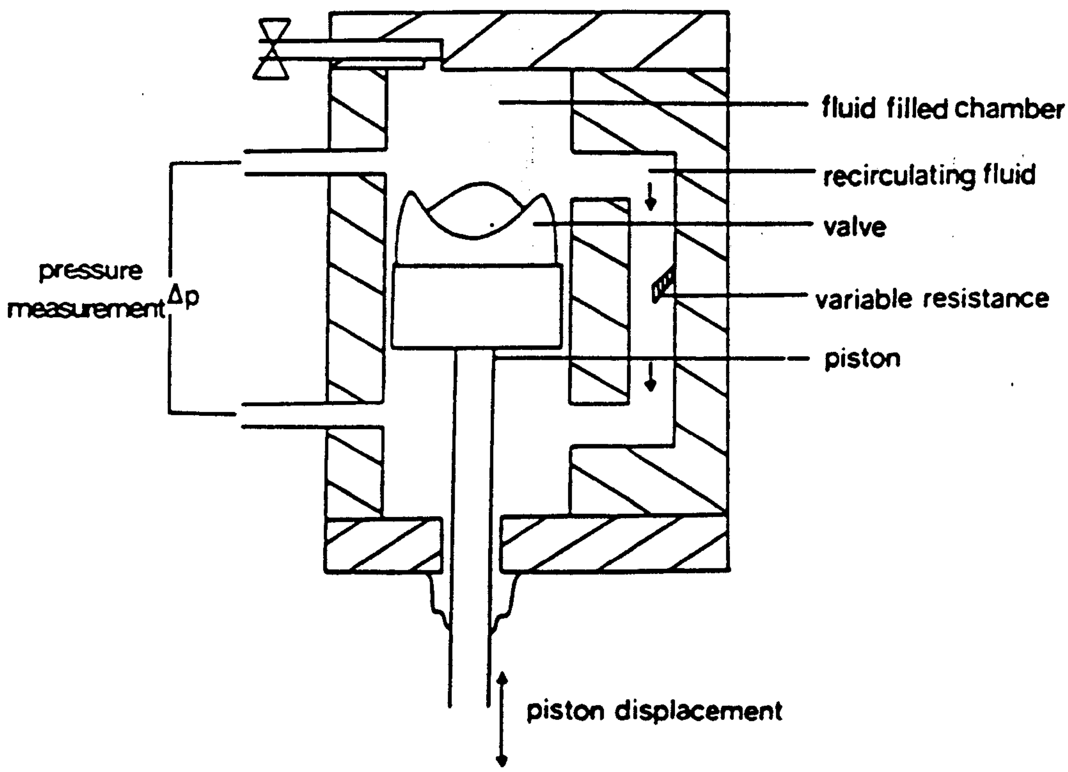

Figure 2.7 Diagram of the test chamber in the Rowan Ash accelerated fatigue tester.

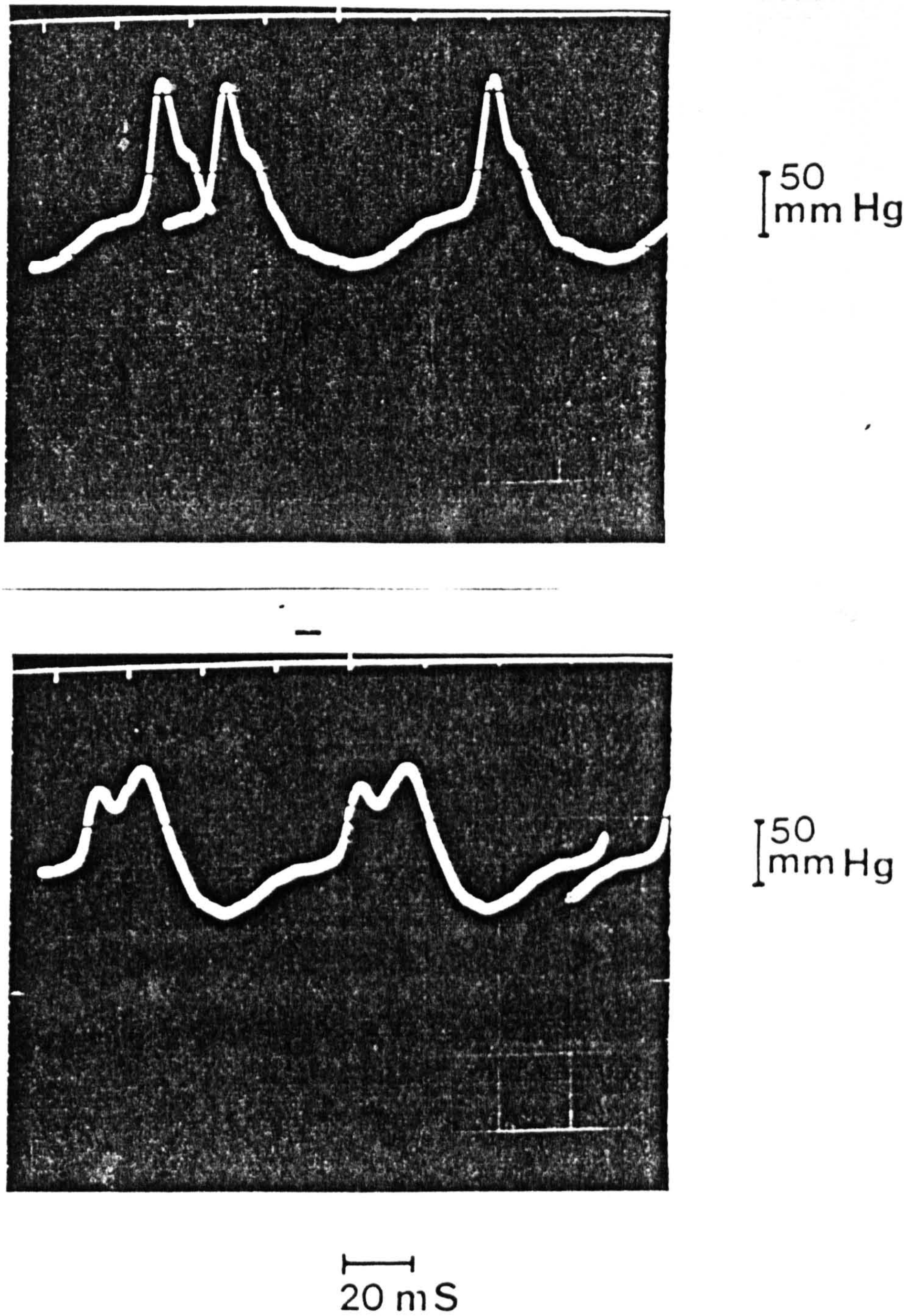

Figure 2.8 Differential pressure waveforms for two Ionescu-Shiley Low Profile valves in the fatigue tester. The top trace corresponds to the valve that closes first.

Figure 2.9 Closing characteristics of the ISLP size 29 mm valves in the fatigue tester A and the function tester B

A

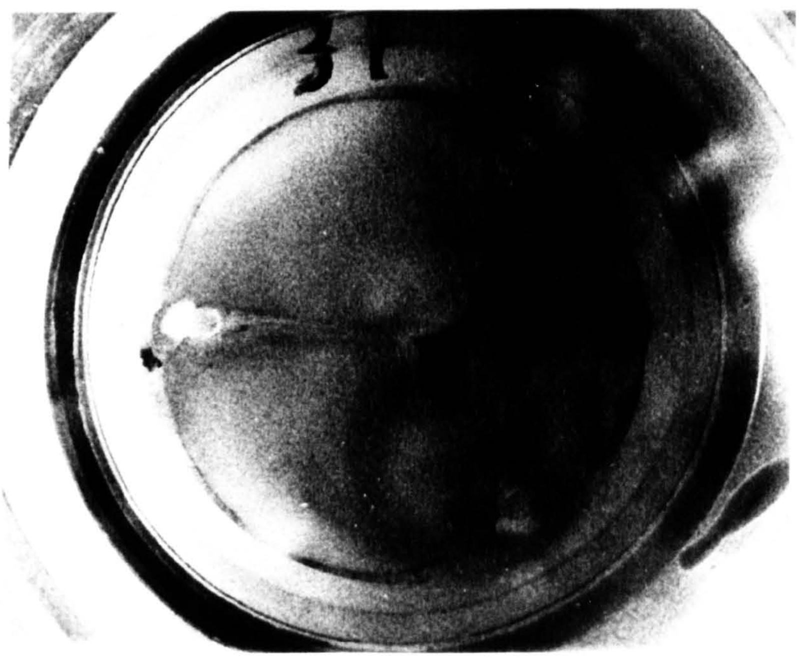

B

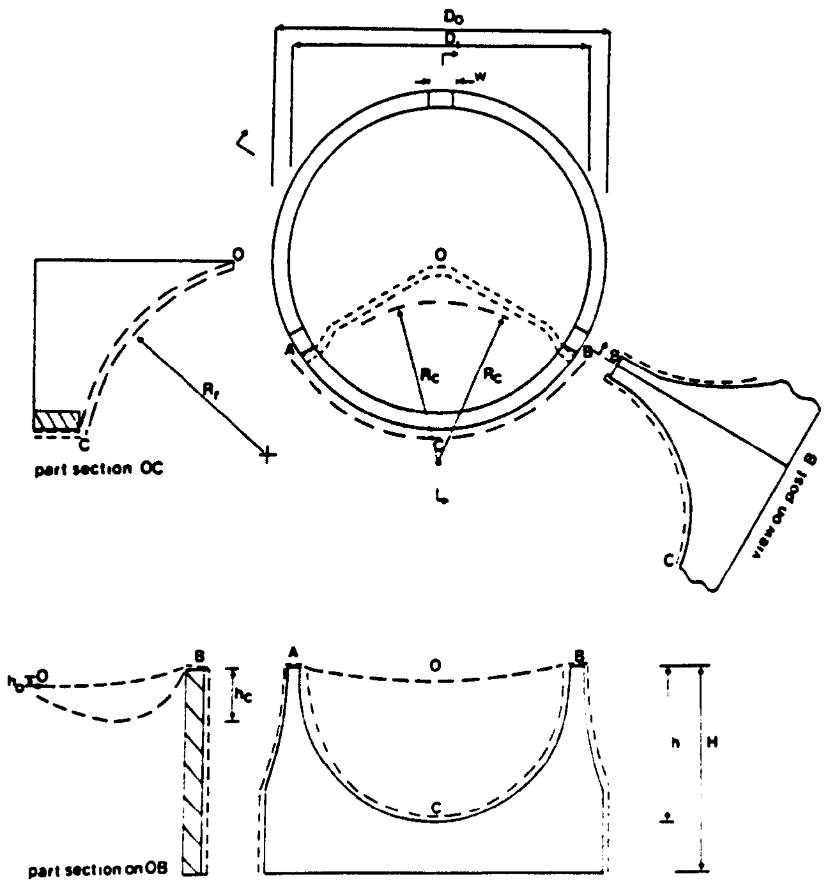

Figure 3.1 Key dimensions and geometries for a three leaflet pericardial valve.

TABLE 3.1

Key dimensions for four size 29 mitral valves

Valve	ISU	ISLP	HP	MM
<u>Dimensions mm</u>				
Outside Diameter D_o	29/28	28.5	28	28
Internal Diameter Di	25	24.5	24	24.5
Height H	20	19	17	16.5
Leaflet height h	16	15	12.5	12.5
Post width w	2	2		2
Coaption depth h_c	4	3	2.5	3.5
Radii Curvature r_c	20	17.5	15	15
Radii Curvature R_r	20	17.5	15	15
Implant Height H_{imp}	18	17	14	14.5
Tissue thickness t	0.35	0.55-0.35	0.38	0.5

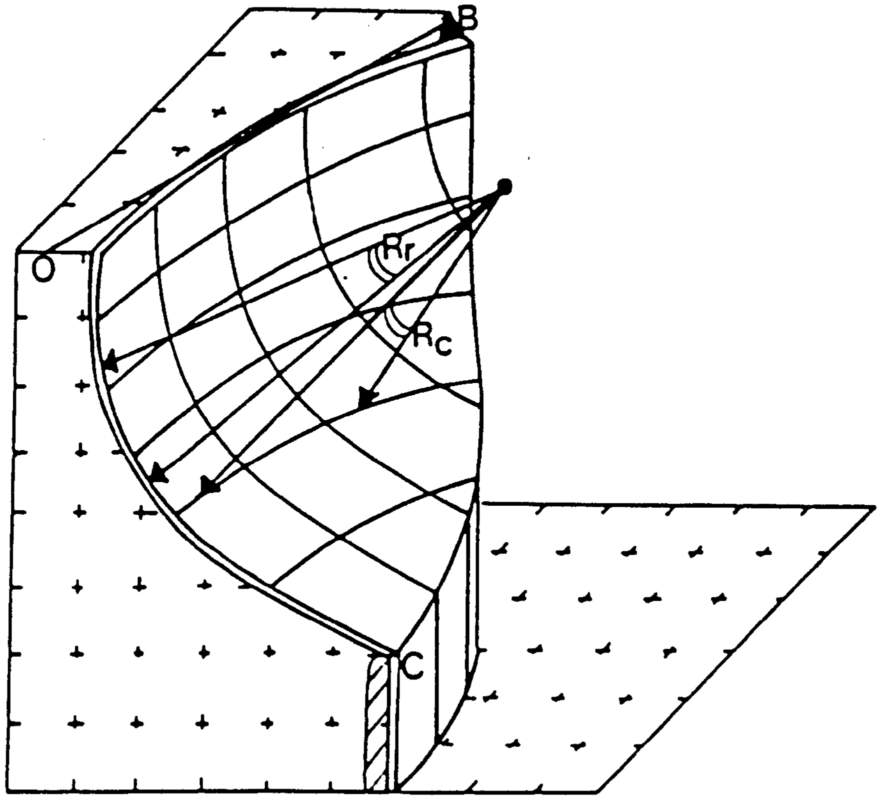

Figure 3.2 A three dimensional plot of the valve leaflet sectioned through the vertical centre line OC, defined by vertical and horizontal sections at 2.5 mm intervals.

Figure 3.3 Photographs of the size 29 mm pericardial valves. a] Ionescu-Shiley Standard (ISU), b] Ionescu-Shiley low profile (ISLP), c] Hancock pericardial (HP), d] Mitral Medical (MM)

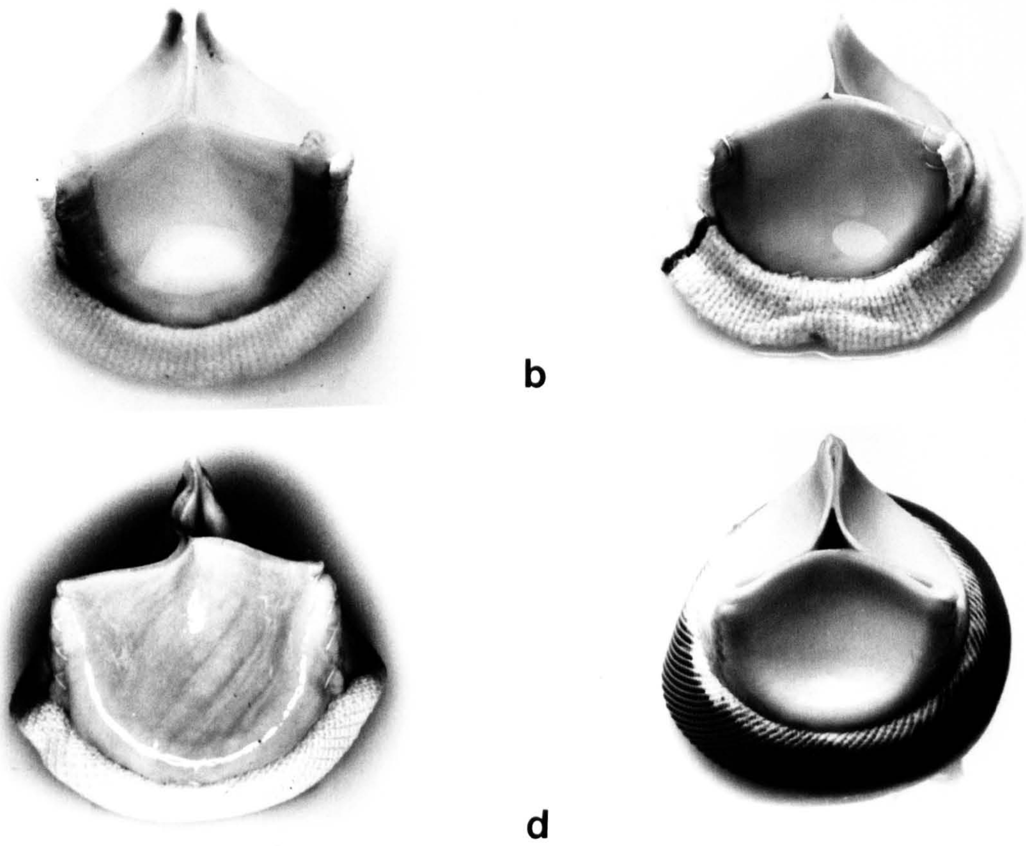
a
b
c
d

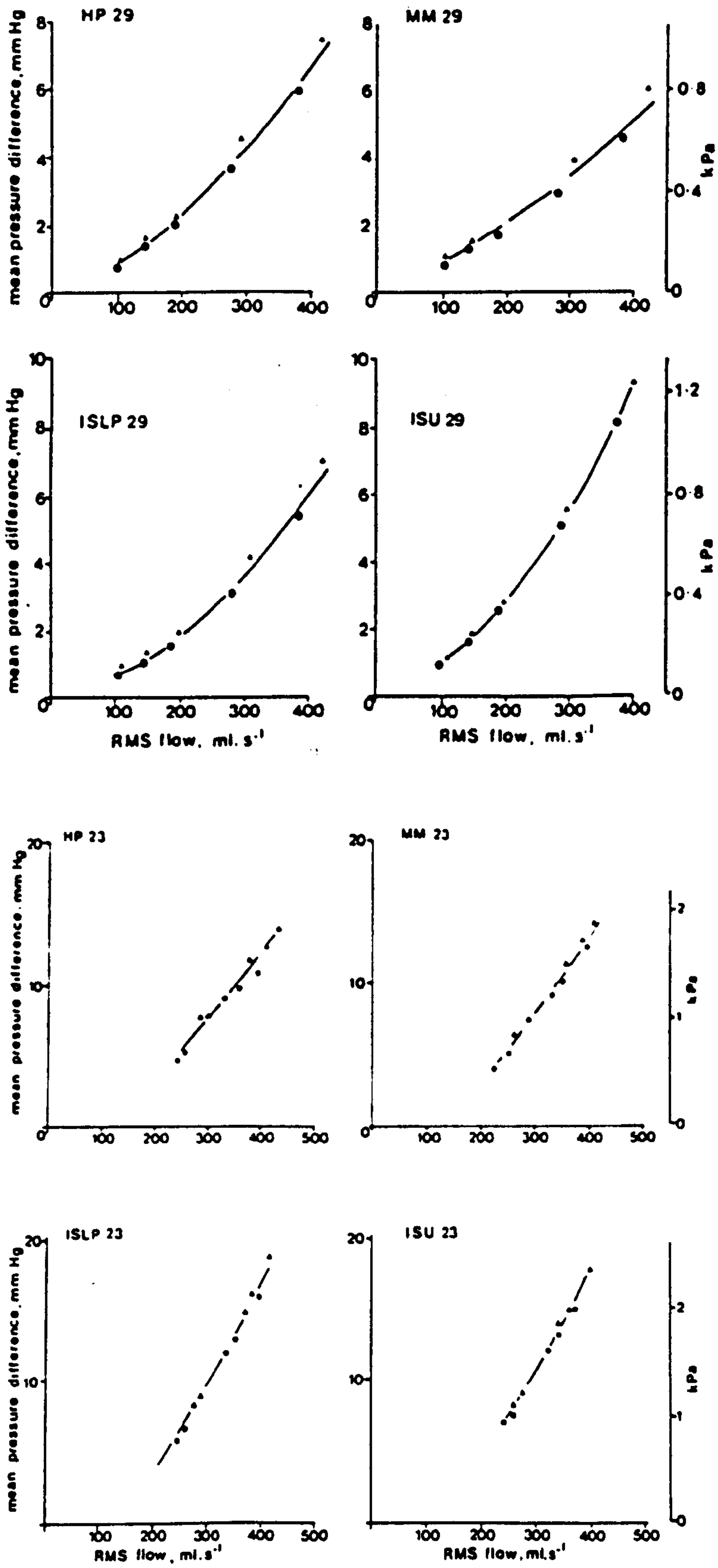

Figure 3.4 The mean pressure difference plotted against RMS forward flow for size 29 mm mitral and size 23 mm aortic valves. ● indicates averge taken over the pressure–flow interval and ▲ indicates the average

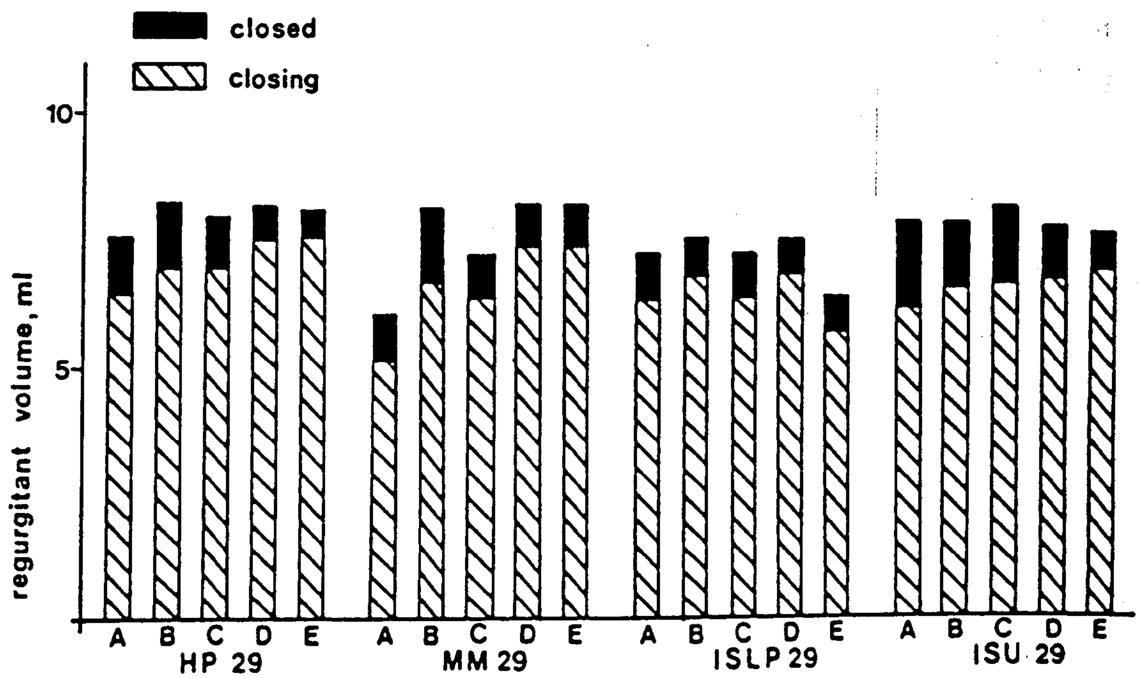

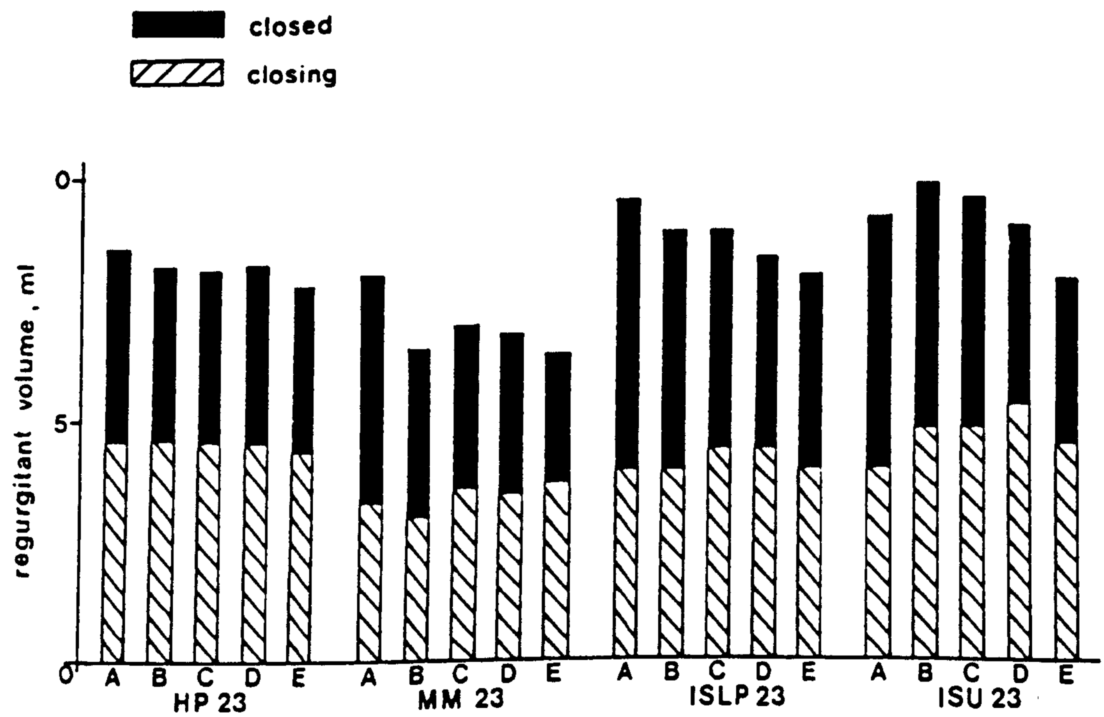

Figure 3.5 Regurgitant volumes for the size 29 mm mitral and size 23 mm aortic pericardial valves.

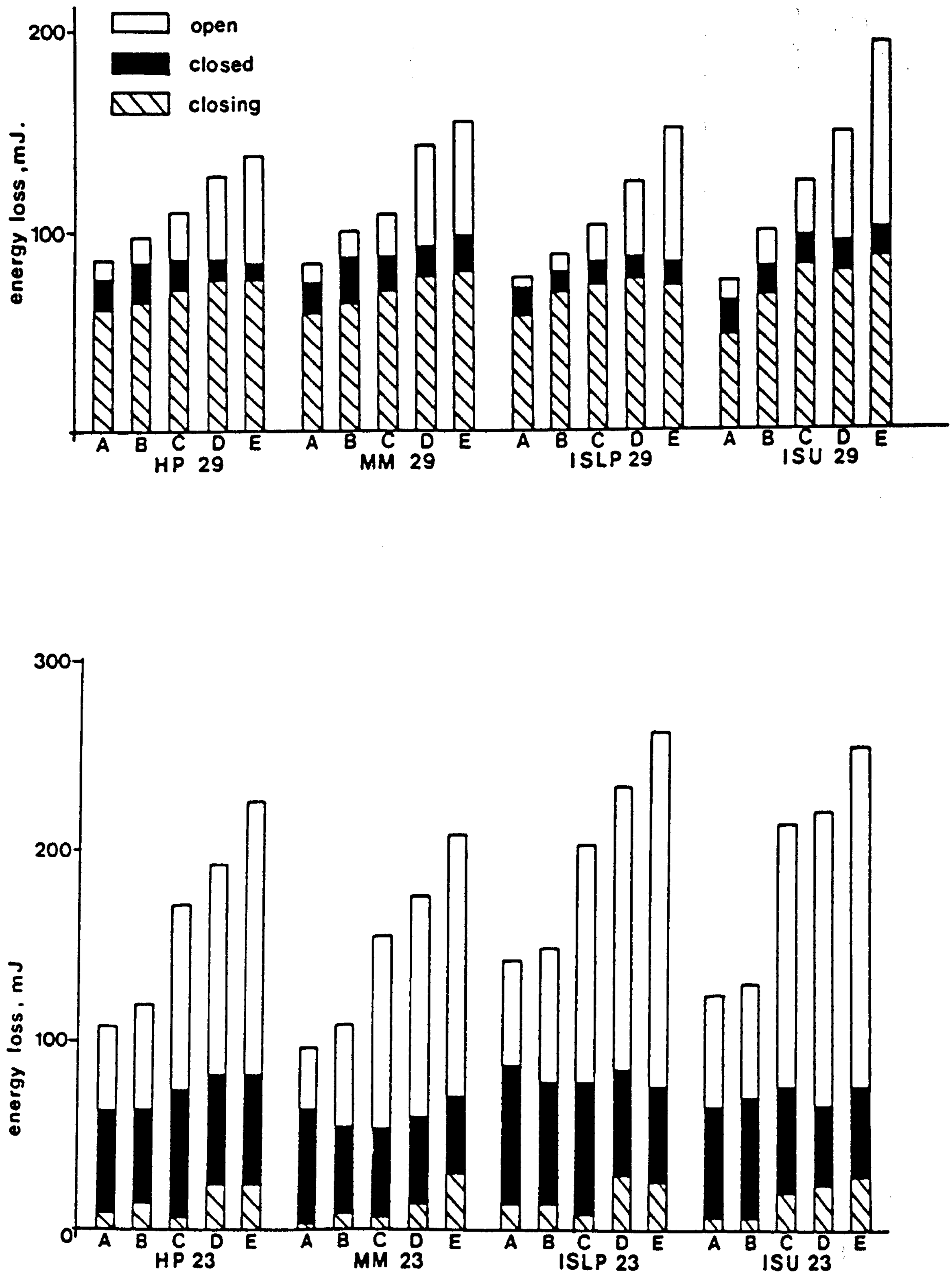

Figure 3.6 Energy losses across the pericardial valves during forward flow (open) and during regurgitation (closing and closed).

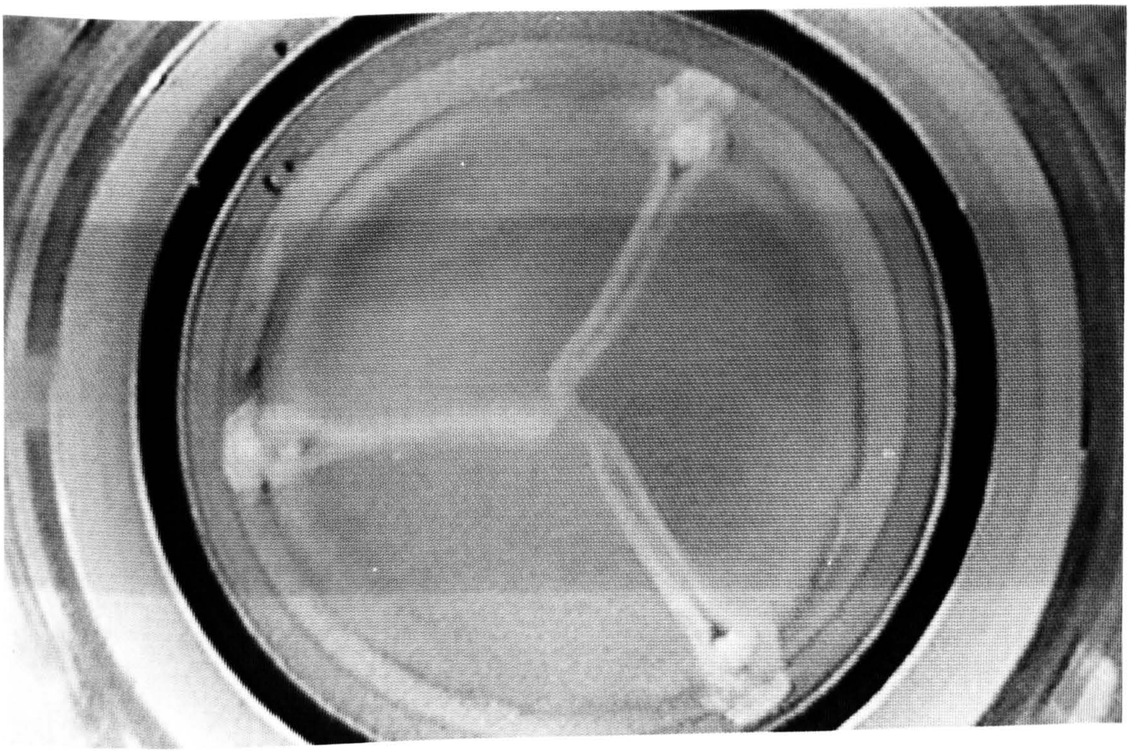

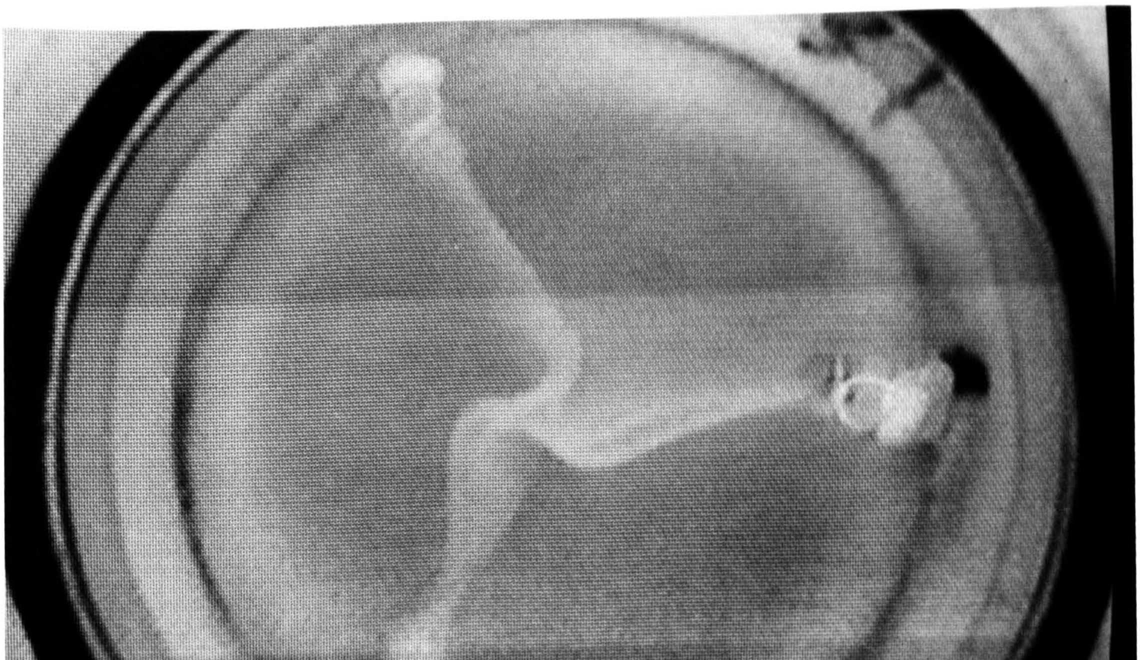

Figure 3.7 The closed position of the Ionescu-Shiley standard valve (ISU) above, and the Ionescu-Shiley low profile valve (ISLP) below, under 100 mm back pressure in the pulse duplicator.

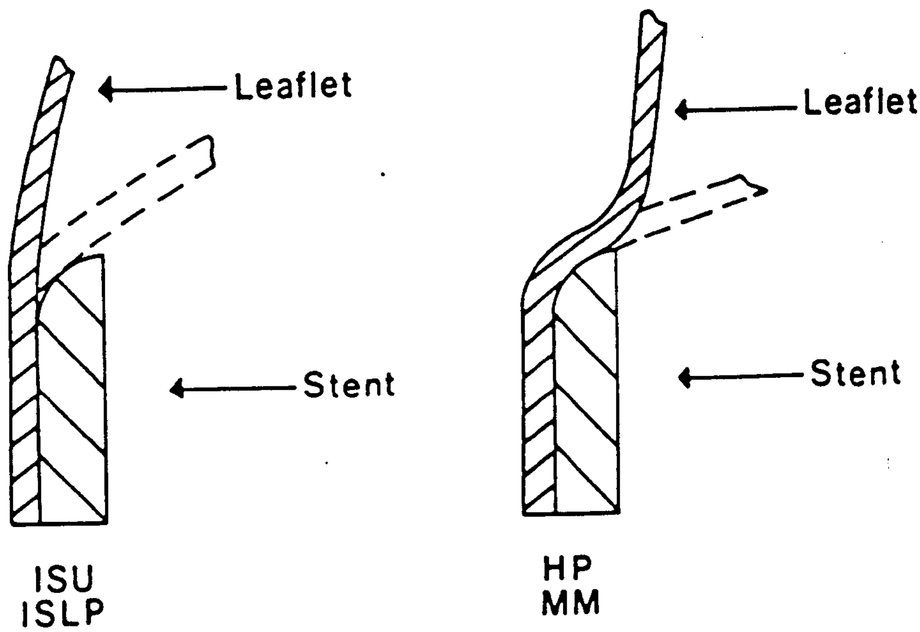

Figure 3.8 The geometries of the open valve leaflets in the base of the leaflet close to the edge of the stent (shown by a section through the leaflet centre line OC).

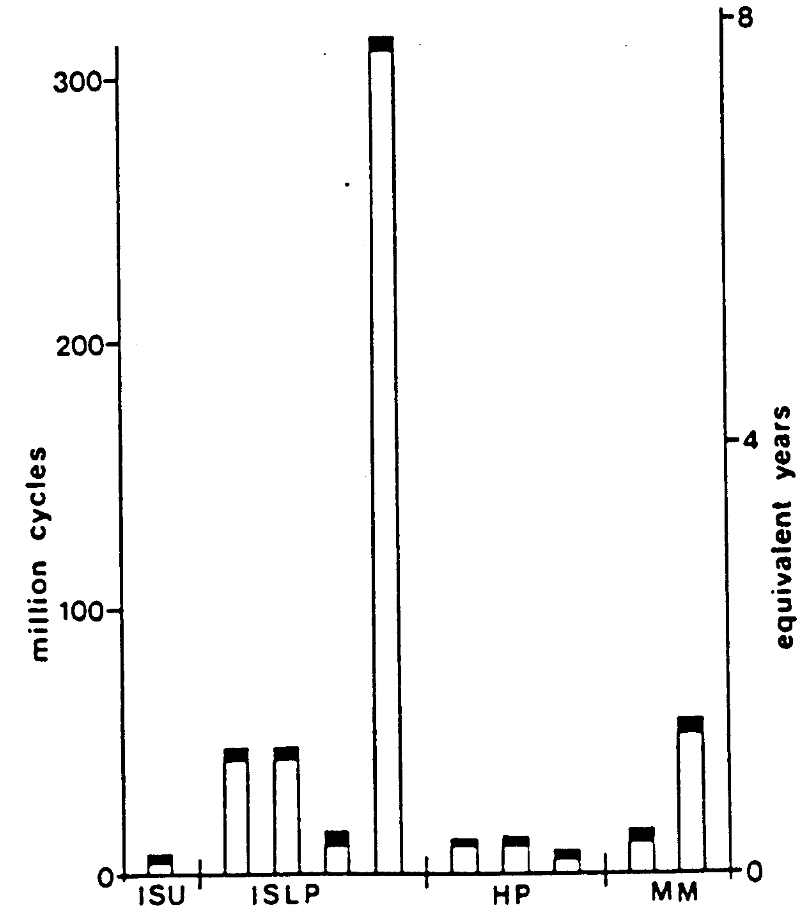

Figure 3.9 Results of the accelerated fatigue tests on the size 29 mm pericardial valves.

Figure 3.10 Four failed Ionescu-Shiley valves after the fatigue tests.


1


2

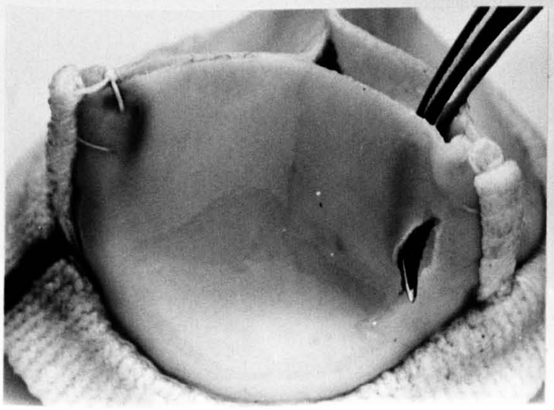
3

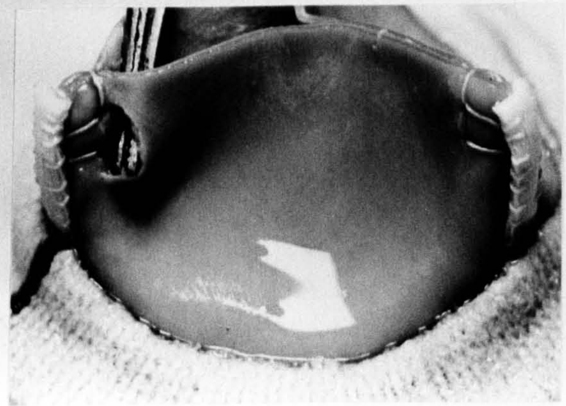
4

Figure 3.11 Leaflets from a failed Ionescu-Shiley low profile valve (1) and a failed Hancock pericardial valve (5) transilluminated and showing wear and abrasion along the edge of the cloth-covered frame on the inflow surface

1

5

Figure 3.12 One failed Ionescu-Shiley standard valve after the fatigue tests

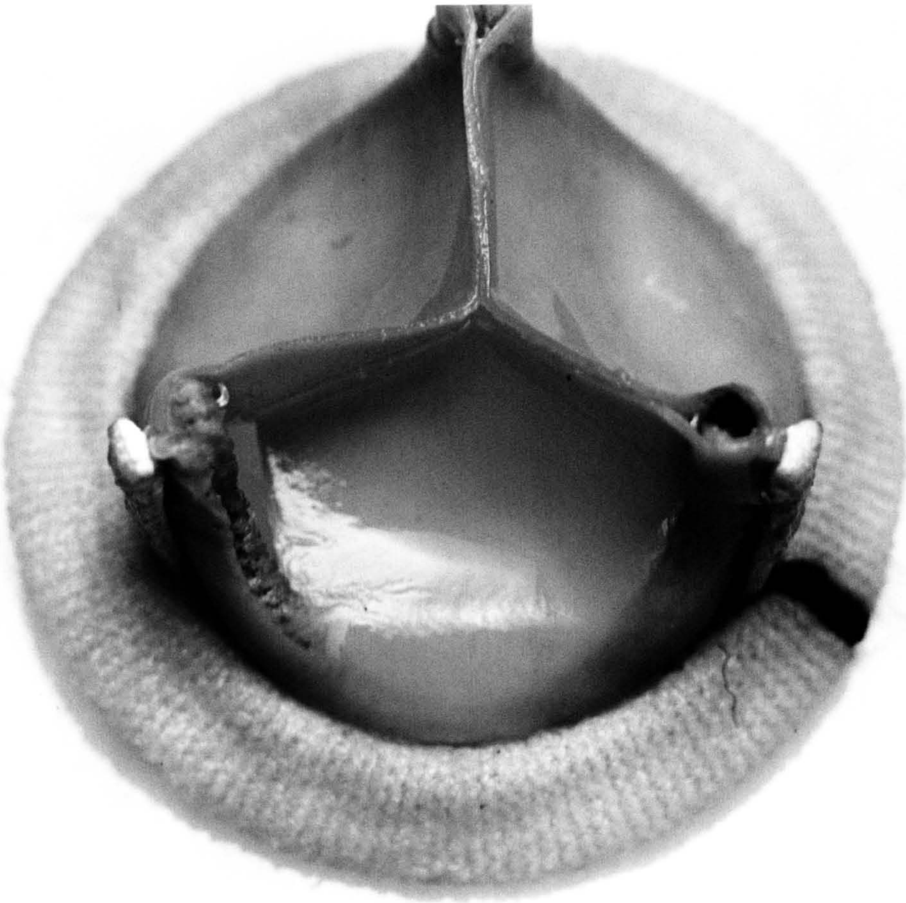

Figure 3.13 Three failed Hancock pericardial valves after the fatigue tests.

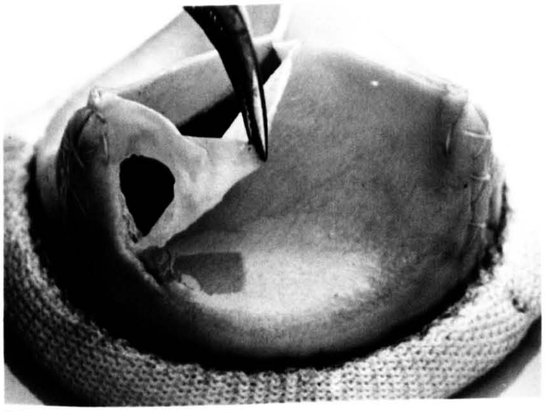

5

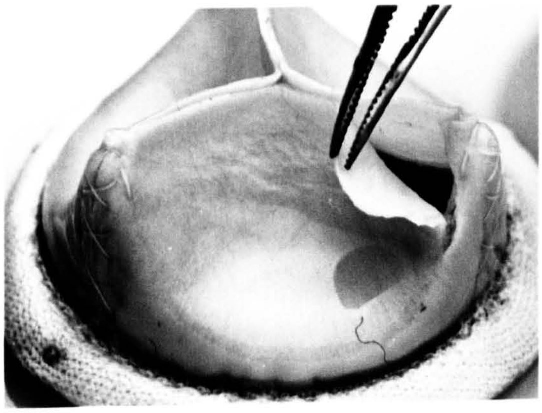

6

7

Figure 3.14 Two failed Mitral Medical valves after the fatigue tests

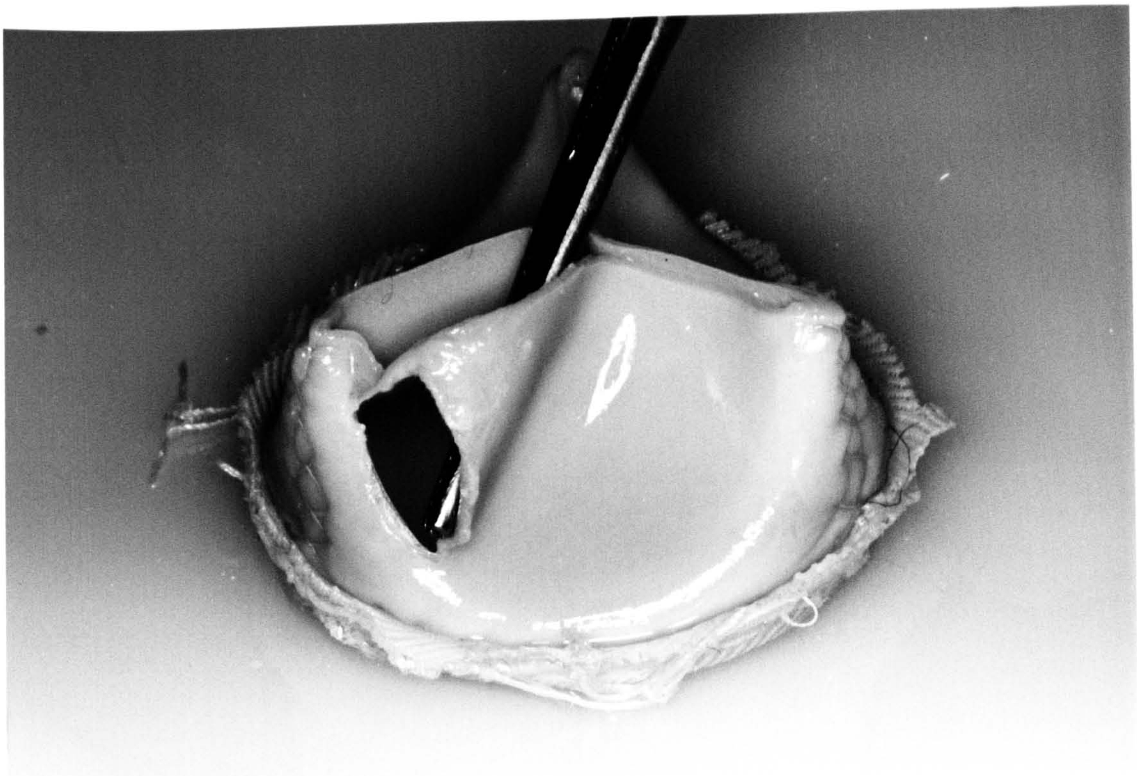

Figure 4.1 Photographs of the cast of a bovine heart showing the anterior surface and position of the two ligaments (above) and the posterior surface and posterior descending artery (below).

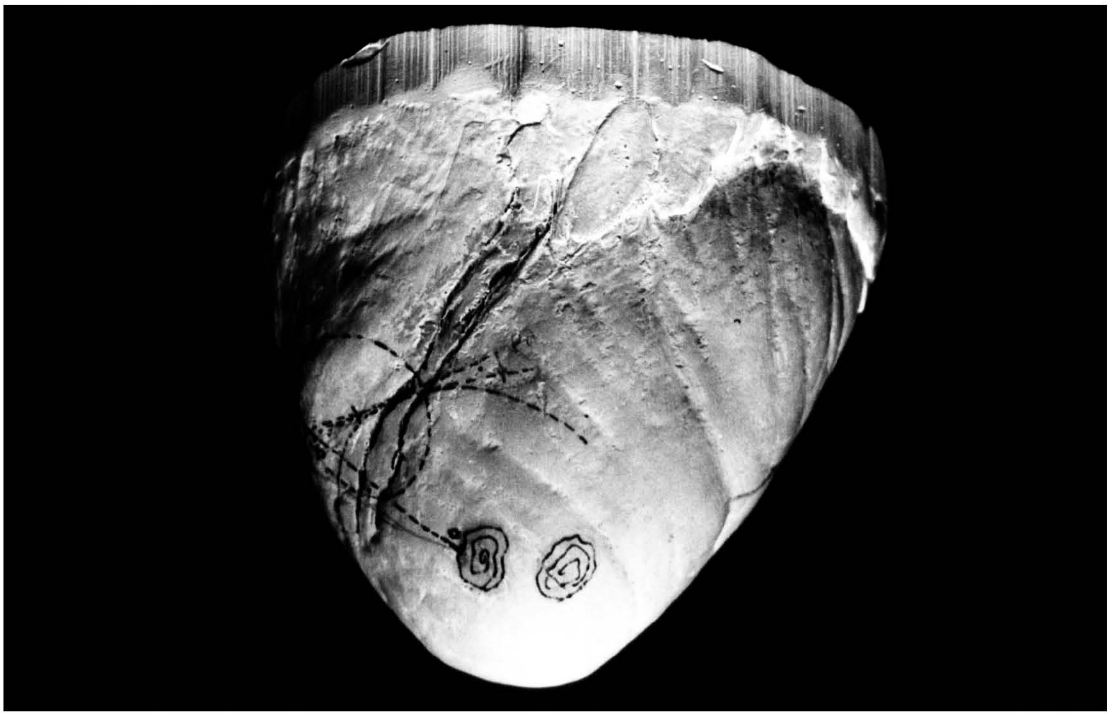

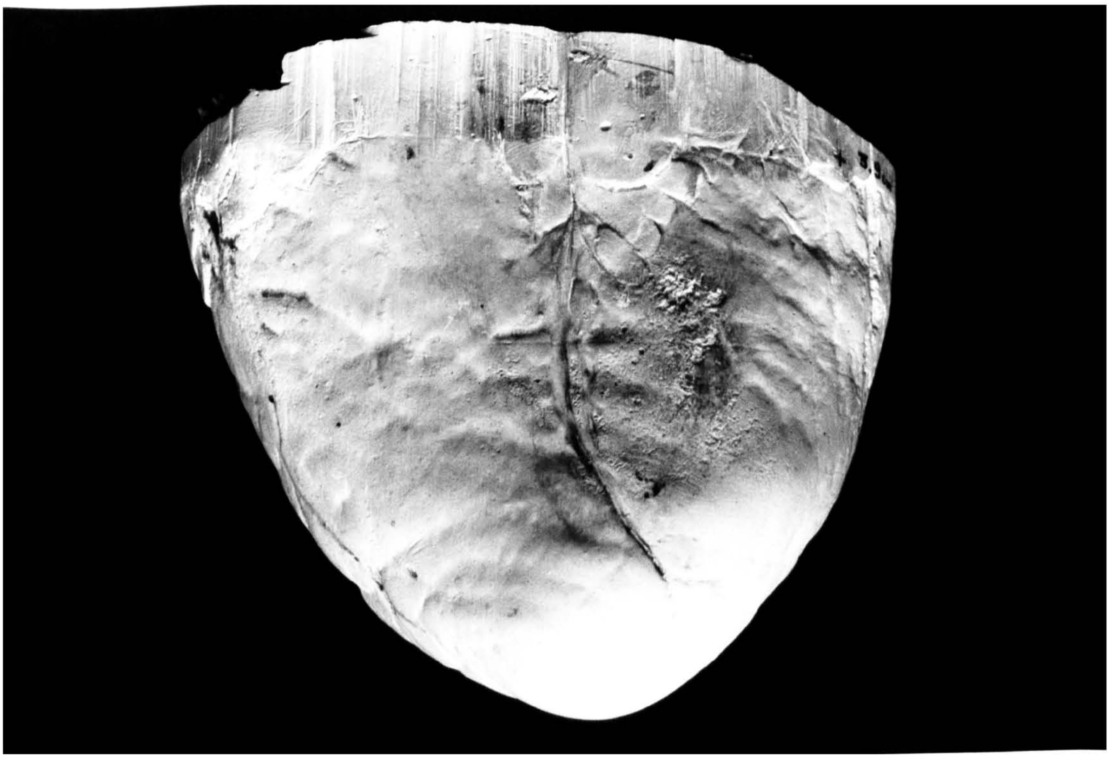

Figure 4.2 Bovine pericardial membrane dissected down the posterior surface, opened out flat and transilluminated looking at the epipericardial surface

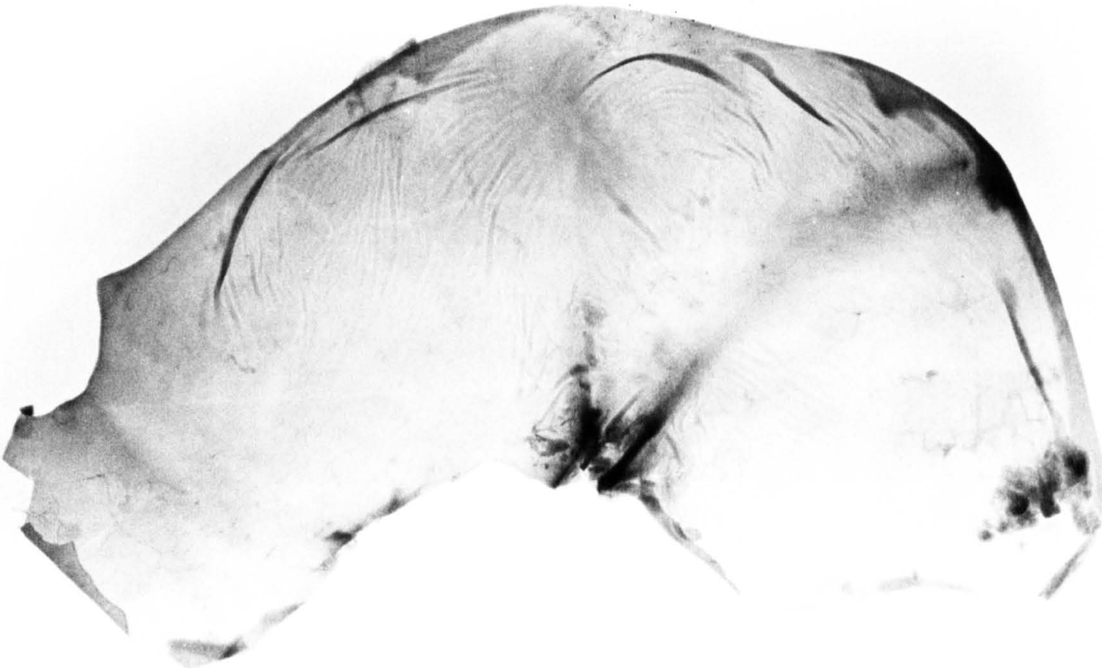

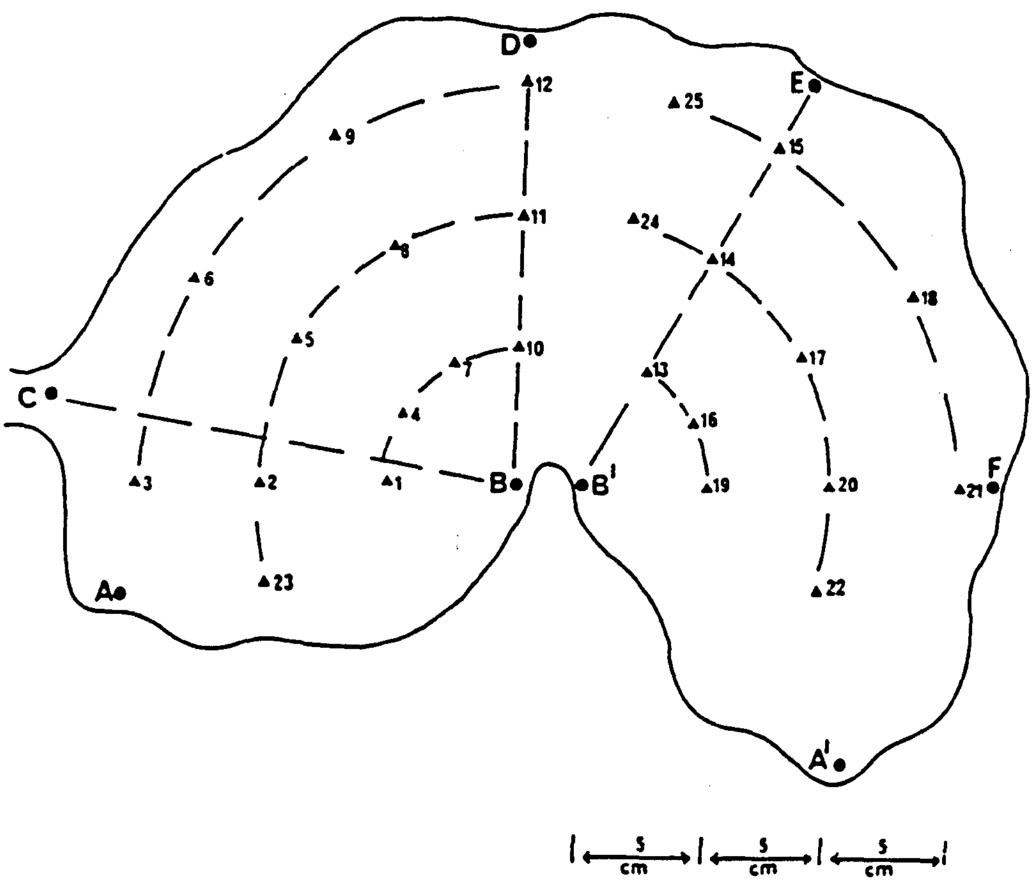

Figure 4.3 A frame of reference for the pericardial membrane with the position of the thickness measurements.

TABLE 4.1

Average tissue thickness in ten sizes

Position	Mean thickness ± 1SD	Position	Mean thickness ± 1SD
1	0.41 ± 0.07 mm	13	0.58 ± 0.09 mm
2	0.42 ± 0.07 mm	14	0.55 ± 0.13 mm
3	0.5 ± 0.08 mm	15	0.65 ± 0.1 mm
4	0.35 ± 0.05 mm	16	0.37 ± 0.05 mm
5	0.31 ± 0.05 mm	17	0.33 ± 0.03 mm
6	0.32 ± 0.09 mm	18	0.28 ± 0.05 mm
7	0.32 ± 0.04 mm	19	0.35 ± 0.04 mm
8	0.3 ± 0.05 mm	20	6.35 ± 0.07 mm
9	0.26 ± 0.03 mm	21	0.33 ± 0.05 mm
10	0.49 ± 0.09 mm	22	0.36 ± 0.04 mm
11	0.47 ± 0.11 mm	23	0.45 ± 0.04 mm
12	0.55 ± 0.14 mm	24	0.34 ± 0.05 mm
		25	0.31 ± 0.04 mm

Figure 4.4 Polarised light micrograph of the mesothelial surface of the pericardial membrane (x 100)

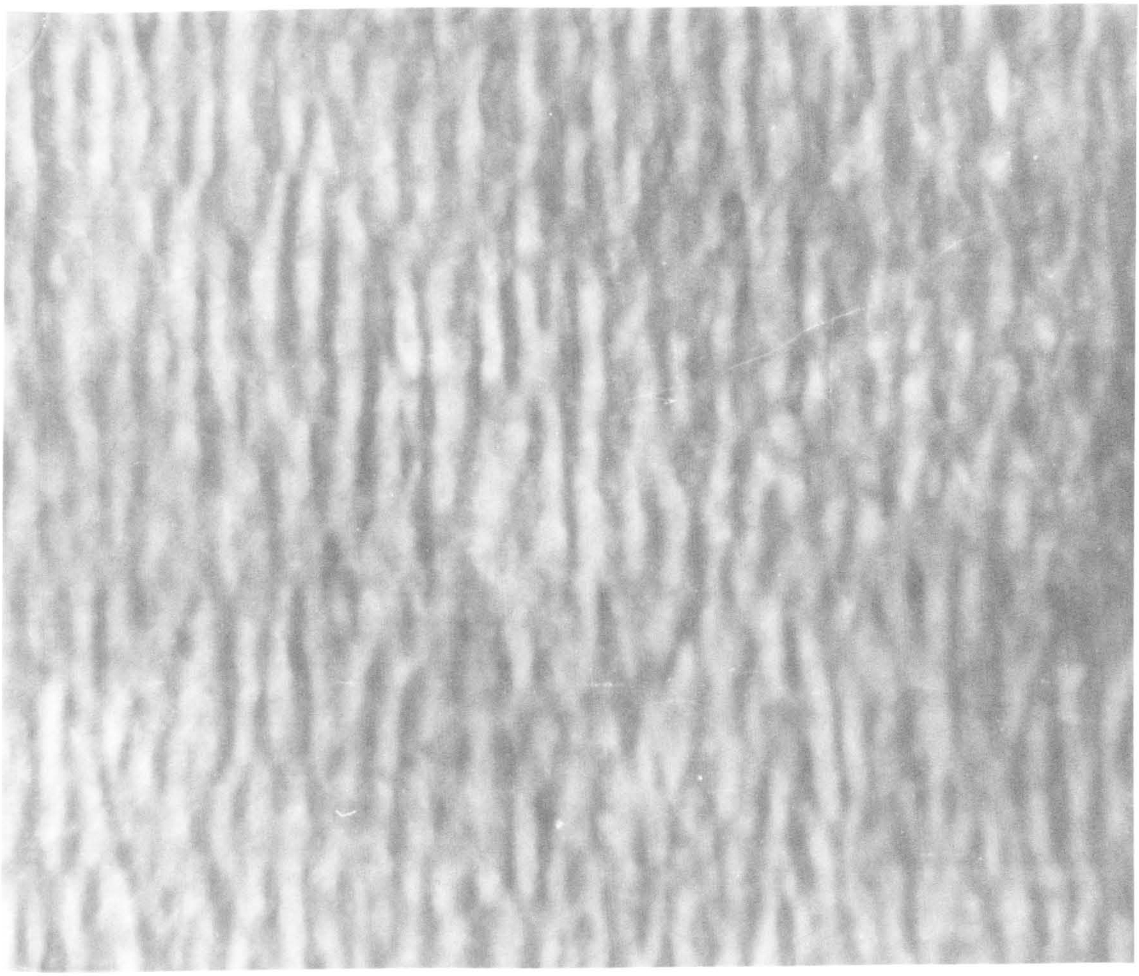

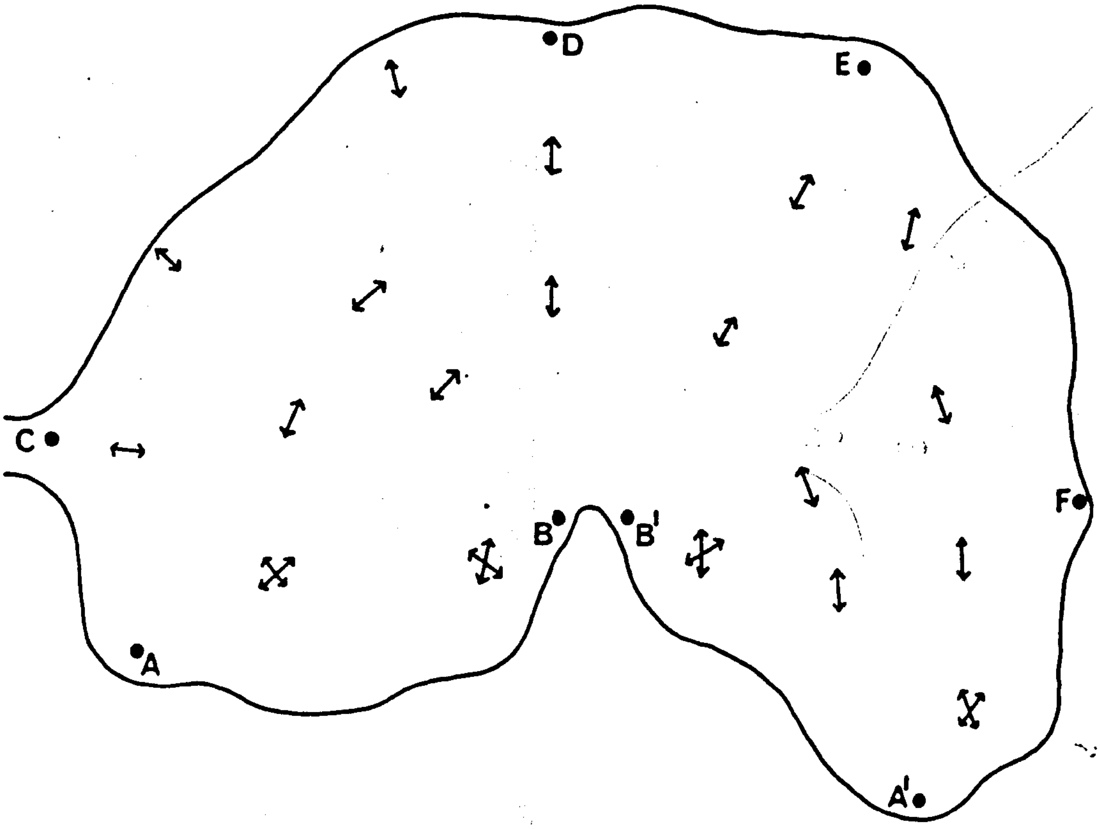

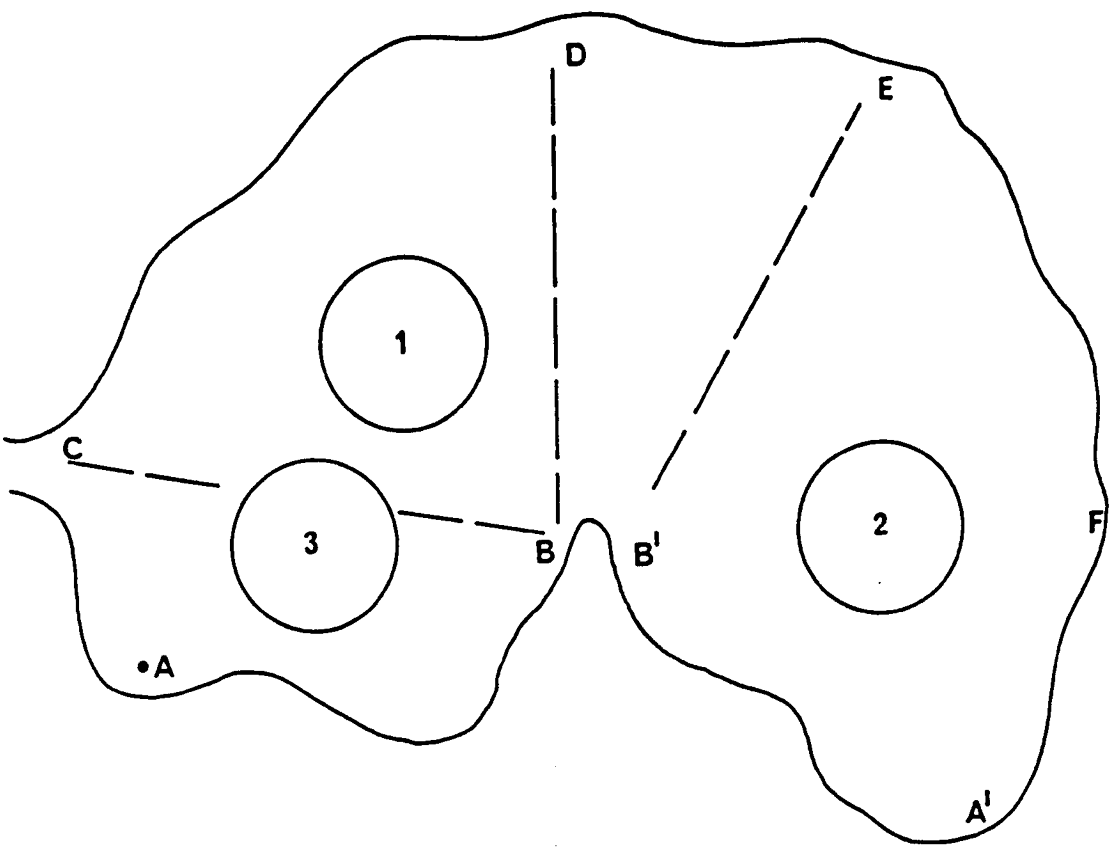

Figure 4.5 A diagram of the membrane showing the average orientation of the fibrils (top) and the areas of uniform thickness which were possible sites for leaflet manufacture (below).

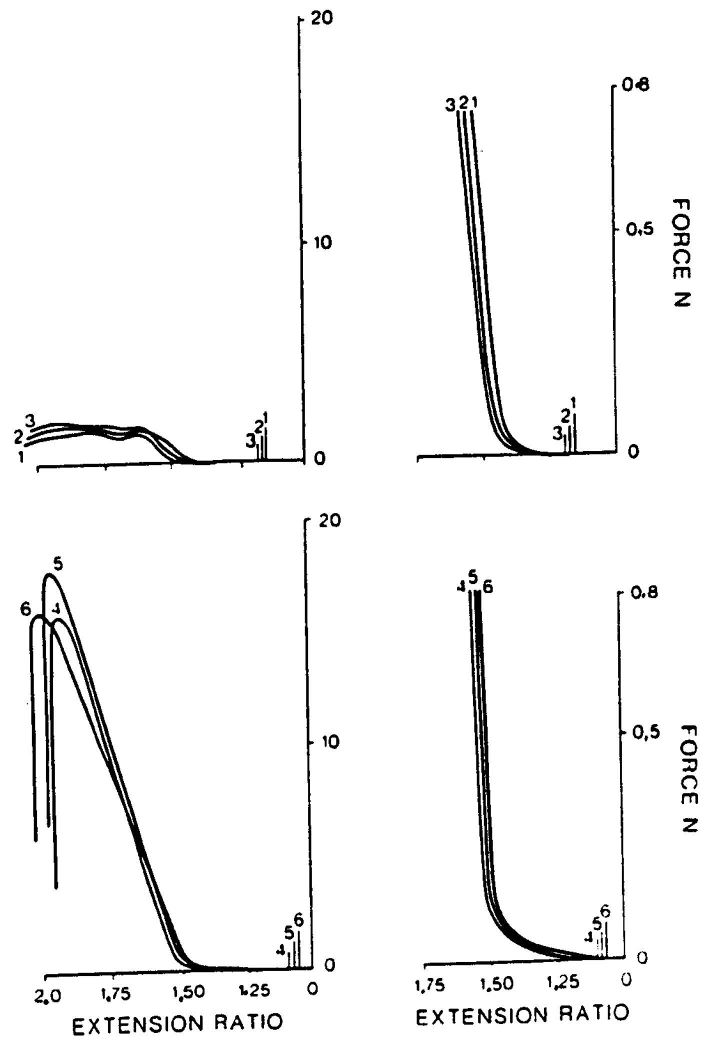

Figure 4.6a Force extension curves for fresh tissue from sac G showing the conditioned fifth cycle, first load points and extension to ultimate failure for each strip.

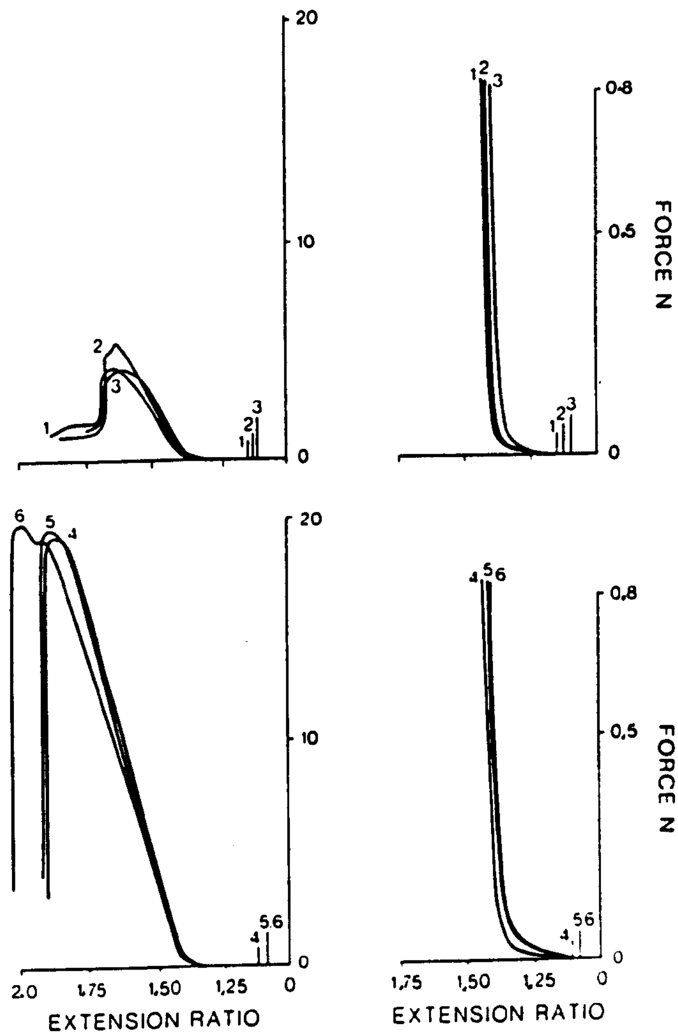

Figure 4.6b Force extension curves for fresh tissue from sac H showing the conditioned fifth cycle, first load points and extension to the ultimate failure for each strip.

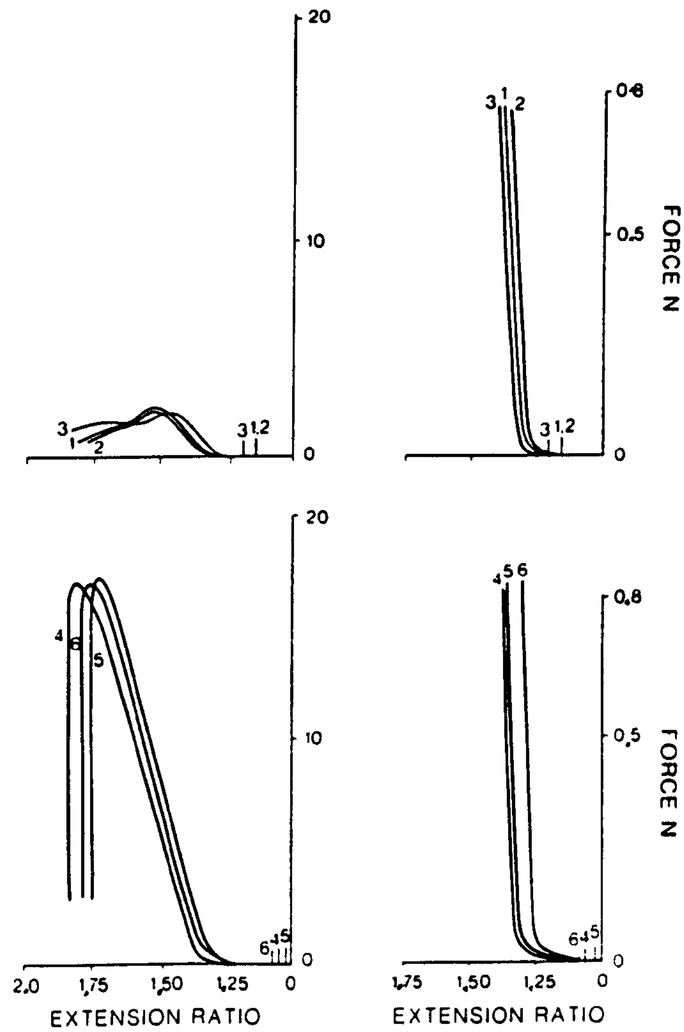

Figure 4.6c Force extension curves for fresh tissue from sac J showing the conditioned fifth cycle, first loadpoints and extension to ultimate failure for each strip.

TABLE 4.2

Fresh tissue specimens

Sac	Average thickness mm	Specimen Number	First load extension ratio on the conditioned curve
G	0.33	1	1.16
		2	1.17
		3	1.17
		4	1.06
		5	1.07
		6	1.09
H	0.33	1	1.14
		2	1.14
		3	1.17
		4	1.02
		5	1.06
		6	1.08
J	0.34	1	1.13
		2	1.12
		3	1.10
		4	1.12
		5	1.08
		6	1.08

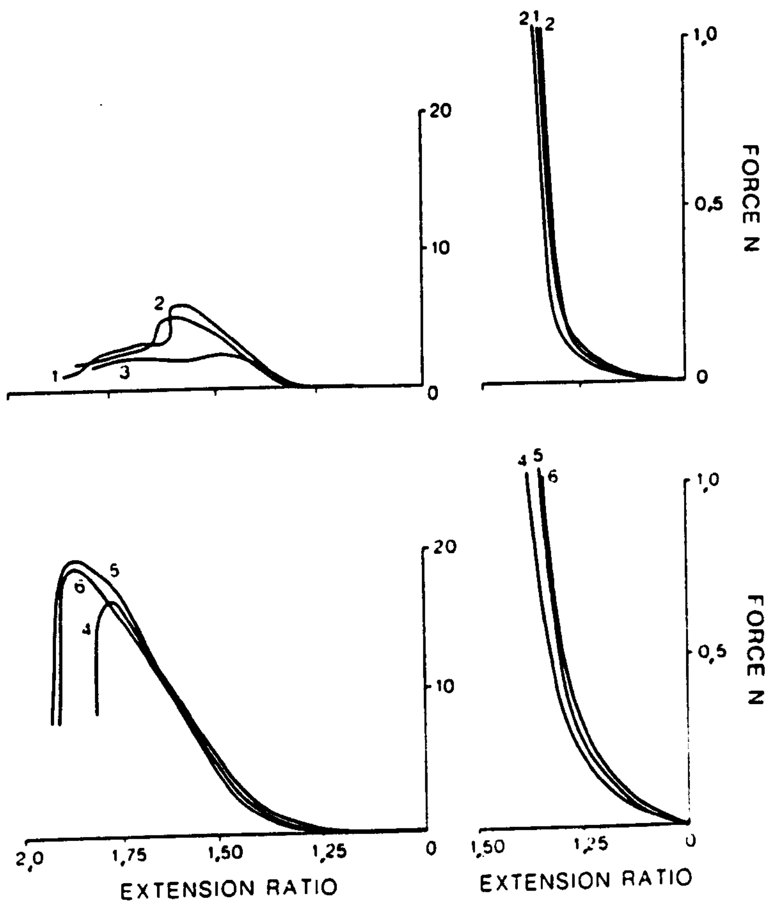

Figure 4.7a Force extension curves for fixed tissue from sac D showing the conditioned fifth cycle and extension to ultimate failure for each strip.

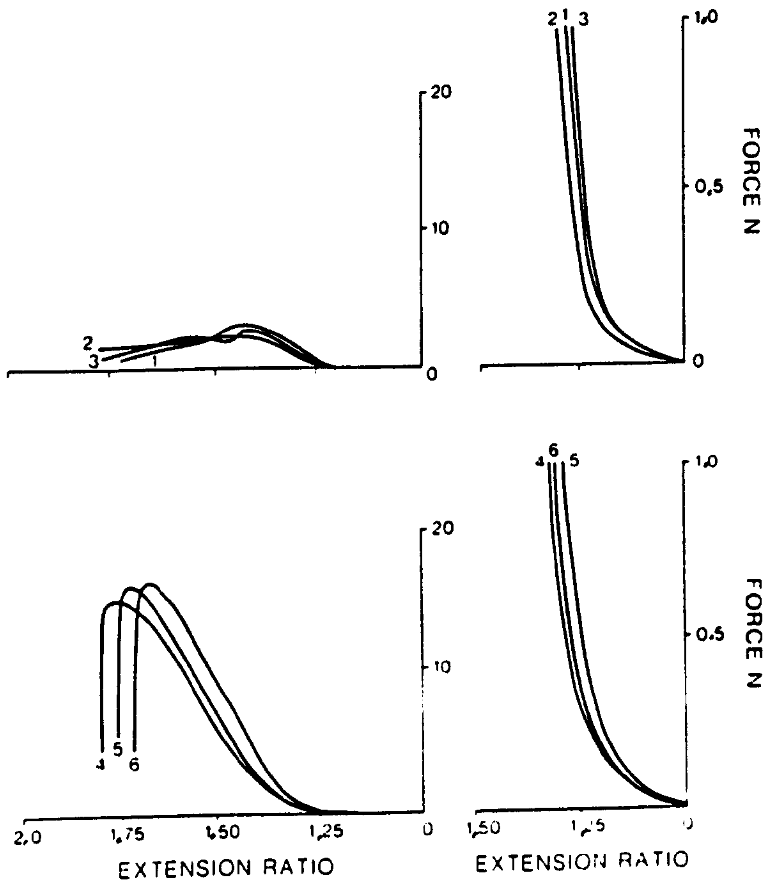

Figure 4.7b Repeat test for 4.7a using sac E.

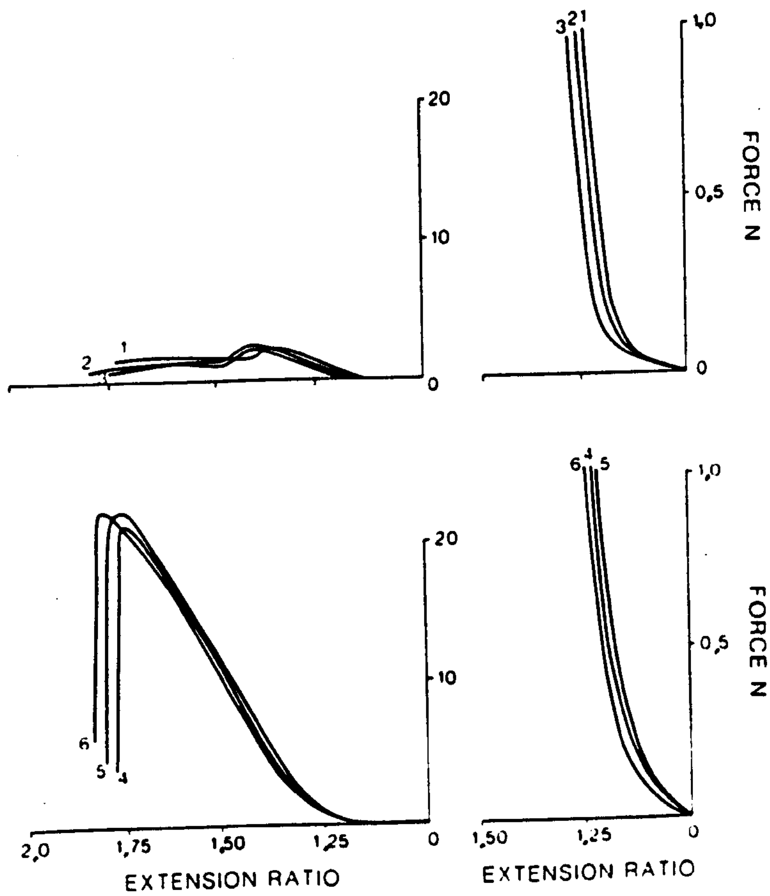

Figure 4.7c Repeat test for 4.7a using sac F.

TABLE 4.3

Properties of the fixed tissue

Sac reference	First load extension ratio for the conditioned tissue	Thickness t
D	1.02 to 1.07	0.4
E	1.02 to 1.05	0.36
F	1.02 to 1.04	0.42

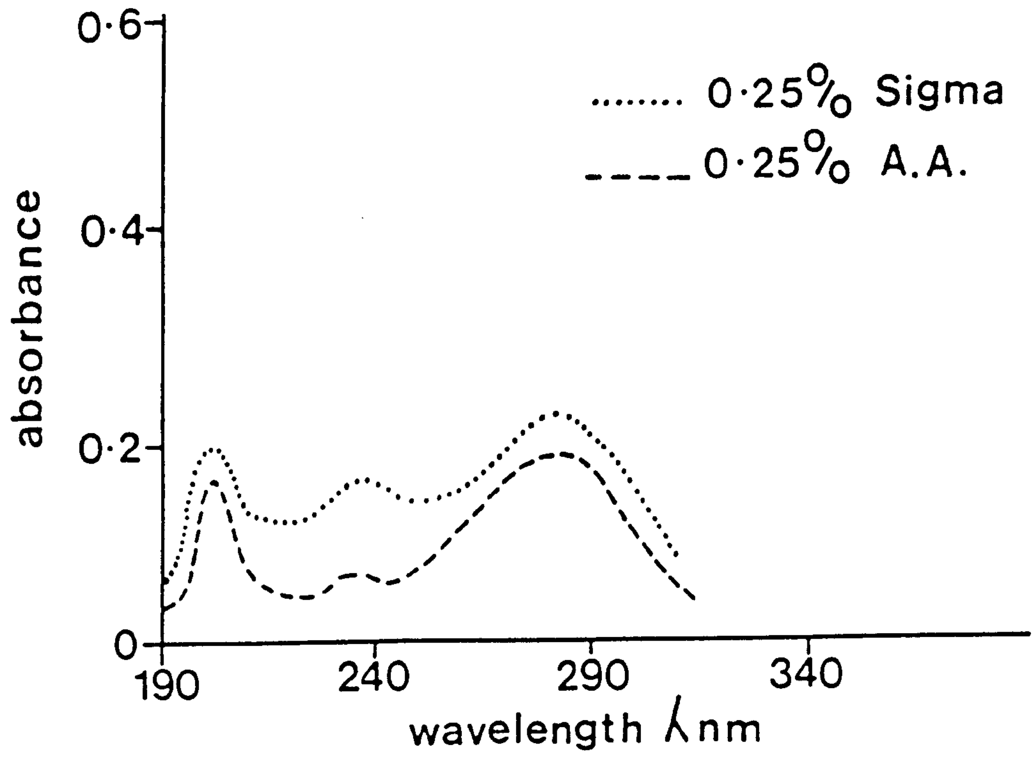

Figure 4.8 Absorbance spectra for 0.25% Sigma and 0.25% Agar Aids (AA) glutaraldehyde.

TABLE 4.4

Absorbance of five solutions of glutaraldehyde (concentration 0.25%)

Solution	**Absorbance** 235 nm	**Absorbance** 280 nm
Technical	1.5	0.24
Agar Aids	0.08	0.20
Sigma	0.15	0.22
Distilled Technical	0.25	0.24
Filtered Technical	0.1	0.24

TABLE 4.5

Concentration	Absorbance at 280 nm	
	Sigma	Distilled Technical
0.5 percent	0.4	0.45
0.25 percent	0.22	0.24
0.125 percent	0.11	0.12
0.06 percent	0.06	0.06

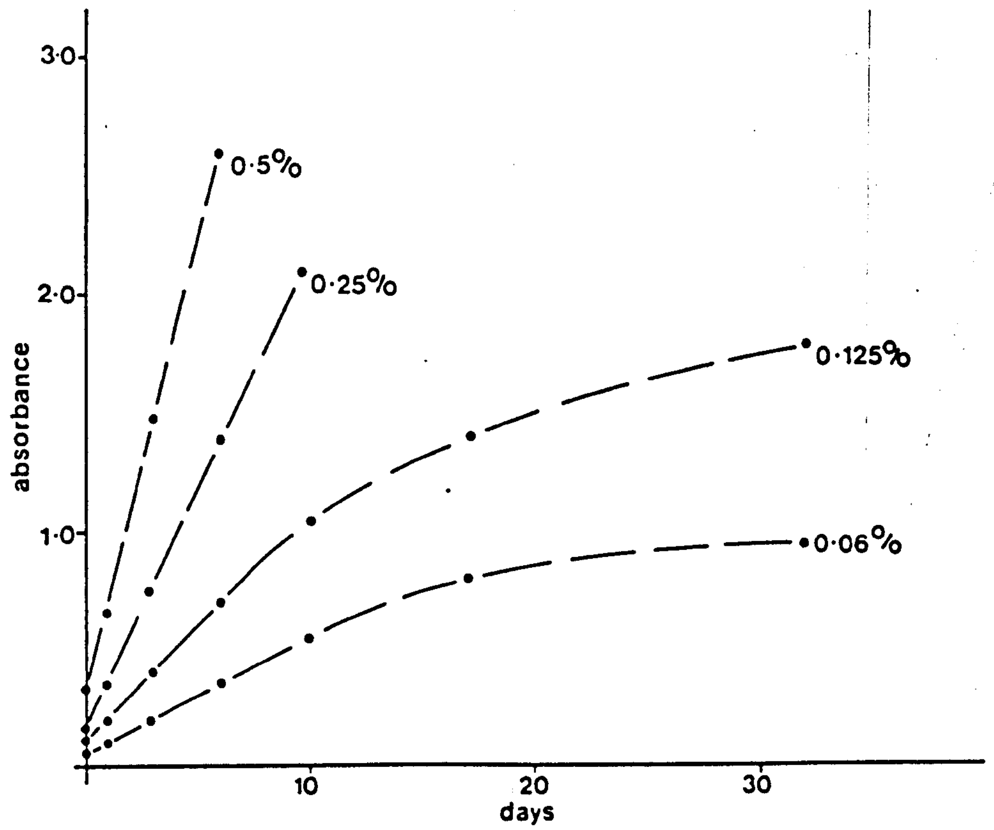

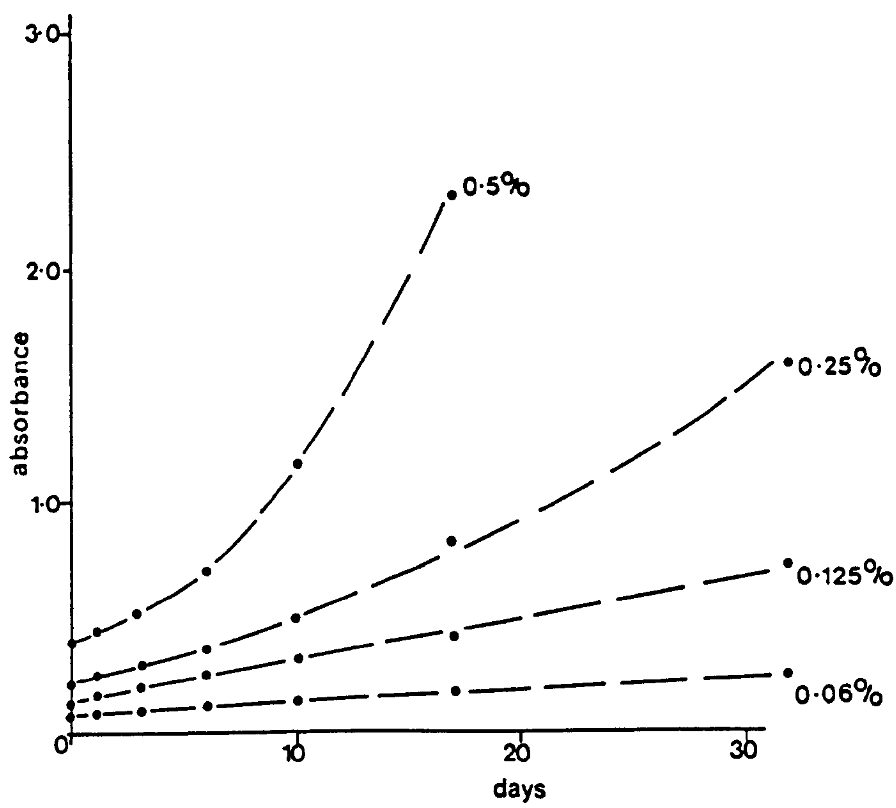

Figure 4.9 Absorbance of dilute solution of Sigma (above) and technical distilled glutaraldehyde (below) at 235 nM, after varying time intervals.

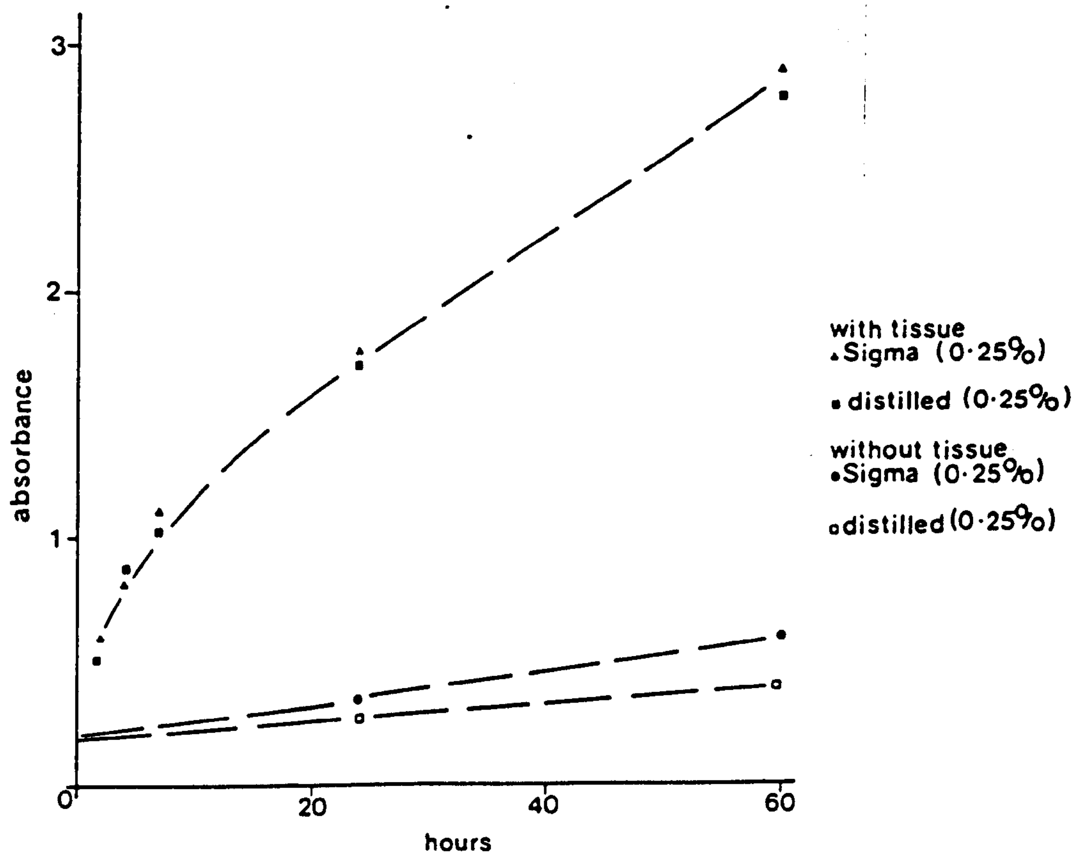

Figure 4.10 Absorbance of dilute solutions of glutaraldehyde at 235 nM at varying time intervals after tissue has been added.

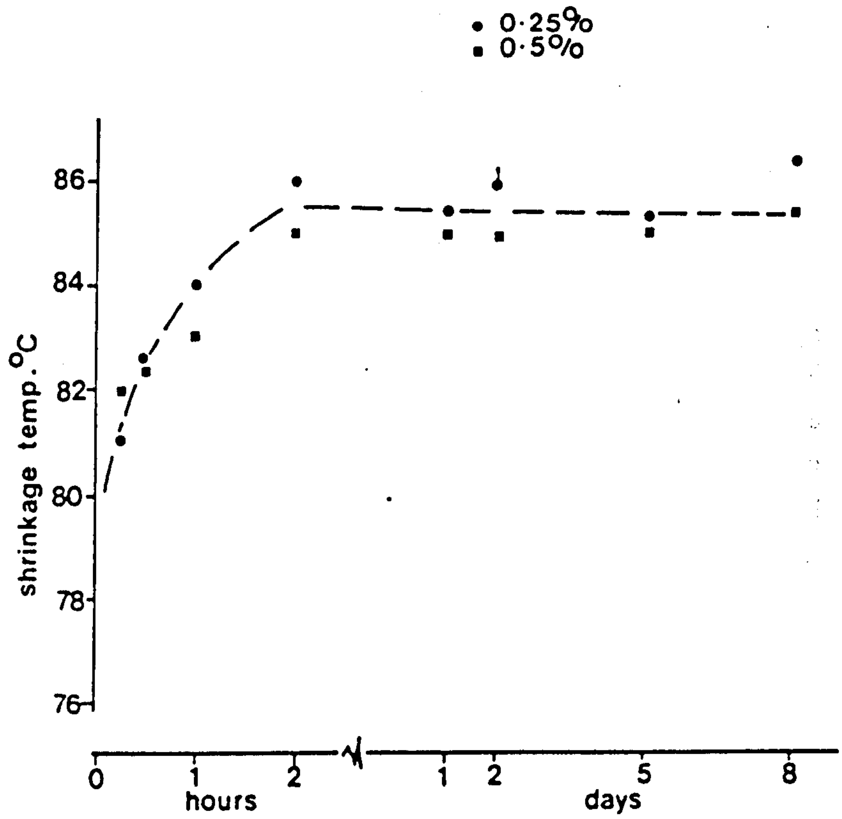

Figure 4.11 Variation in tissue shrinkage temperature with fixation time for fixation with 0.25% and 0.5% glutaraldehyde.

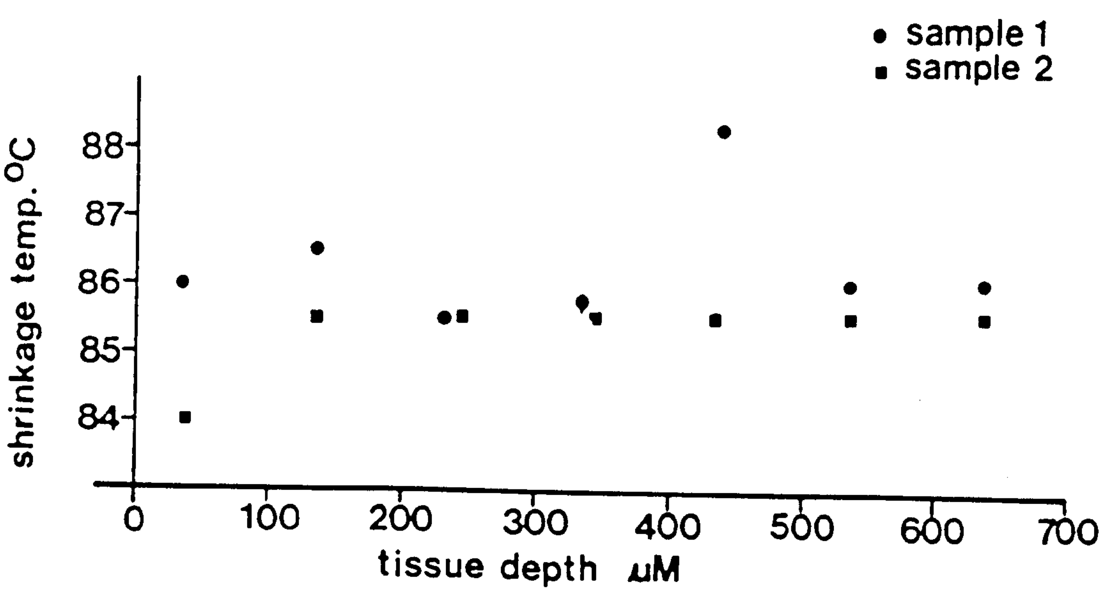

Figure 4.12 Stratographic analysis of the shrinkage temperature of two pieces of tissue fixed with 0.25% glutaraldehyde.

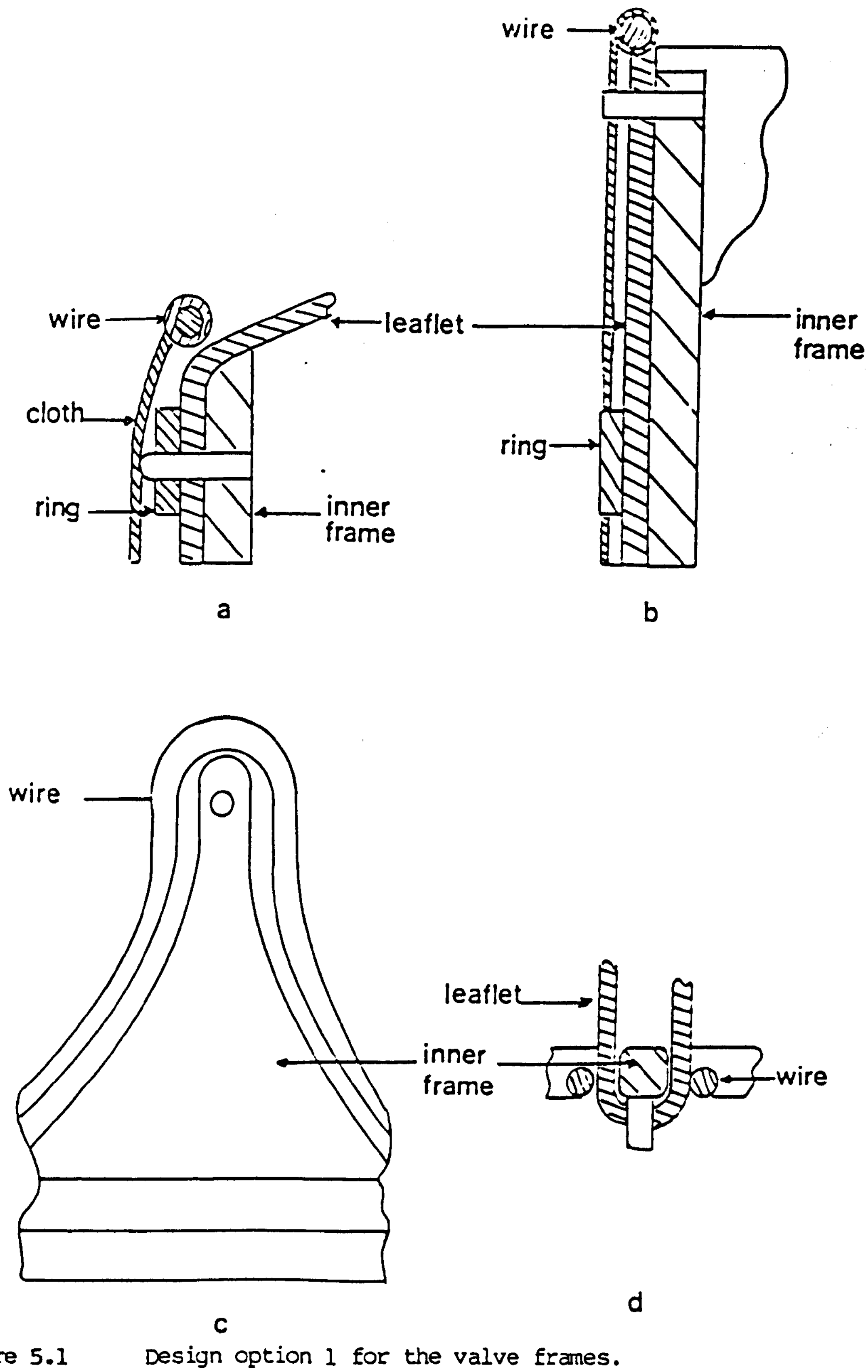

Figure 5.1 Design option 1 for the valve frames.

a] Vertical section through the frame in the base of the scallop.

b] Vertical section through the post.

c] Radial view on the post.

d] Horizontal section through the post.

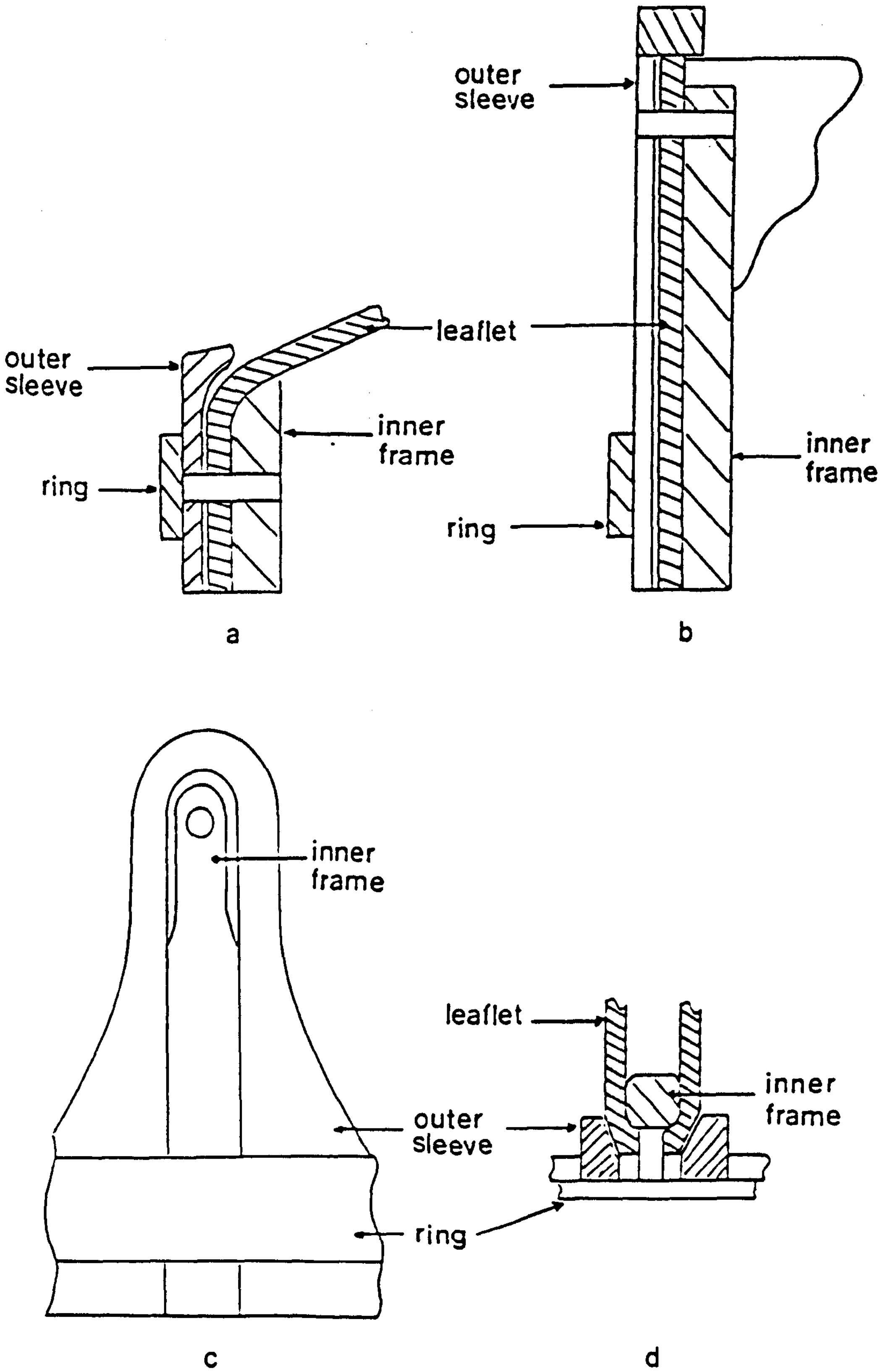

Figure 5.2 Design option 2 for the valve frames.

a] Vertical section through the frames in the base of the scallop.

b] Vertical section through the post.

c] Radial view on the post.

d] Horizontal section through the post.

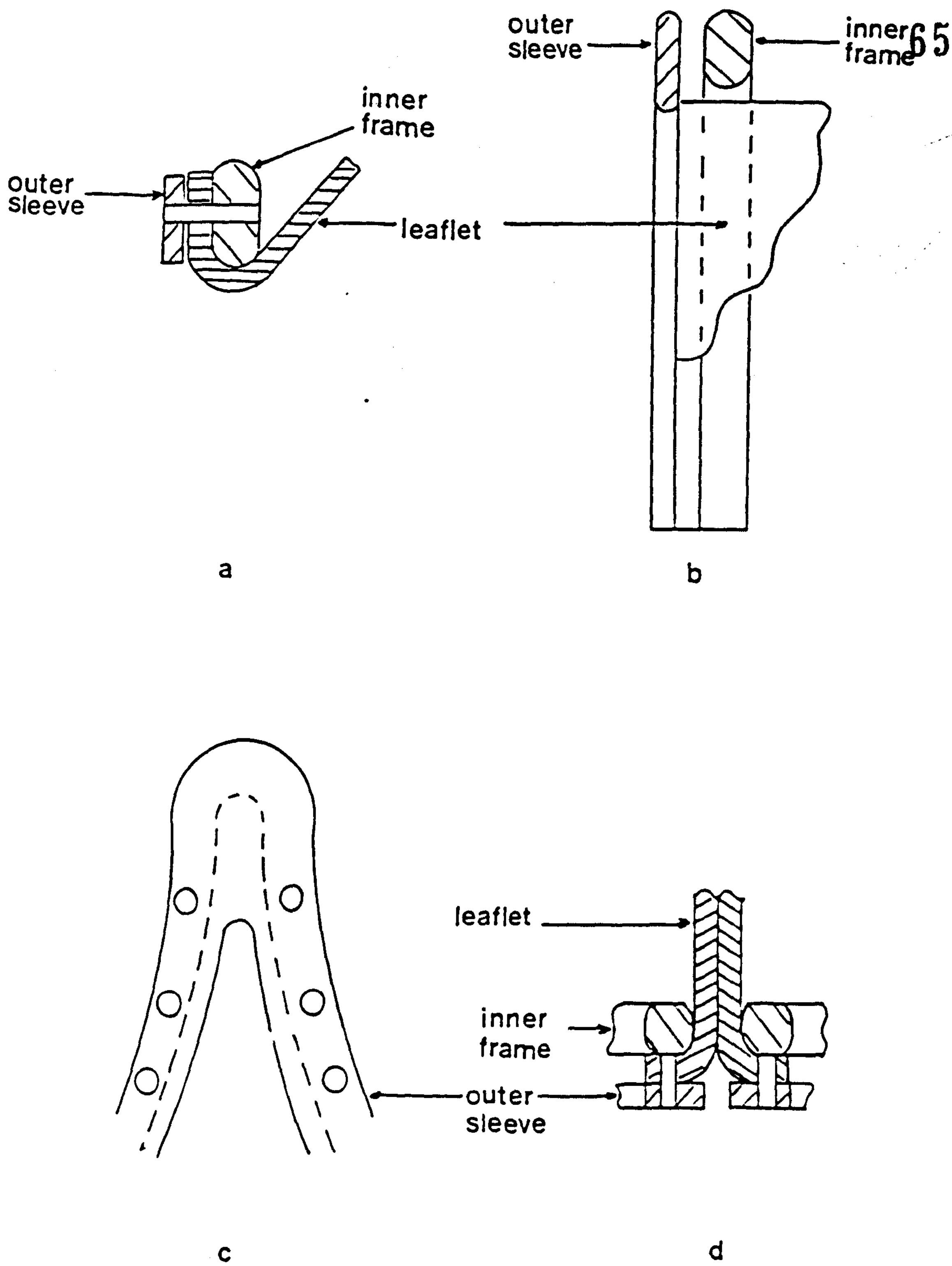

Figure 5.3 Design option 3 for the valve frames.

a] Vertical section through the frames in the base of the scallop.

b] Vertical section through the post.

c] Radial view on the post.

d] Horizontal section through the post.

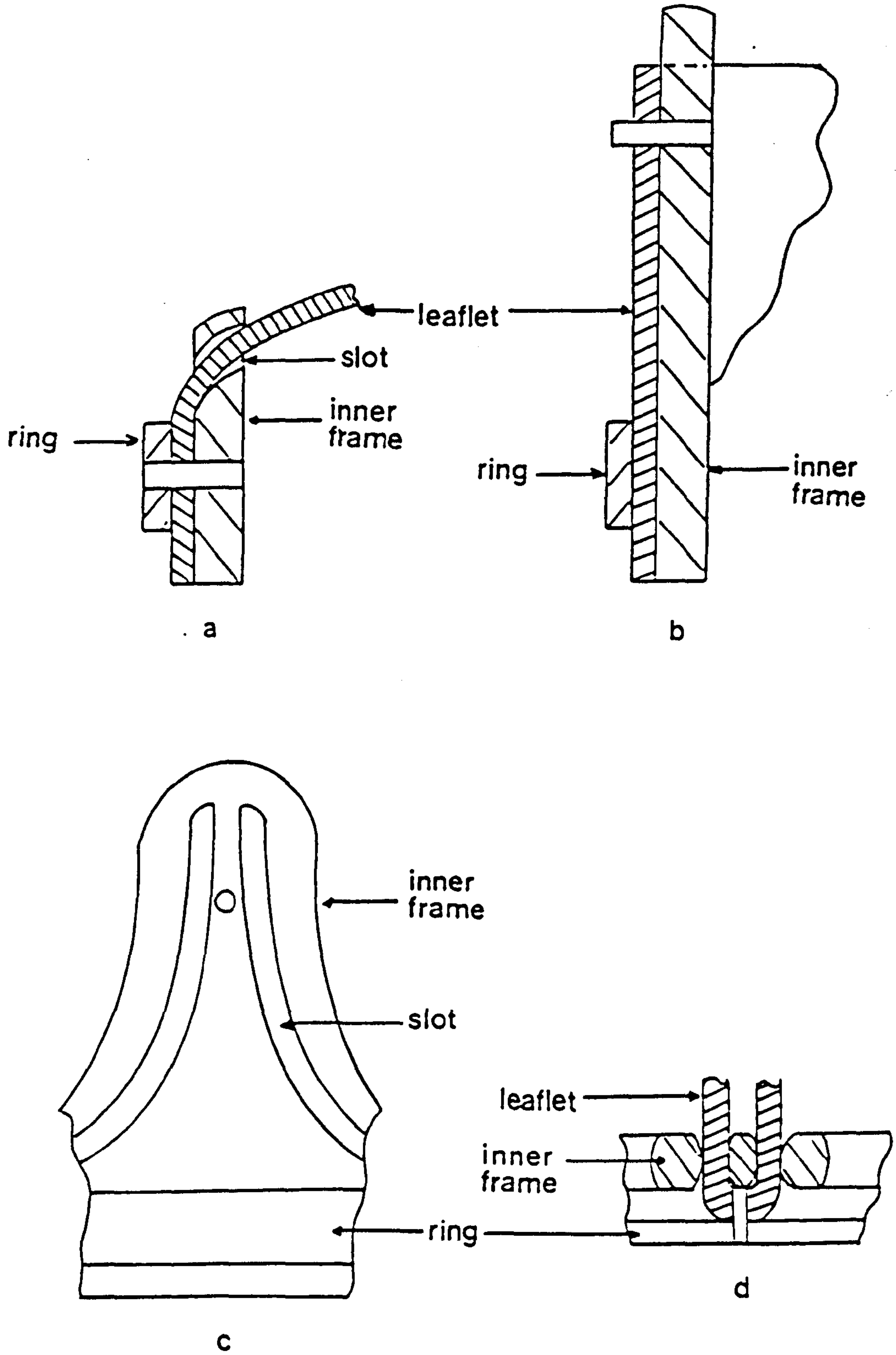

Figure 5.4 Design option 4 for the valve frames.

a] Vertical section through the frames in the base of the scallop.

b] Vertical section through the post.

c] Radial view on the post.

d] Horizontal section through the post.

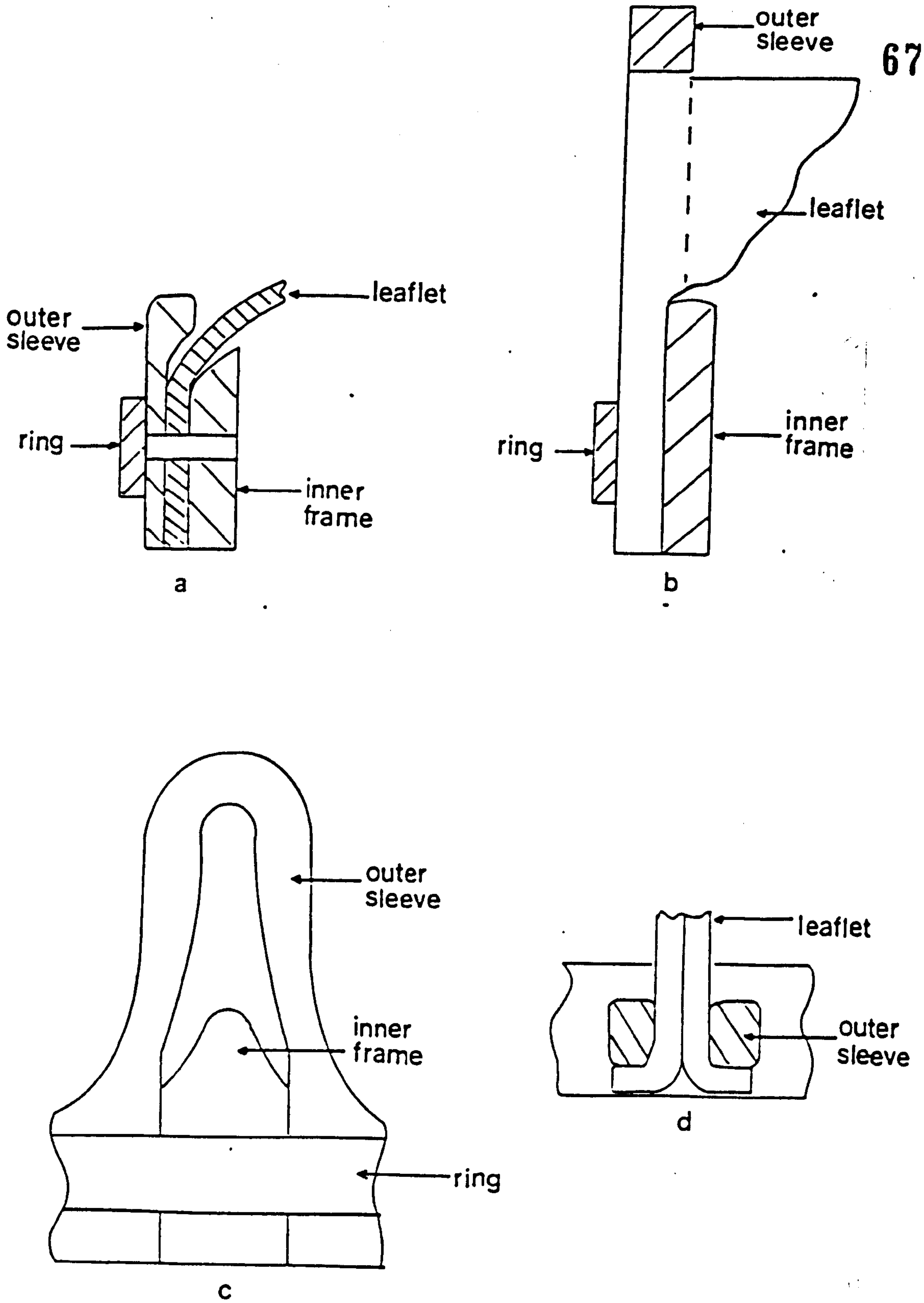

Figure 5.5 Design option 5 for the valve frames.

a] Vertical section through the frames in the base of the scallop.

b] Vertical section through the post.

c] Radial view on the post.

d] Horizontal section through the post.

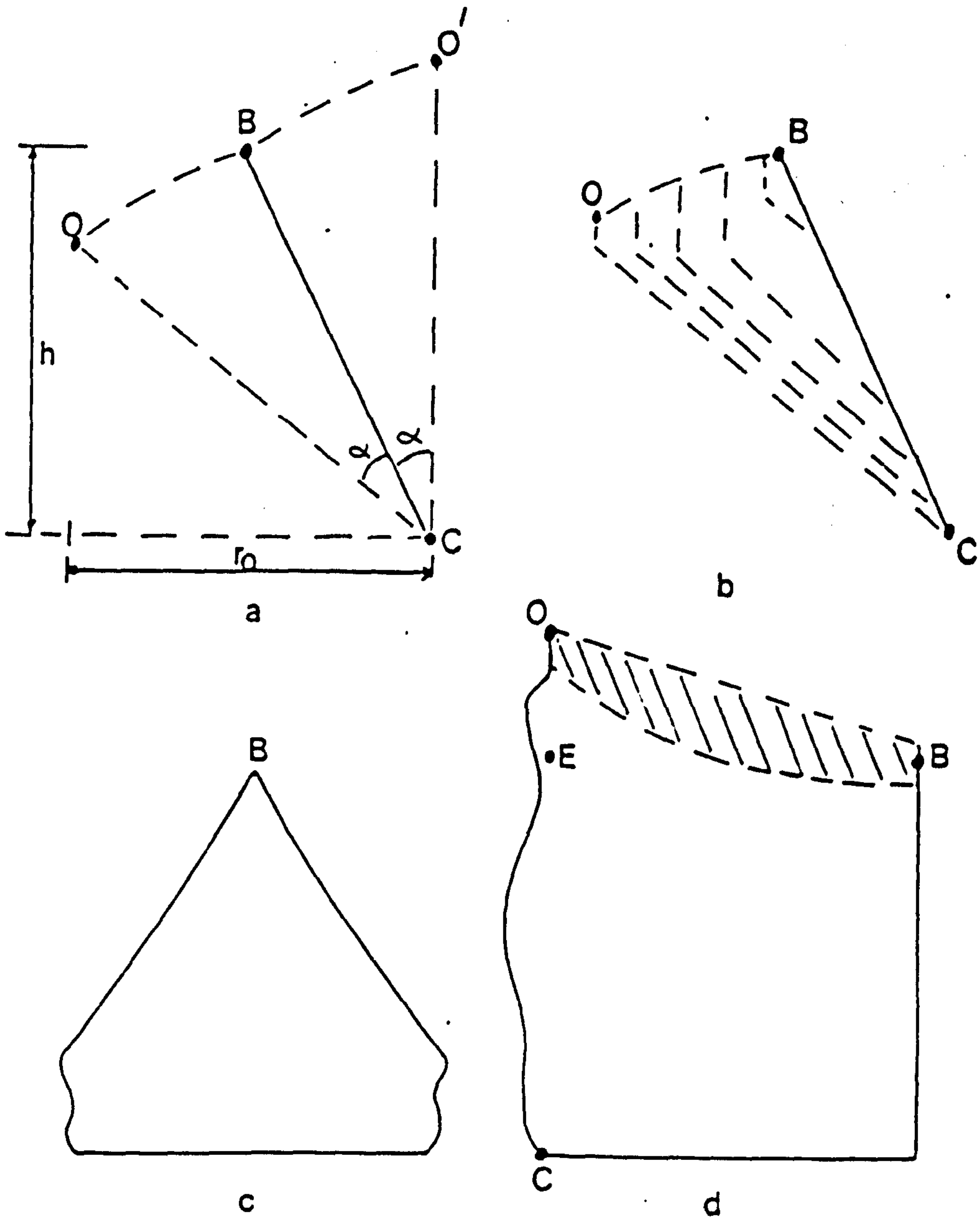

Figure 5.6 Leaflet geometry A

a] Vertical section through the centre line OEC of the leaflet.

b] Vertical sections through the closed leaflets.

c] Radial view on the post.

d] Projection of the leaflet showing the coaption area.

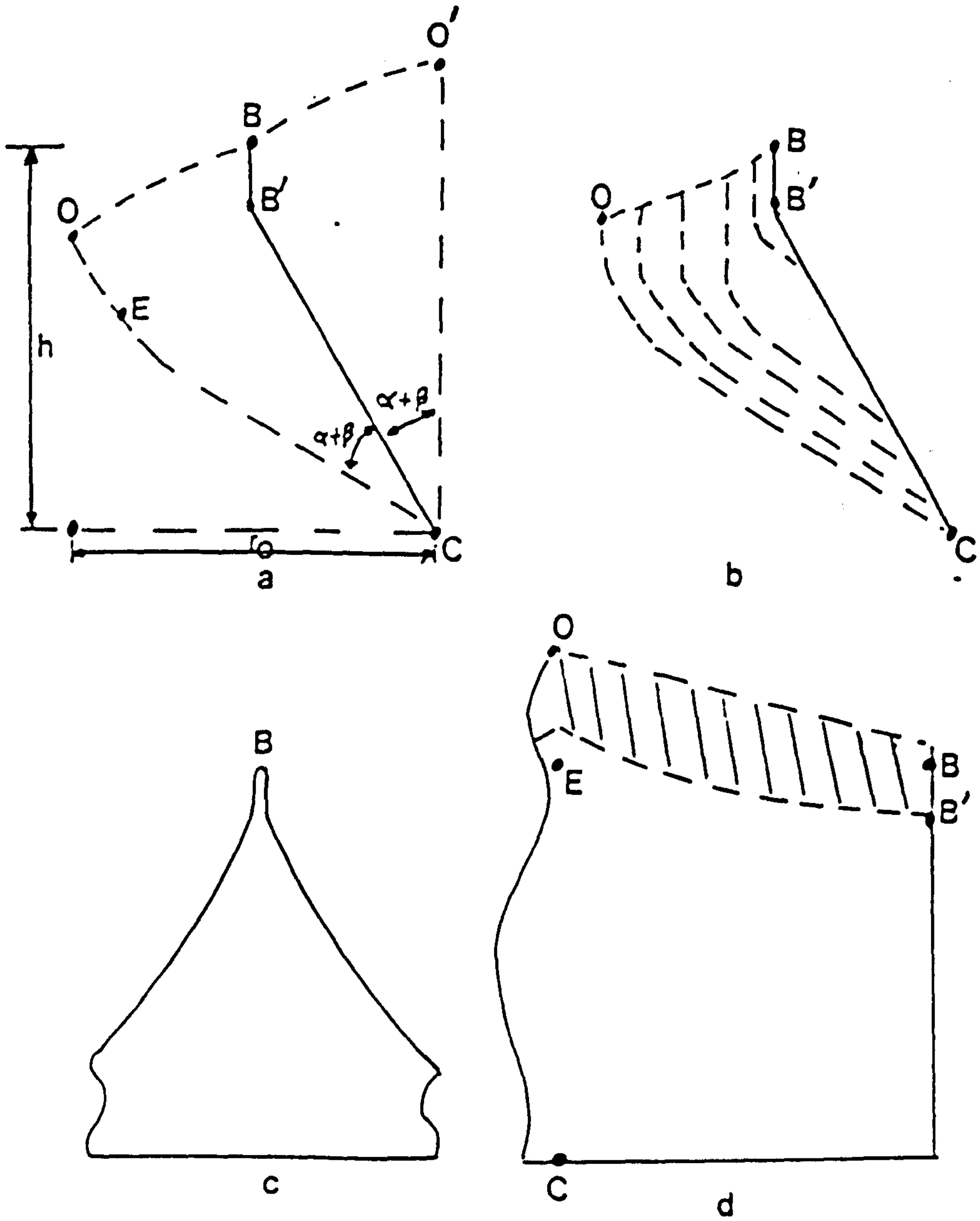

Figure 5.7 Leaflet geometry B

a] Vertical section through the centre line of the leaflet OEC.

b] Vertical sections through the closed leaflet.

c] Radial view on the post.

d] Projection of the leaflet showing the increased coaption area.

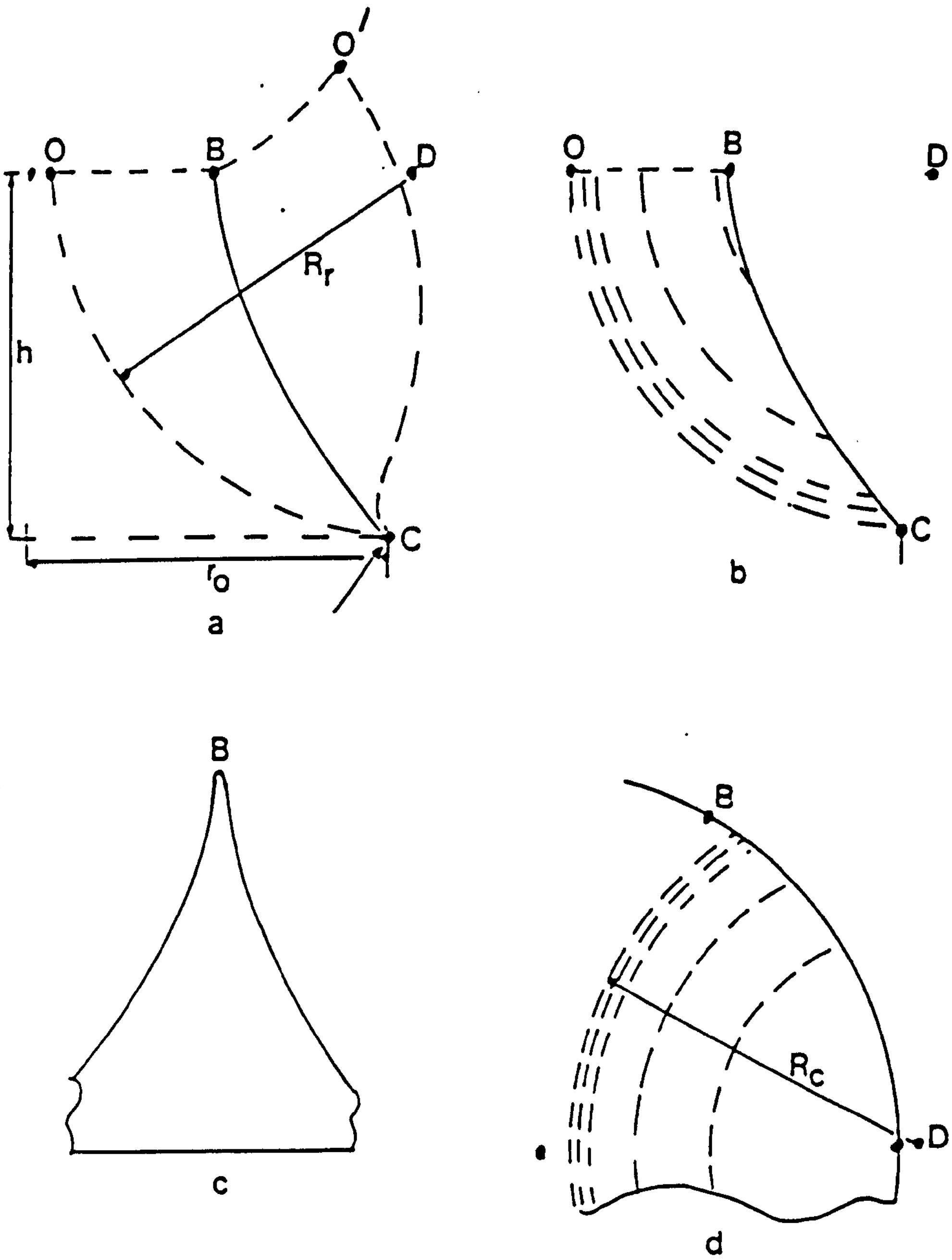

Figure 5.8 Leaflet geometry C

a] Vertical section through the centre line of the leaflet OEC.

b] Vertical section through the closed leaflet.

c] Radial view on the post.

d] Horizontal sections through the closed leaflet.

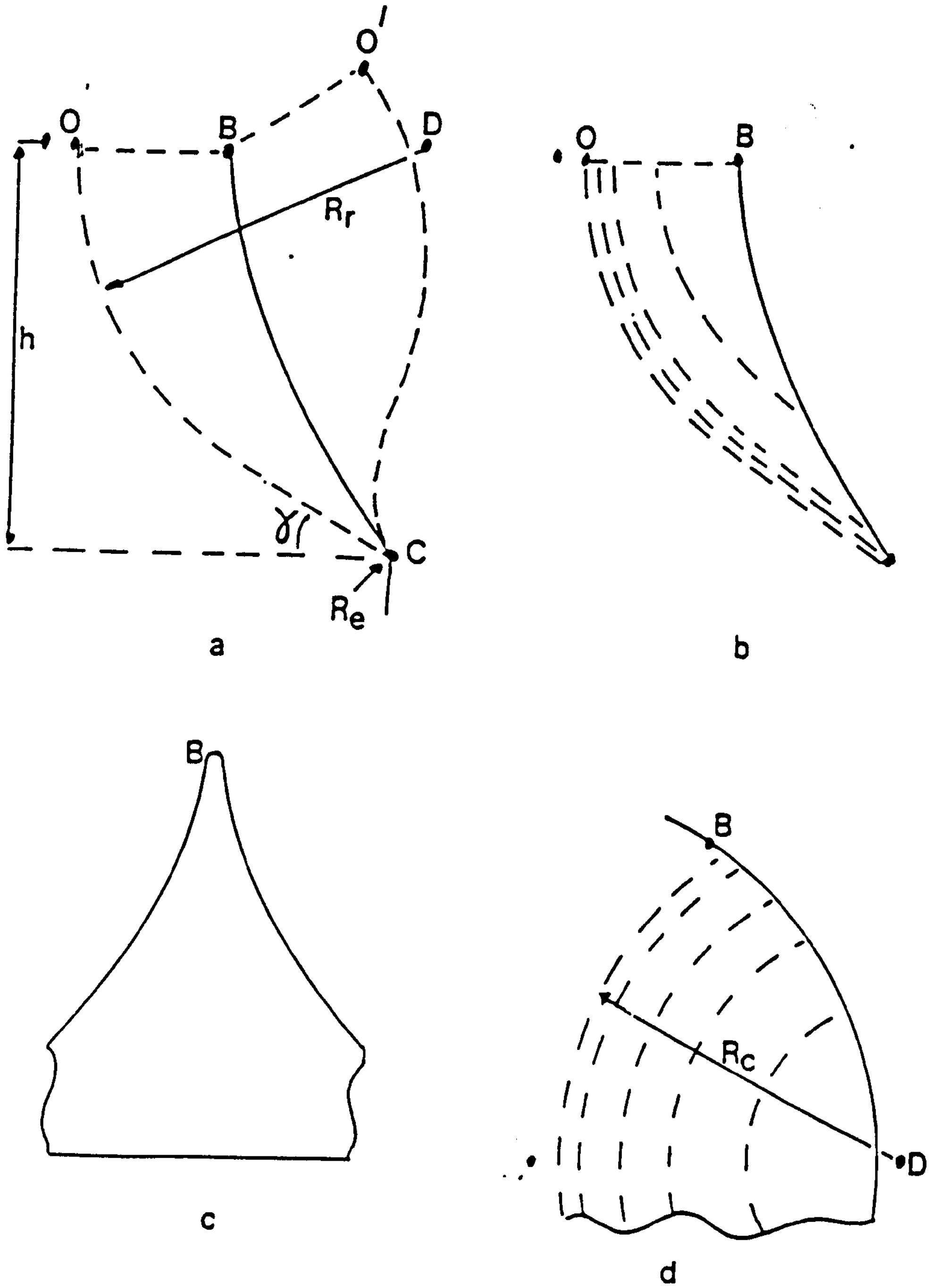

Figure 5.9 Leaflet geometry D.

a] Vertical section through the centre line of the leaflet OE.

b] Vertical sections through the closed leaflet.

c] Radial view on the post.

d] Horizontal sections through the closed leaflets.

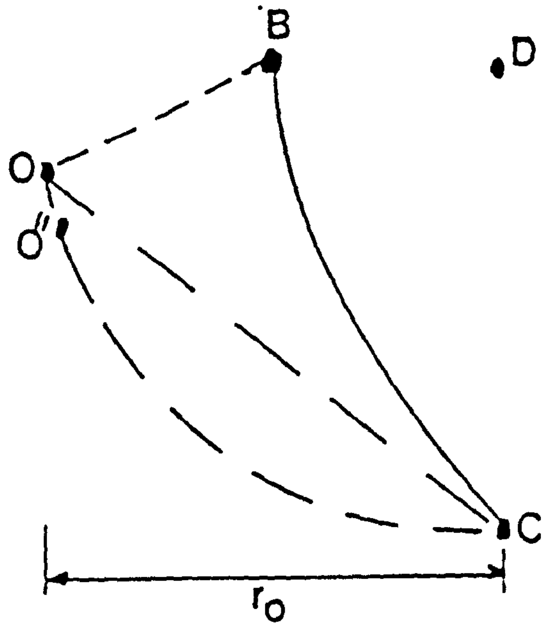

Figure 5.10 Vertical section through a closed leaflet showing the extension of the tissue in a spherical leaflet.

Figure 6.1 Photograph of the inner and outer frame

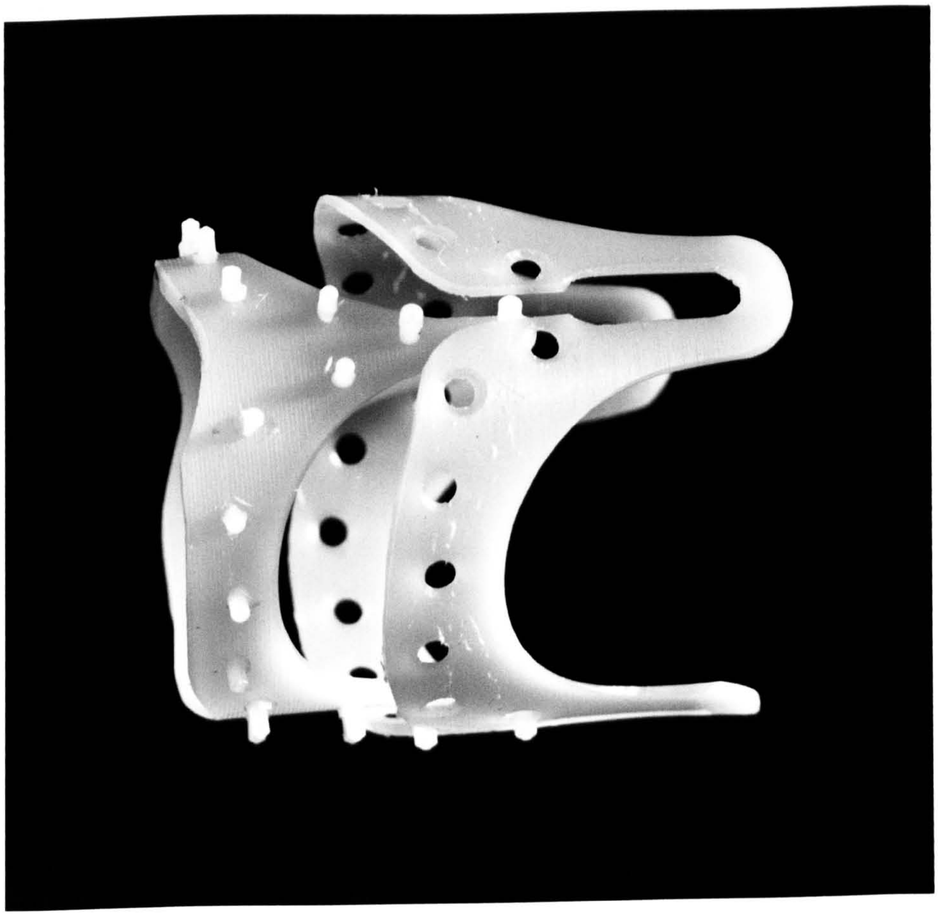

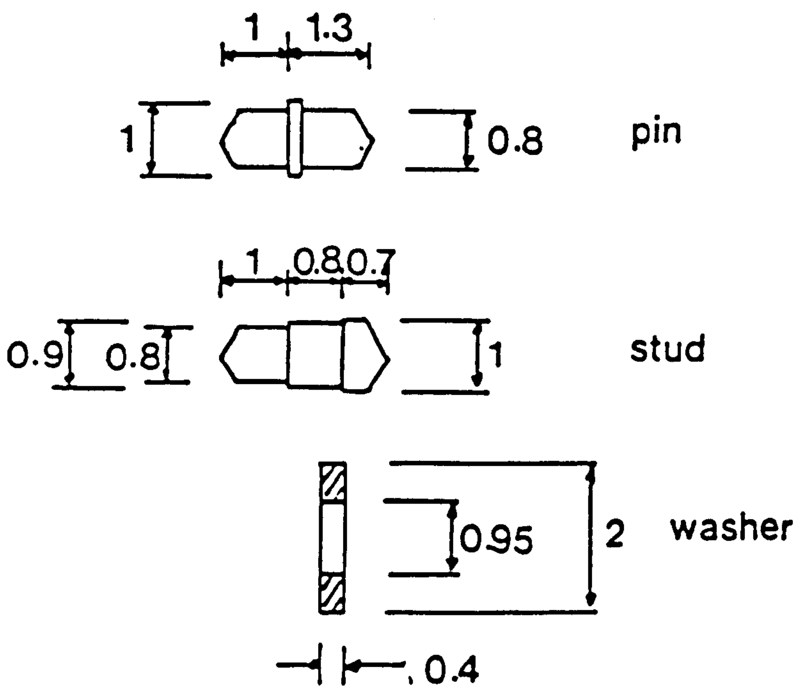

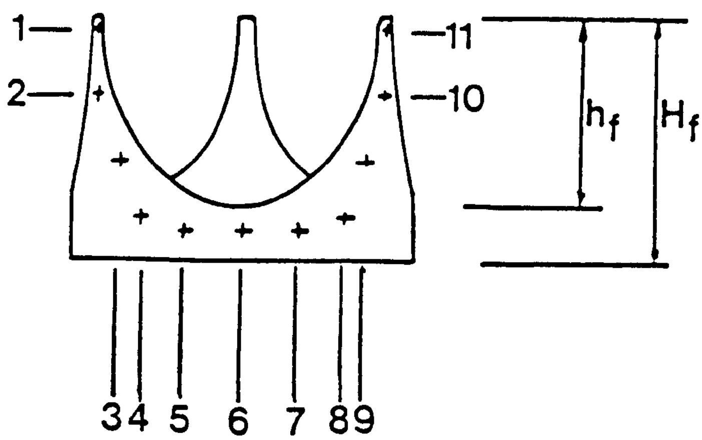

Figure 6.2 Diagram showing the position (above) and dimensions of the pin studs and washers.

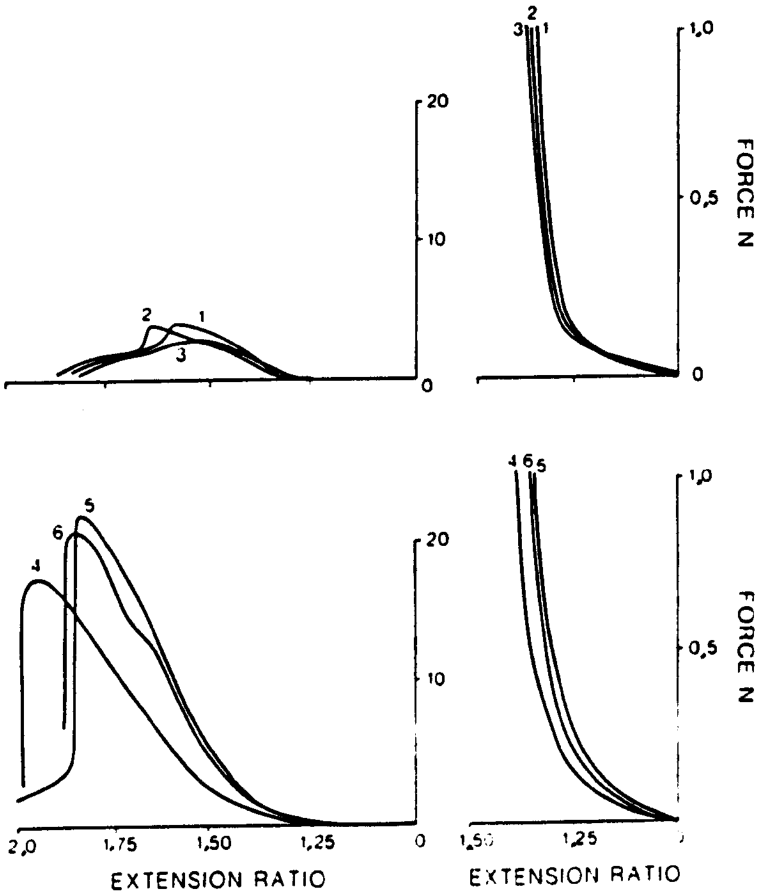

Figure 6.3 Force extension graphs for tissue fixed as a flat sheet.

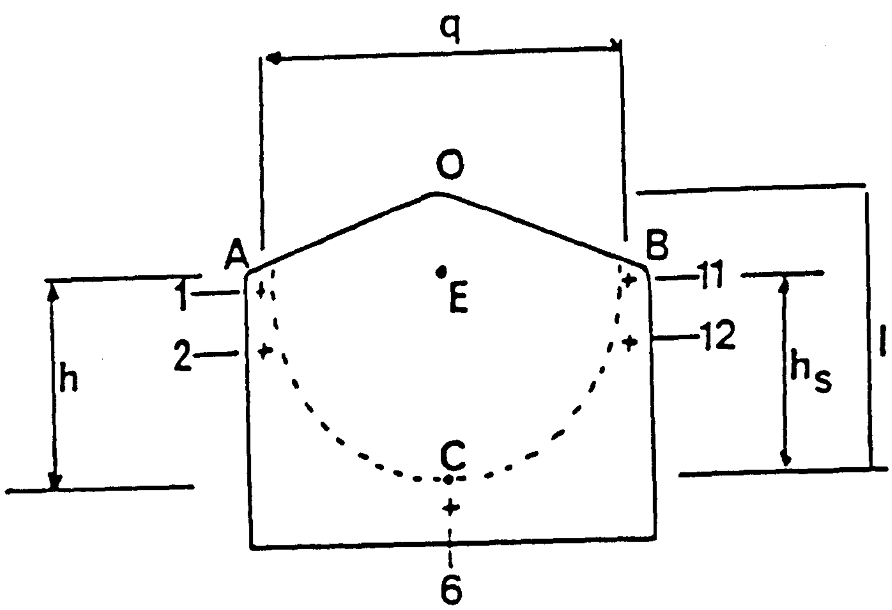

Figure 6.4 Diagram of the leaflet template.

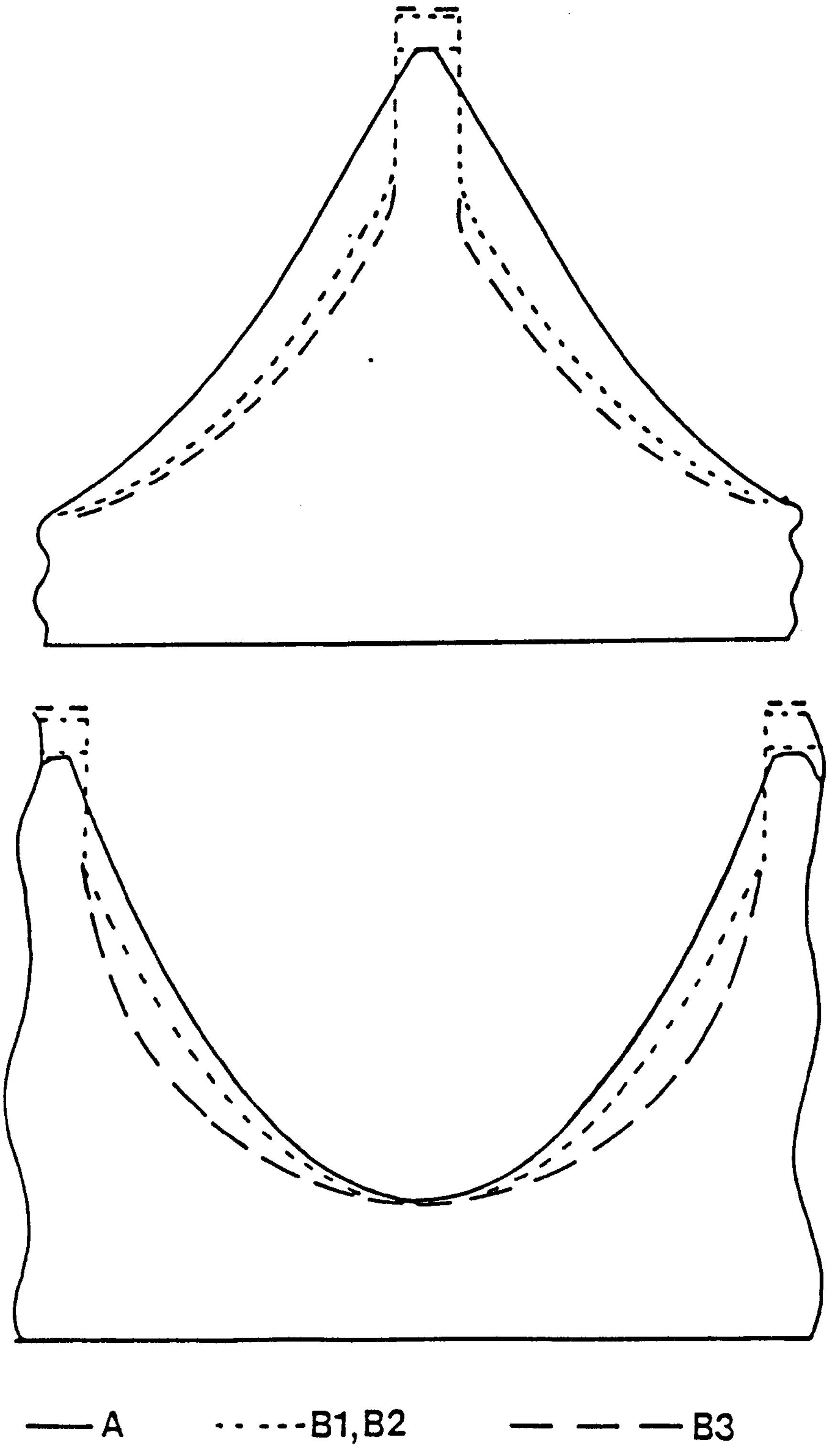

Figure 6.5 Detailed shape of the valve inner frames for configuration A1, B1, B2, B3. A radial view on the post (above) and a radial view on the scallop.

Figure 6.6 Prototype valve configuration A in the function test apparatus showing the open position (above) and the unstable closed position (below)

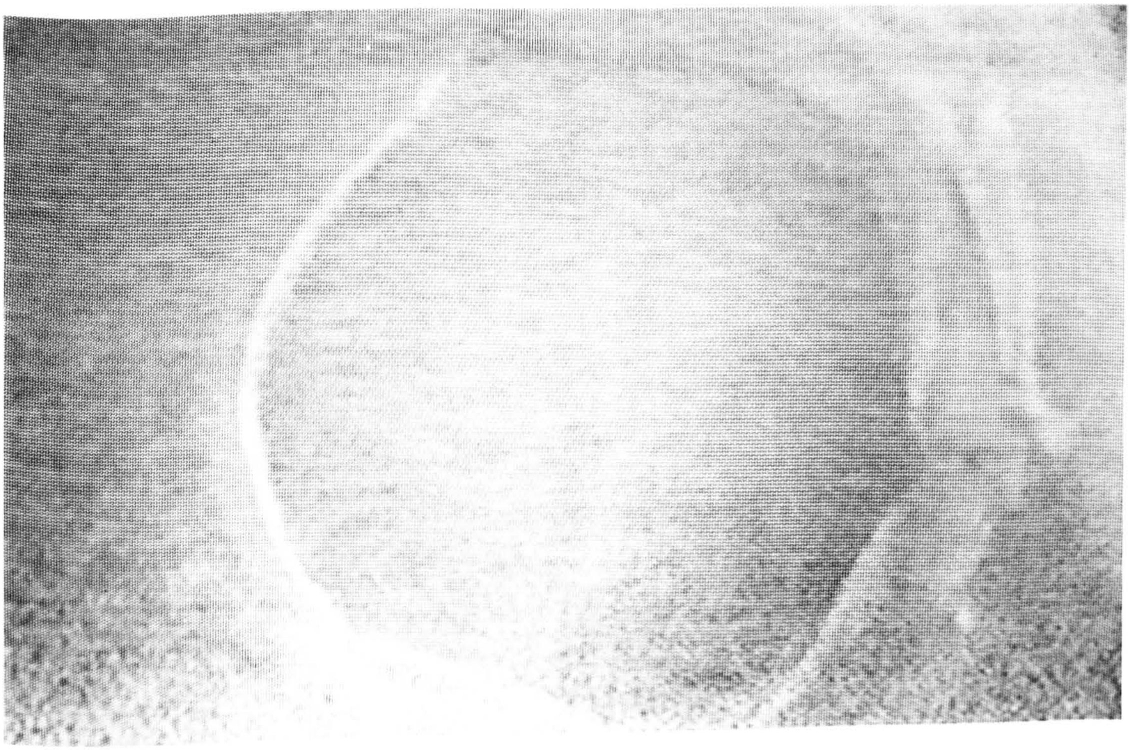

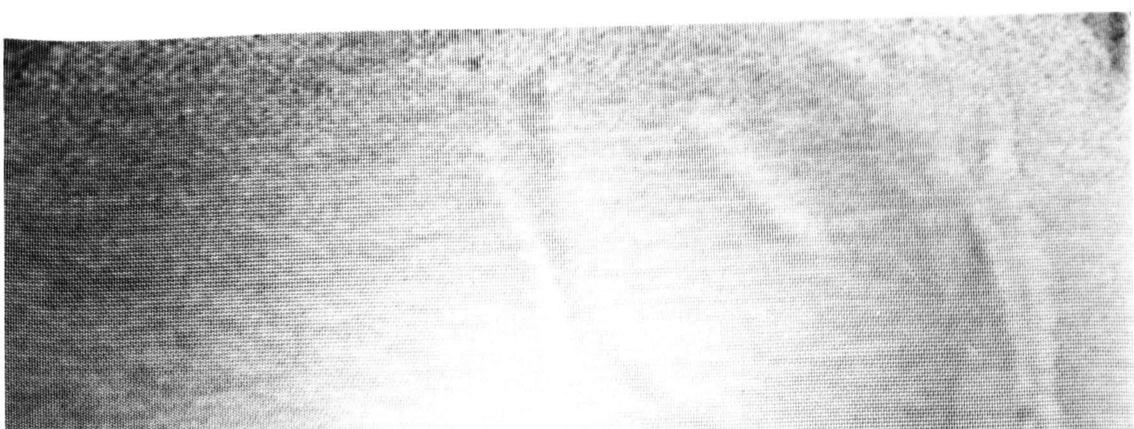

Figure 6.7 Prototype valve configuration B1 in the function test apparatus, showing the open position (above), the unloaded closed position (centre) and the closed position under back pressure (below)

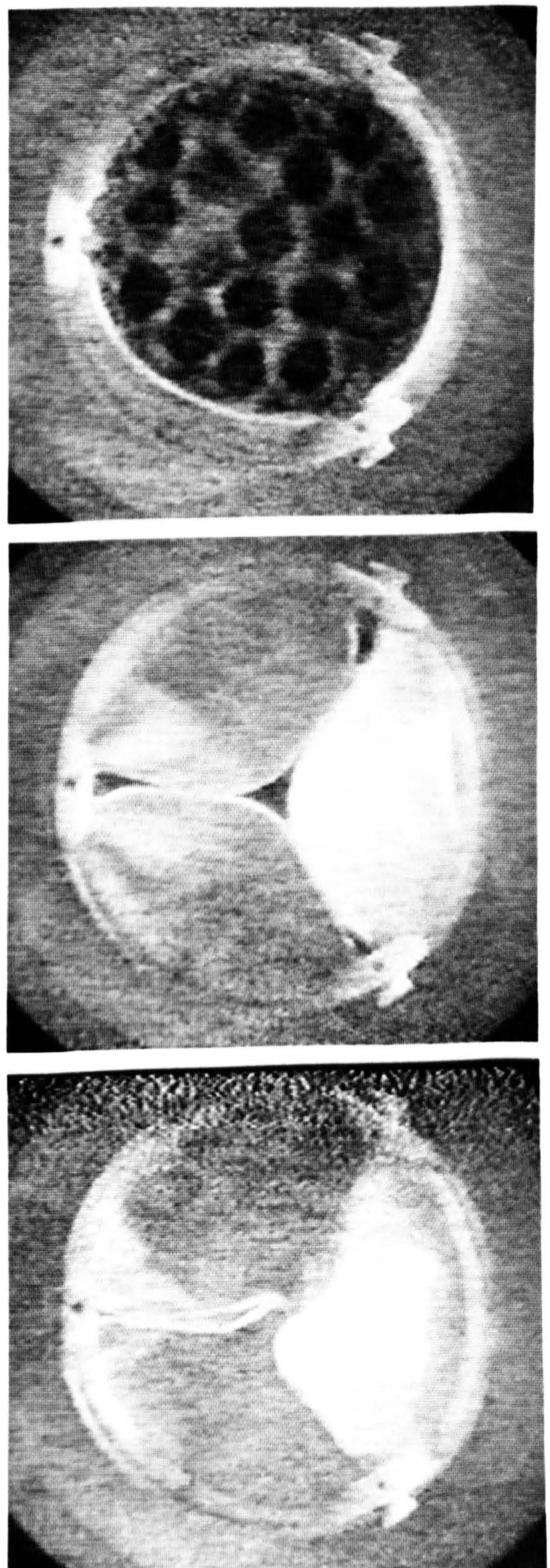

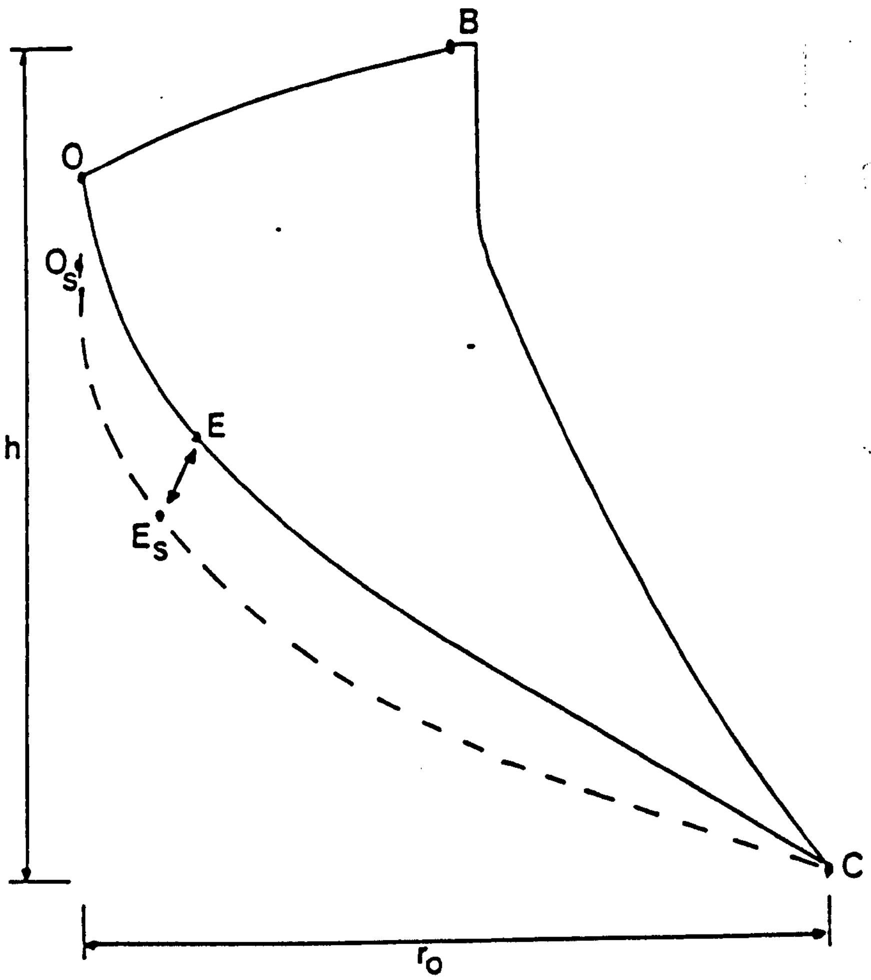

Figure 6.8 A vertical section through the leaflet centre line showing the extension of the leaflet under pressure.

Figure 6.9 Prototype valve configuration B3 in the function test apparatus showing the open position (above), the unloaded closed position (centre) and the closed position under back pressure (below)

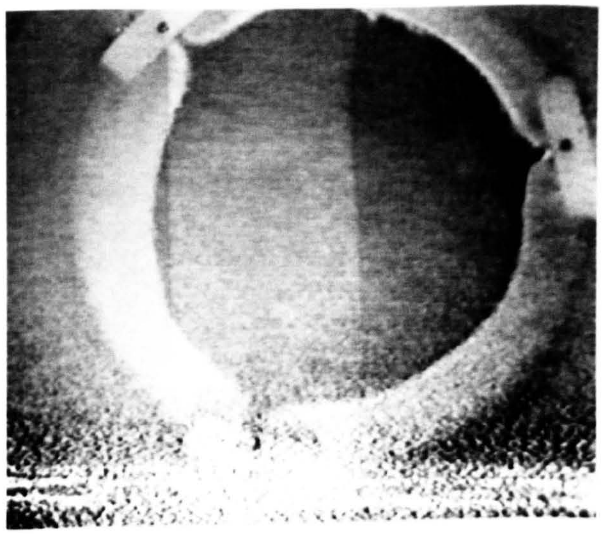

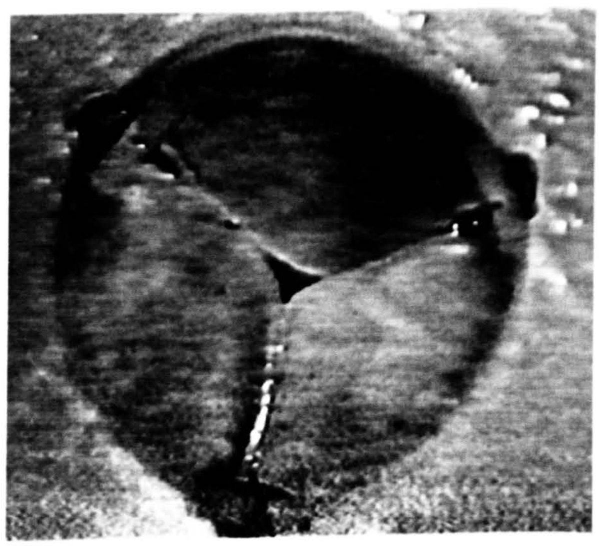

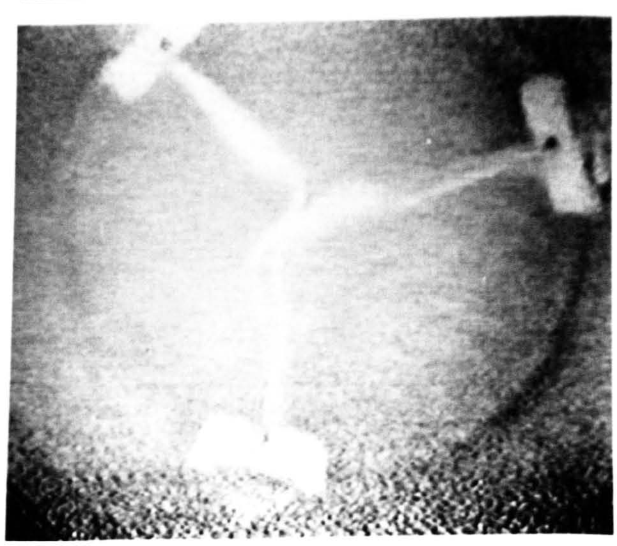

Figure 6.10 Photograph of a size 27 mm mould

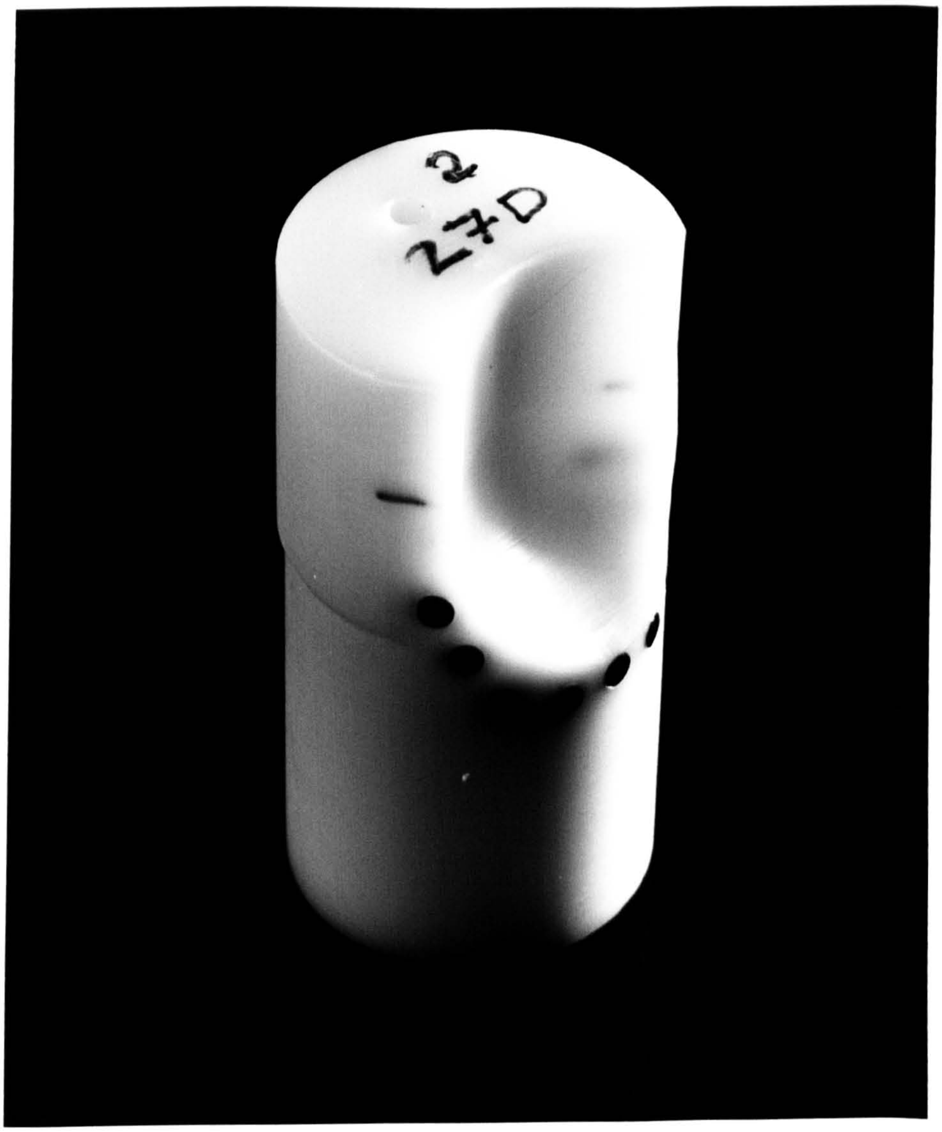
2
27D

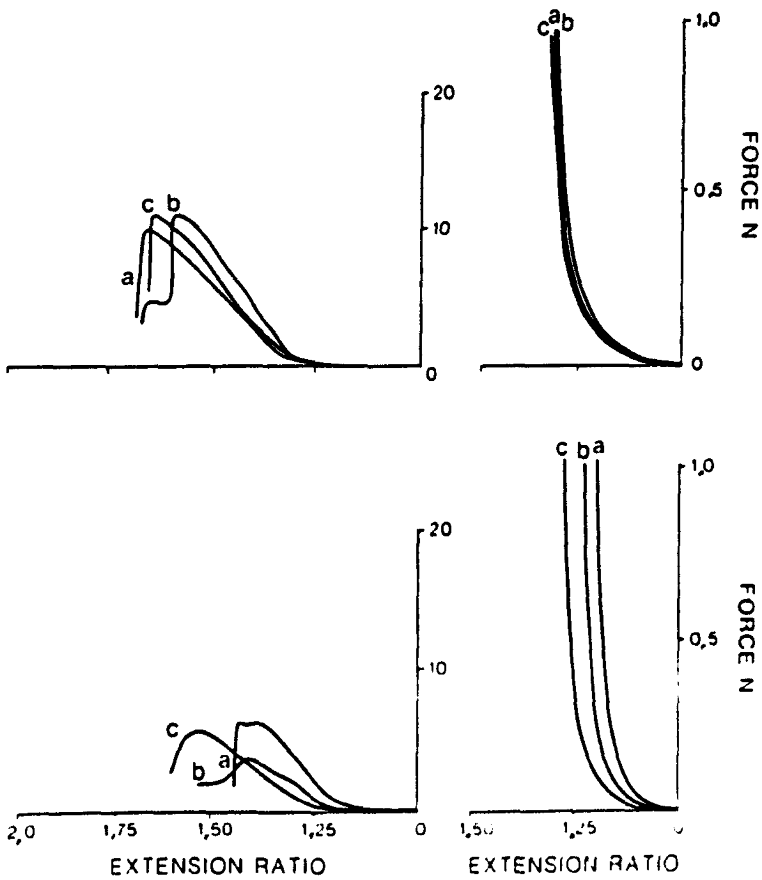

Figure 6.11 Force extension graphs for tissue fixed on a mould.

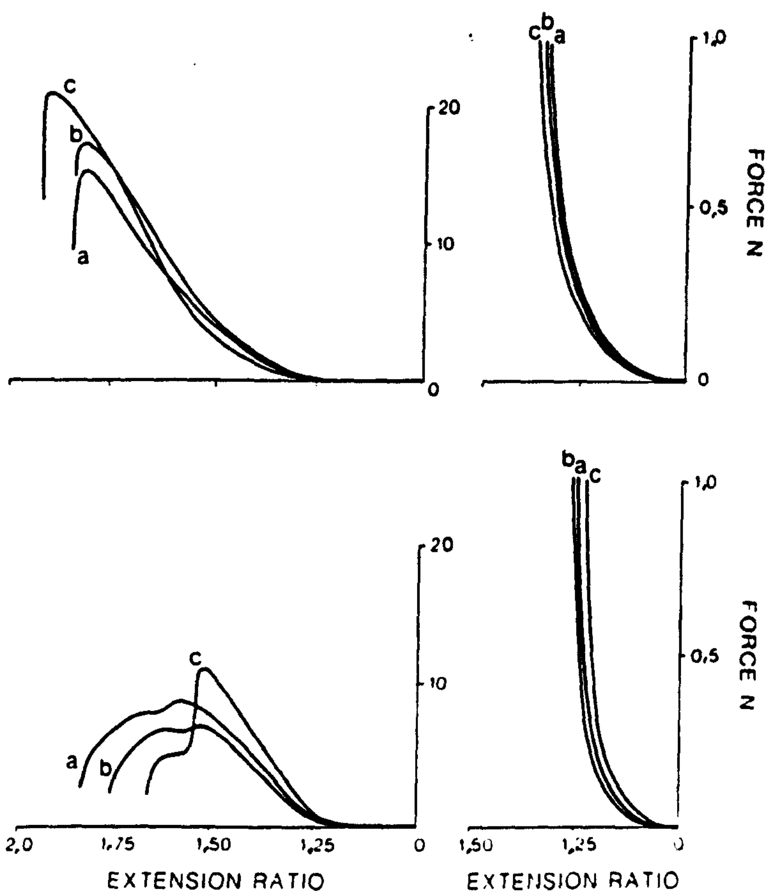

Figure 6.11 Force extension graphs for tissue fixed on a mould.

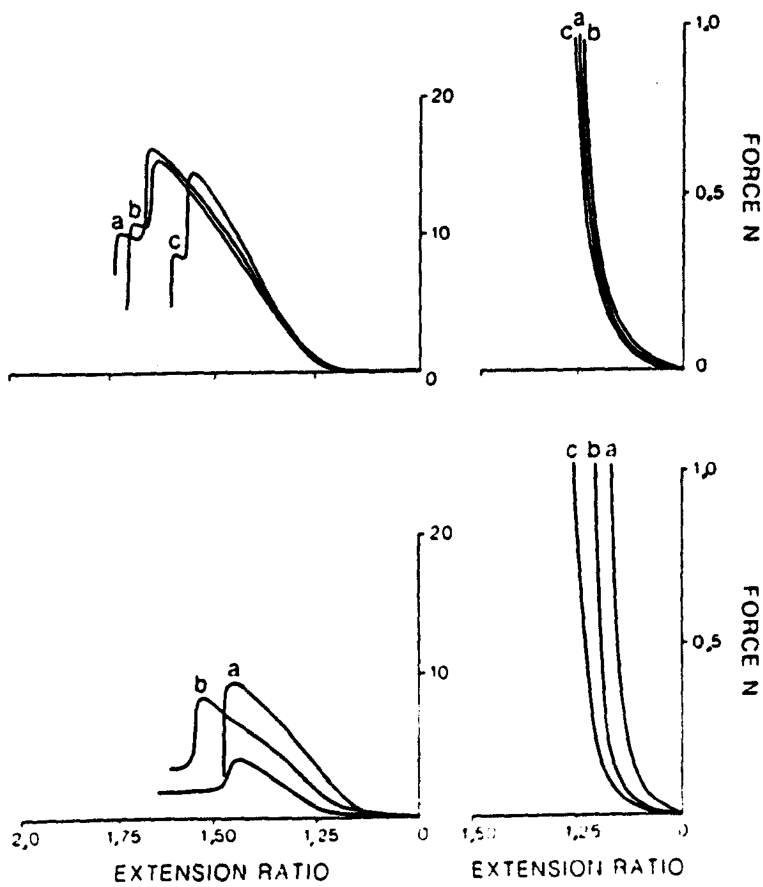

Figure 6.11 Force extension graphs for tissue fixed on a mould.

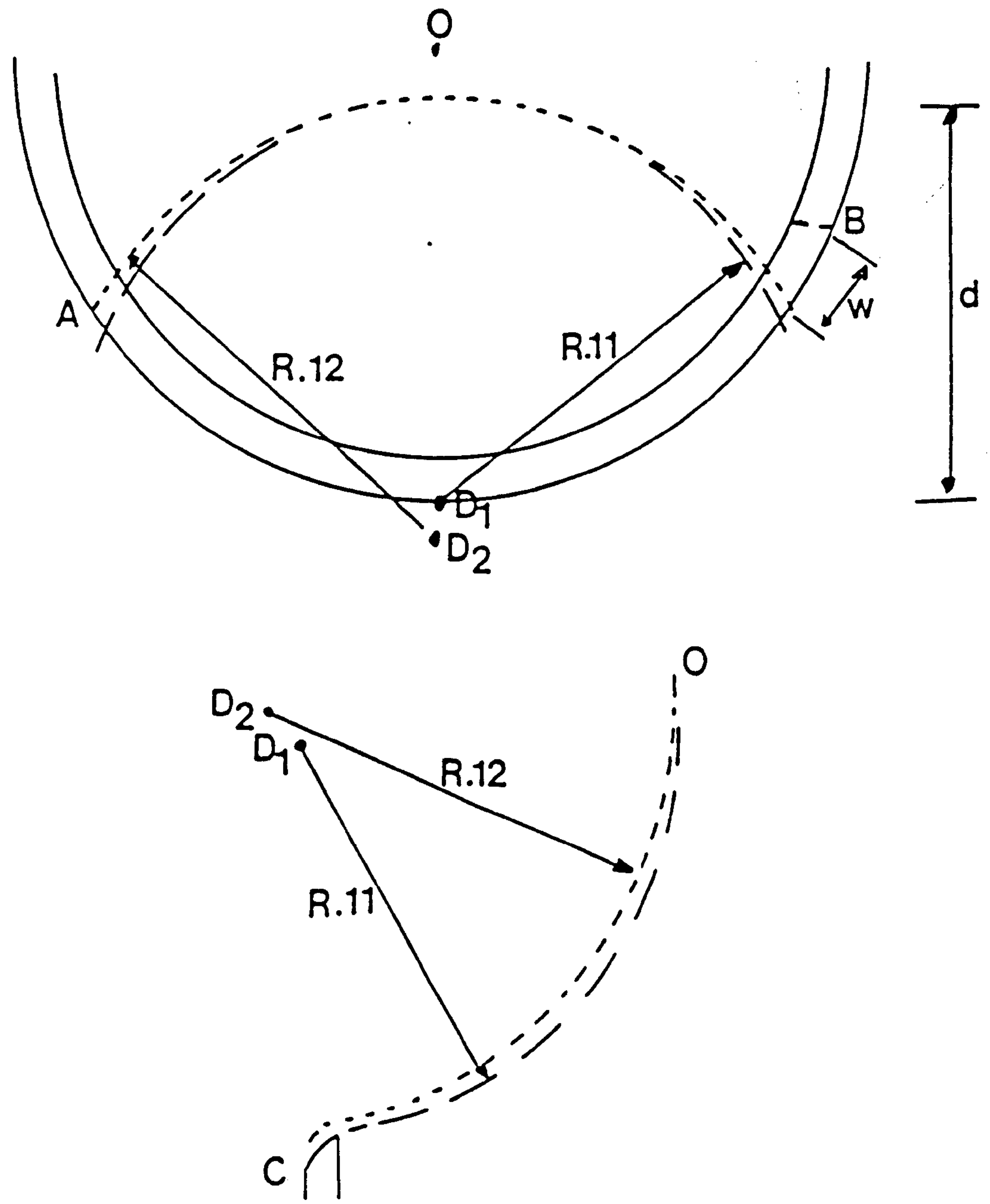

Figure 6.12 Diagram of the leaflet geometries for configurations C1 and C2, showing a horizontal section and a vertical section through the leaflets.

Figure 6.13 Prototype valve configuration C in the function test apparatus showing the open position (above), the unloaded closed position (centre) and the closed position under a back pressure (below)

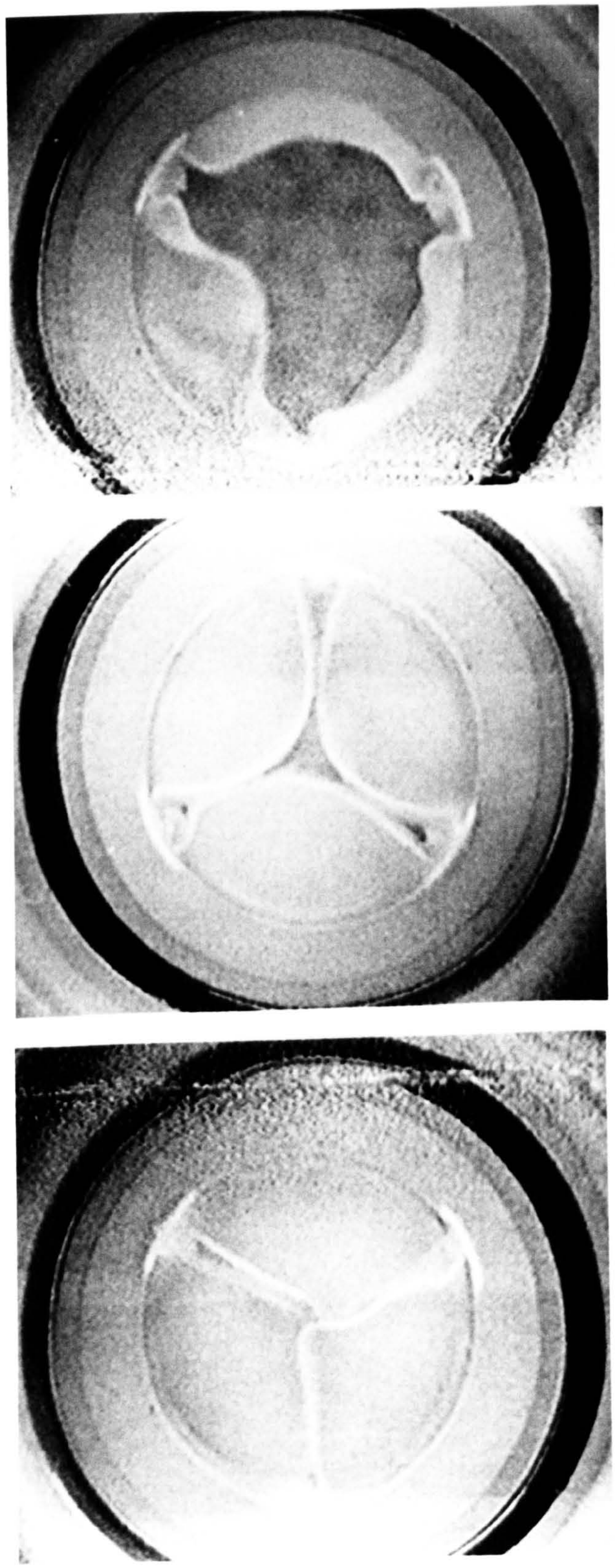

Figure 6.14 Prototype valve configuration D1 in the function test apparatus, showing a] the open position, b] the unloaded closed position, c] the closed position under pressure, and d] the closed position under pressure (side view)

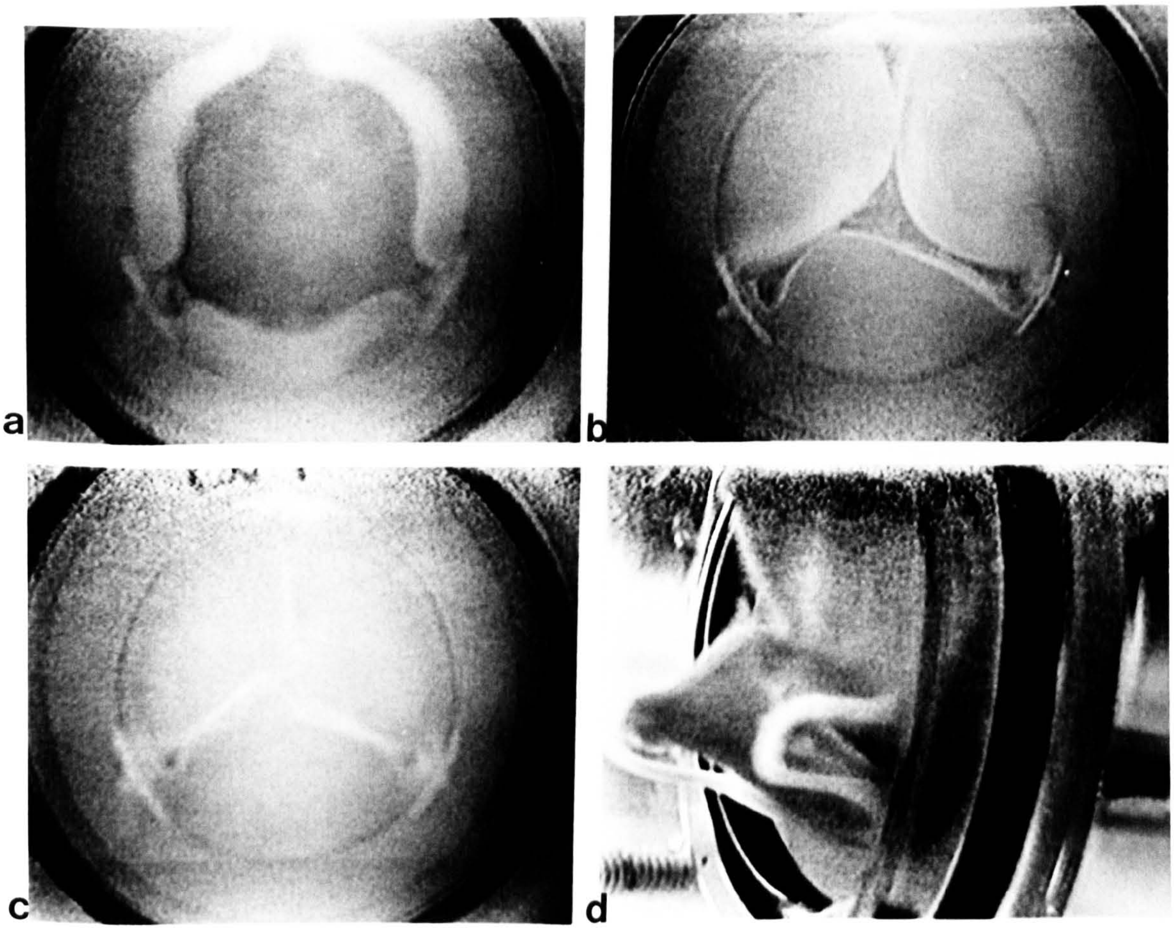
a
b
c
d

Figure 6.15 Prototype valve configuration D2 in the function test apparatus showing a] the open position, b] the closed unloaded position, c] the closed position under back pressure, and d] the closed position under back pressure (side view)

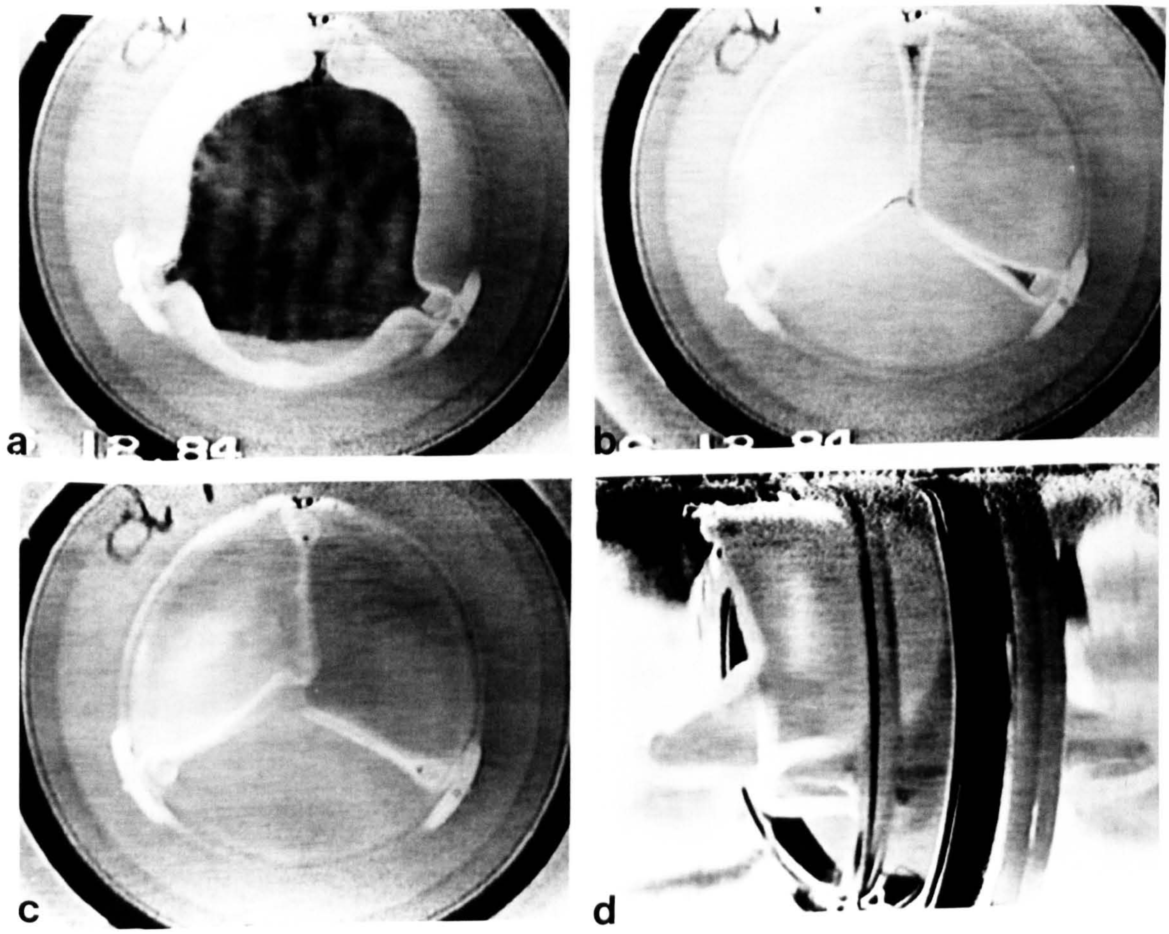
a
b
c
d

Figure 7.1 A cloth-covered outer frame

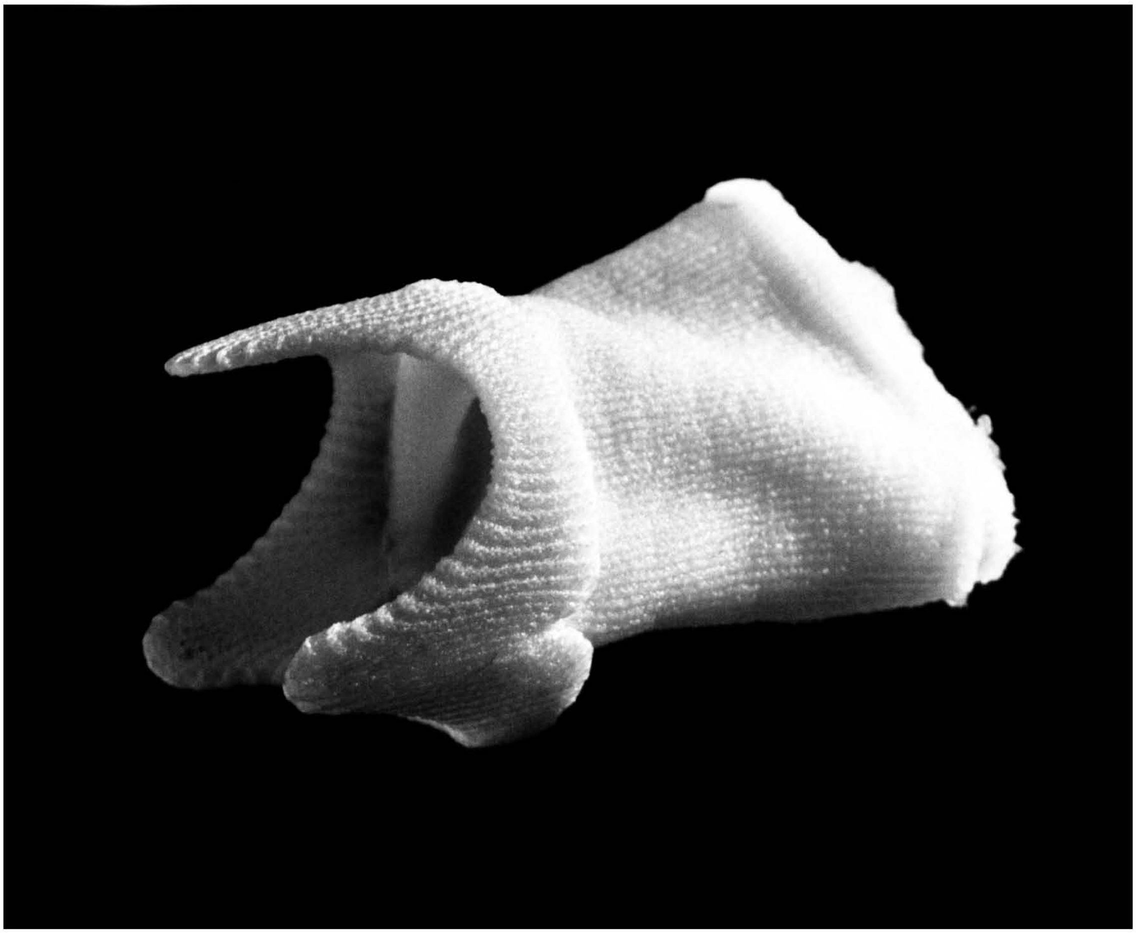

Figure 7.2 A pericardial covered inner frame

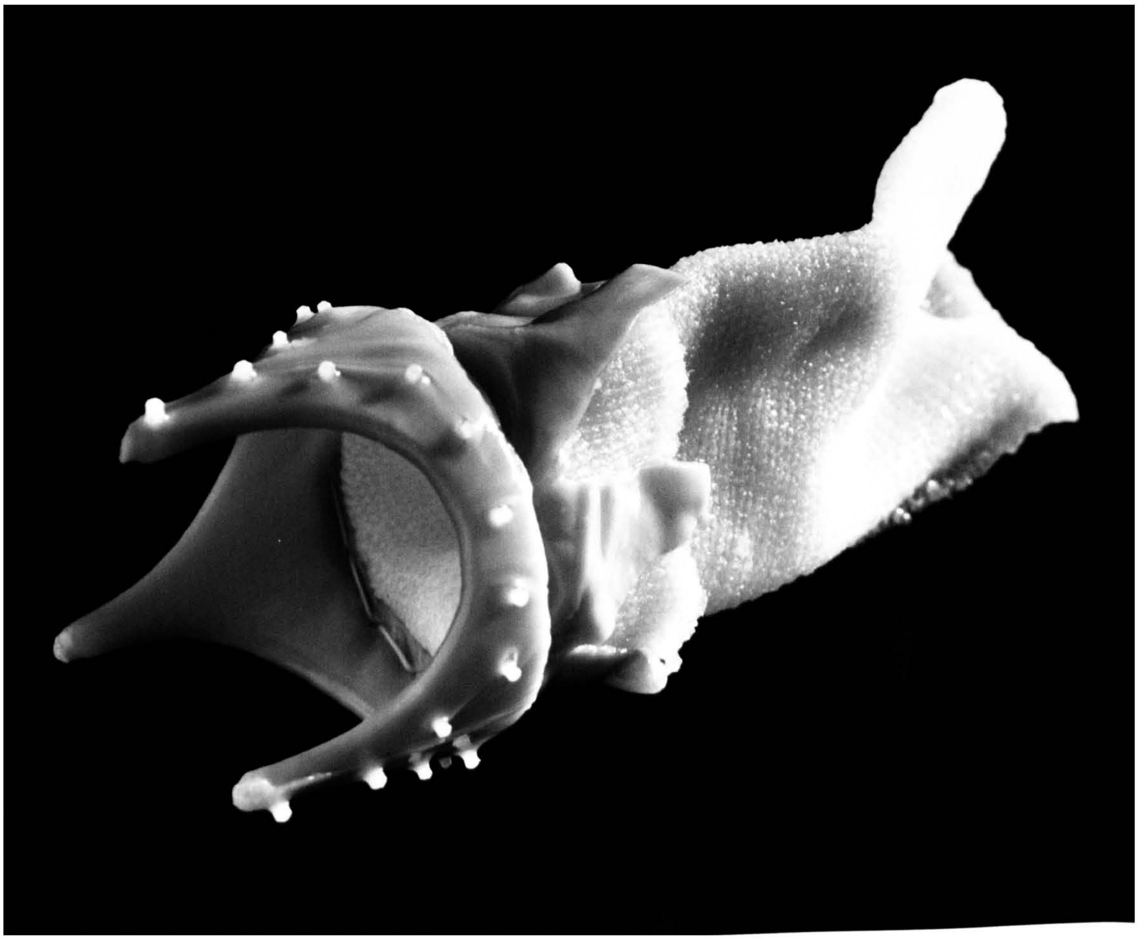

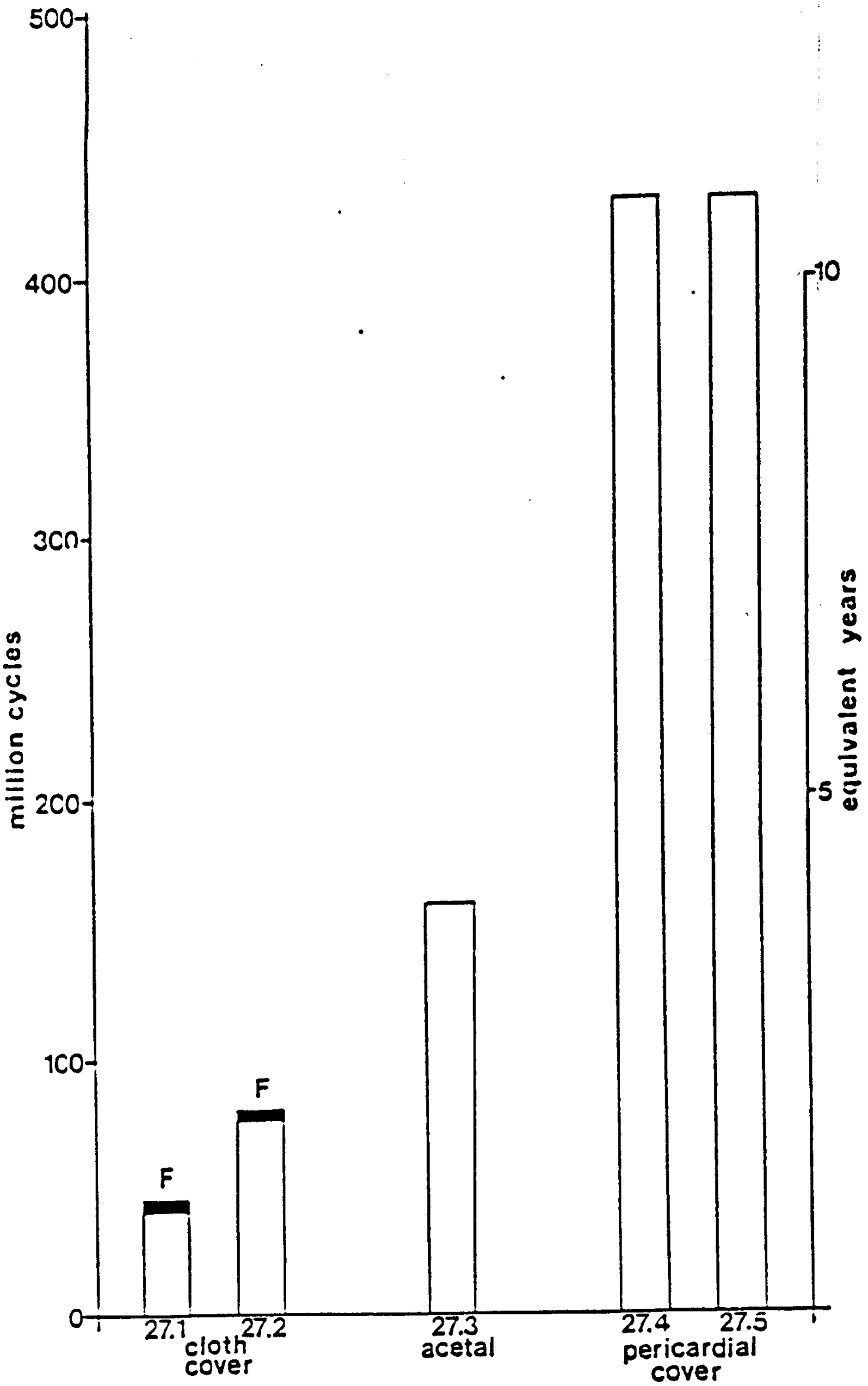

Figure 7.3 Fatigue test results for prototype valves with different frame coverings.

Figure 7.4 Failed valves 27.1 (above) and 27.2 (below) with cloth-covered frames after fatigue tests

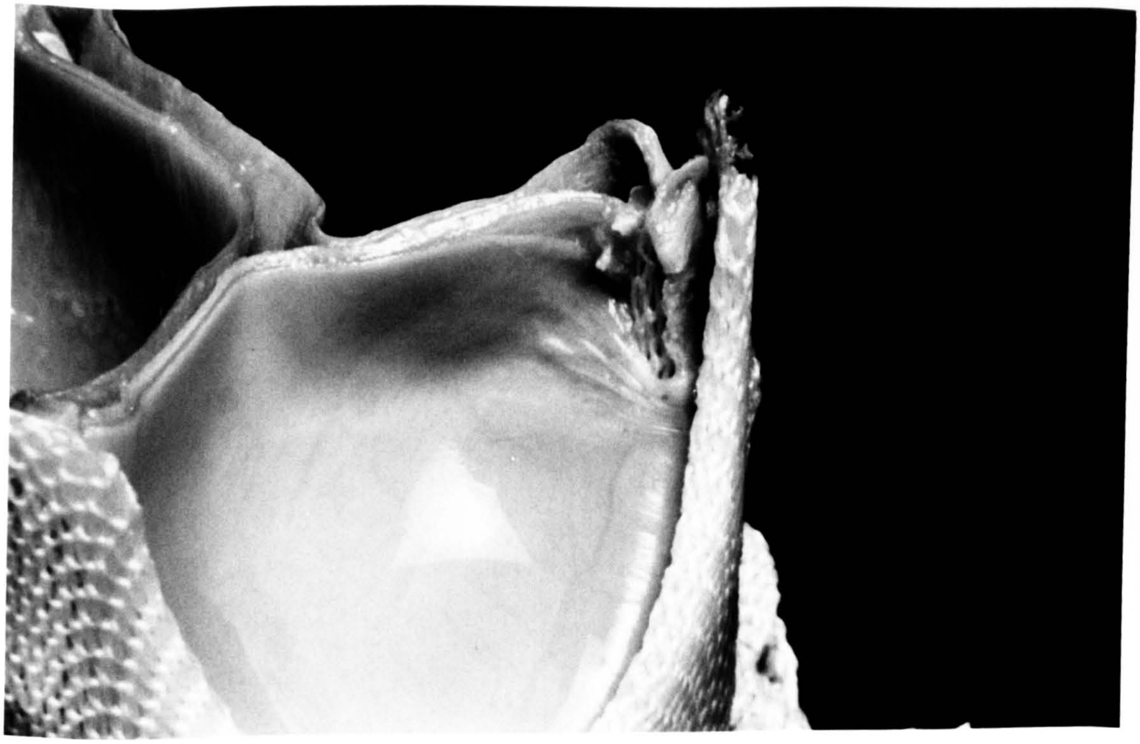

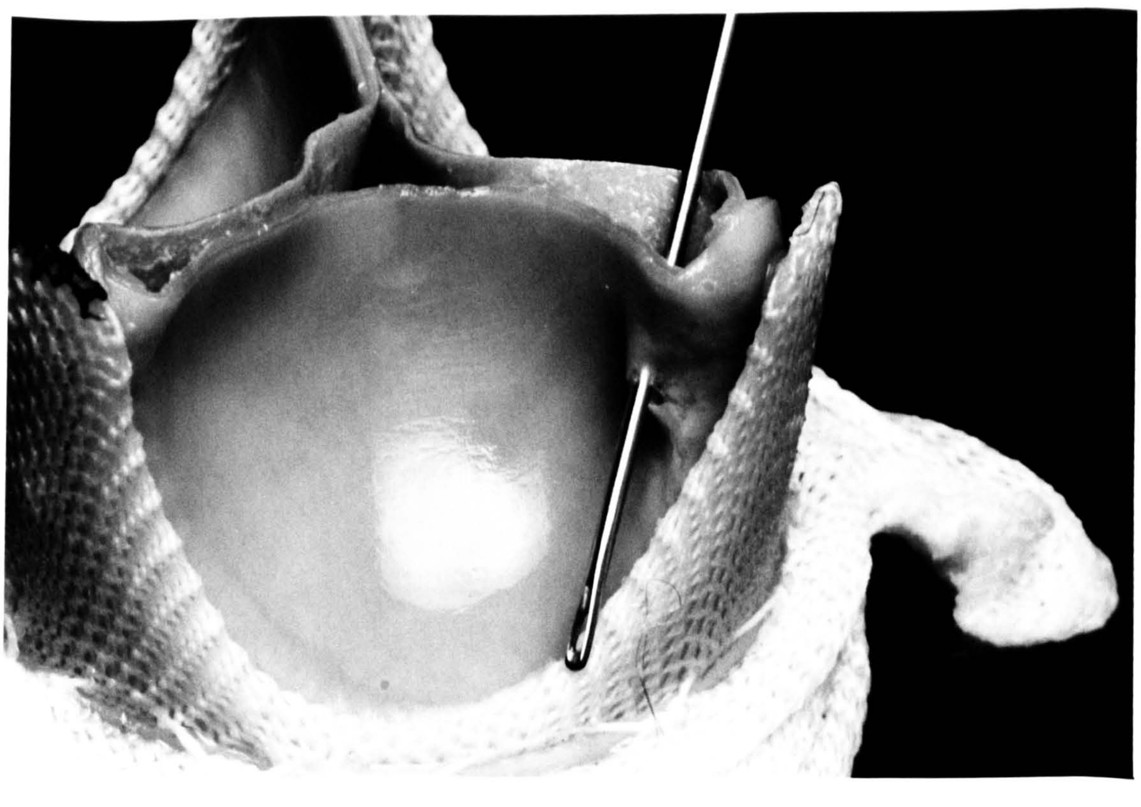

Figure 7.5 Transilluminated leaflets taken from valve 27.1 with a cloth-covered frame (above) and valve 27.4 with a pericardial-covered frame (below)

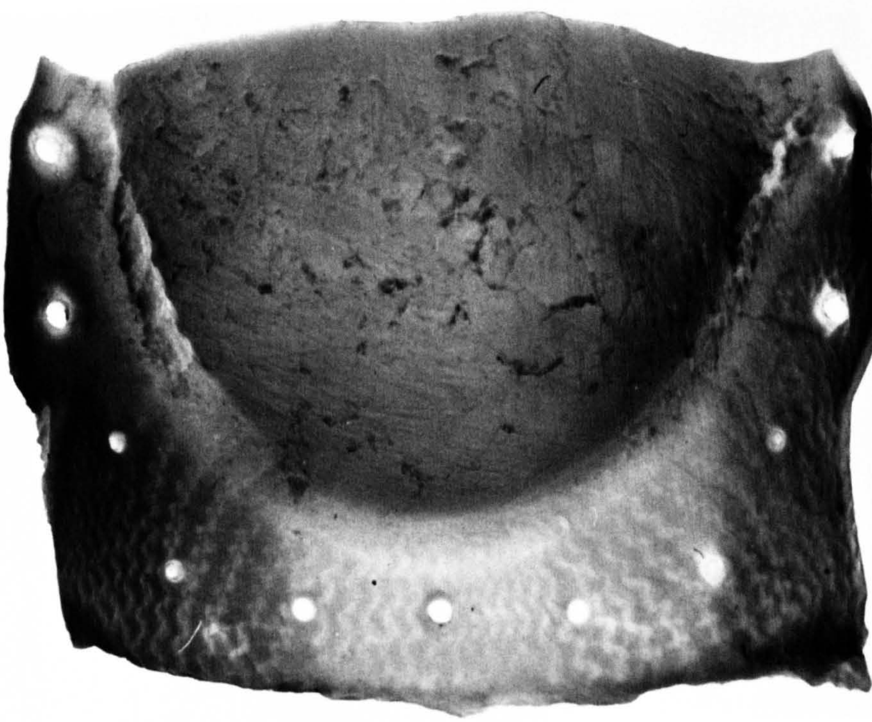

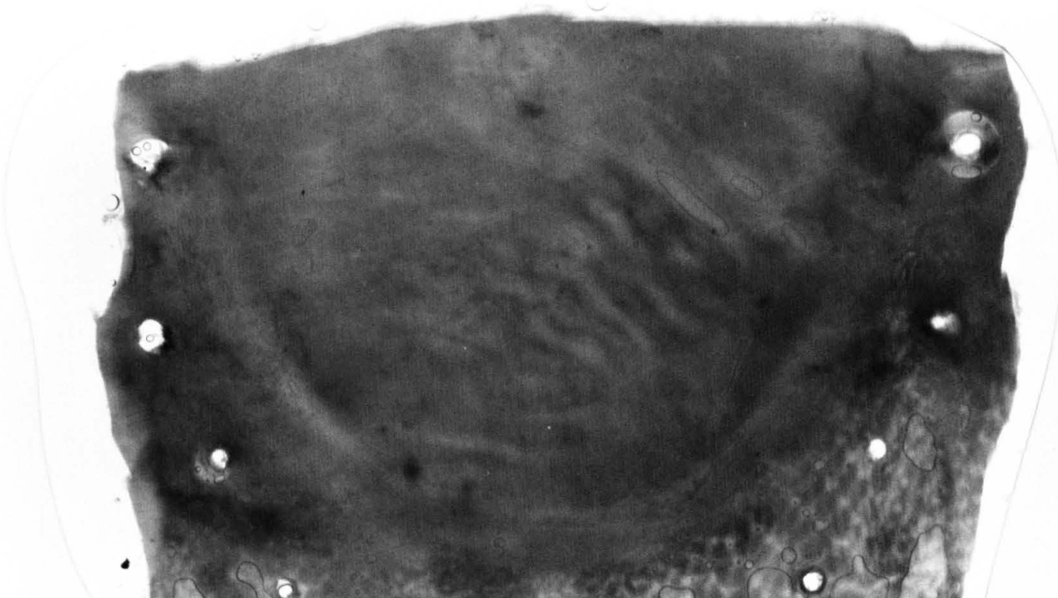

Figure 7.6 Valves 27.4 (above) and 27.5 (below) with pericardial covered frames after 430 million cycles on the fatigue tester

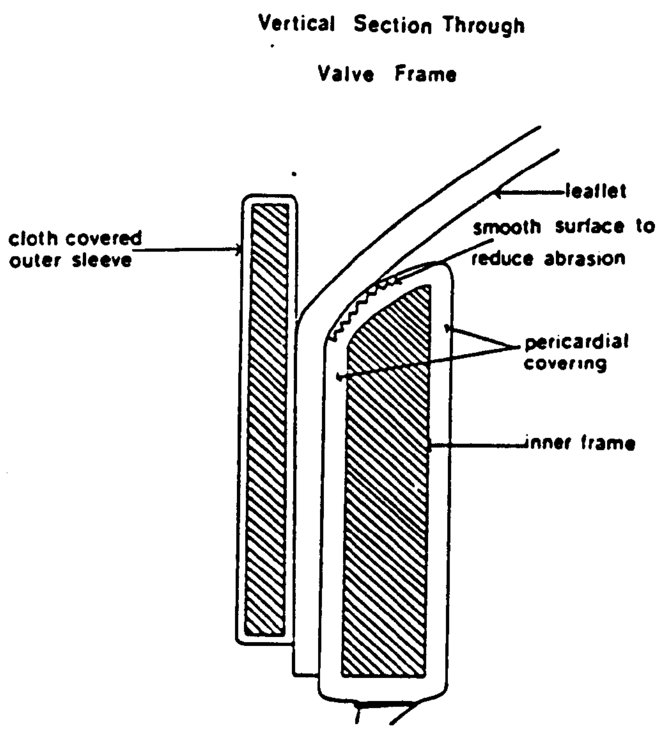

Figure 7.7 A vertical section through the valve frames at the base of the scallop.

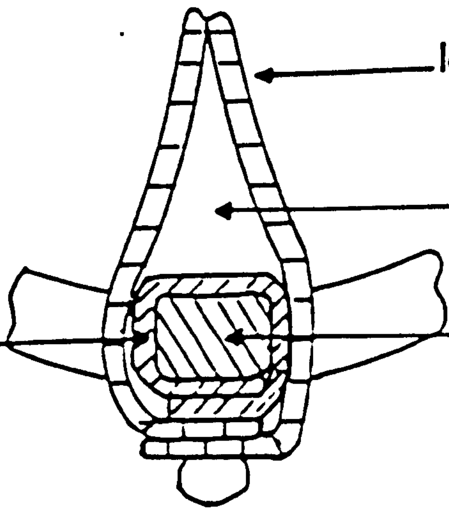

Figure 7.8 A horizontal section through the leaflets at the top of the post showing the space between the leaflets.

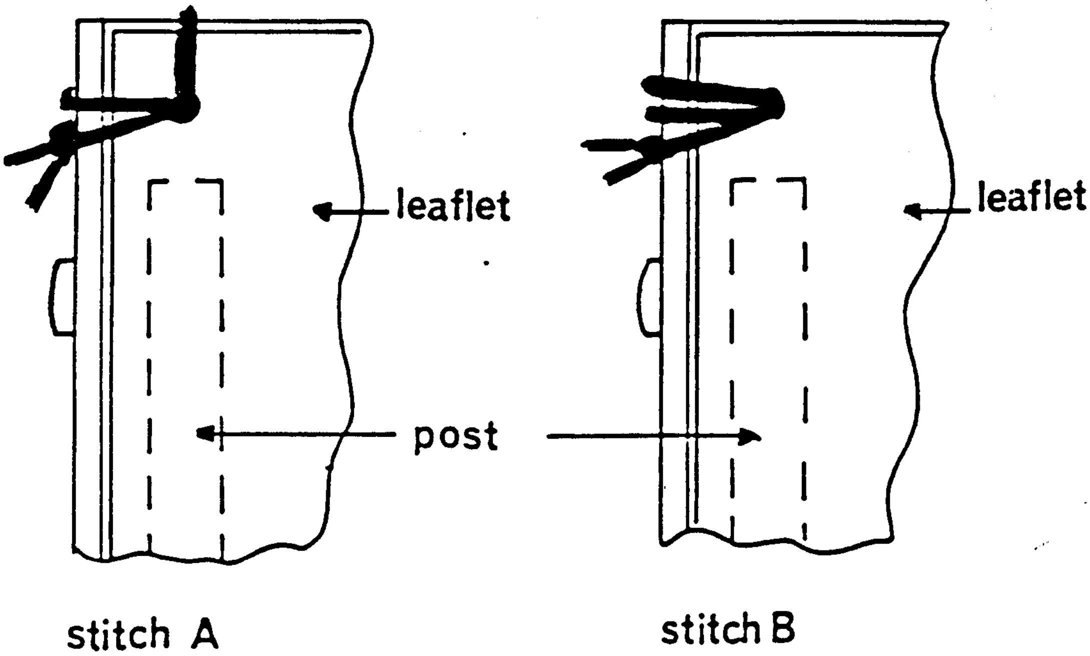

Figure 7.9 Two stitch configurations used to seal the leaflets above the top of the post.

Figure 7.10 Closed valves under back pressure in the function test apparatus without stitches at the top of the posts (above) and with stitches at the top of the posts (below)

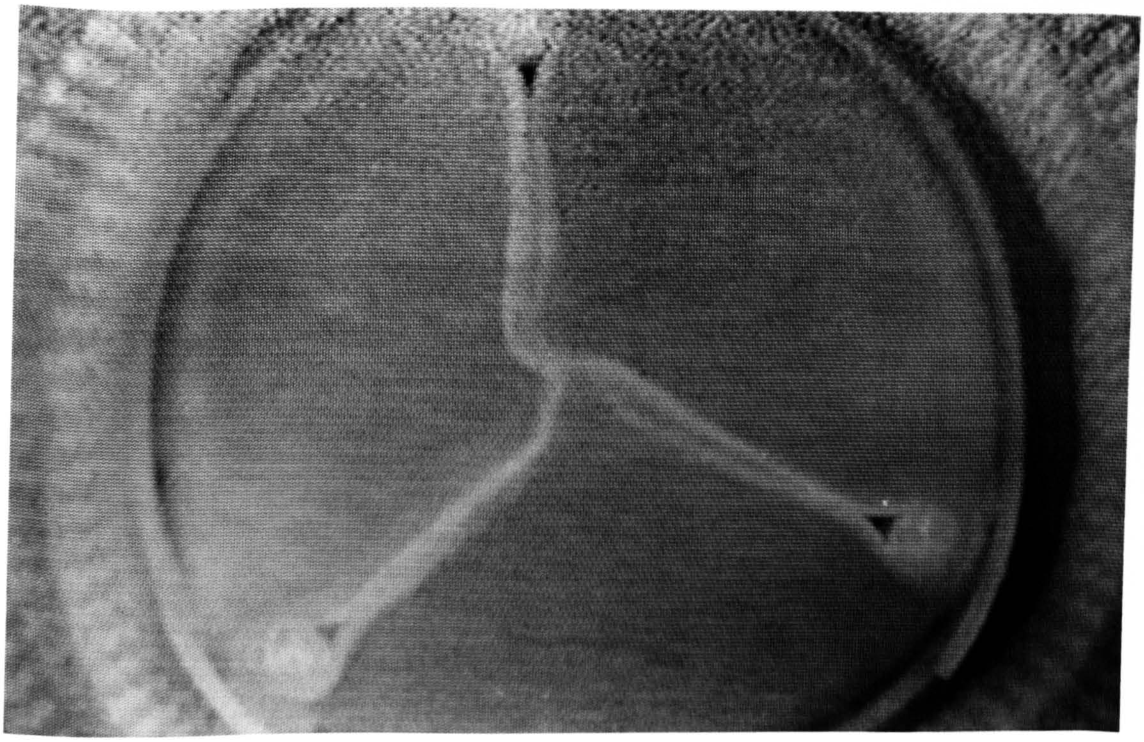

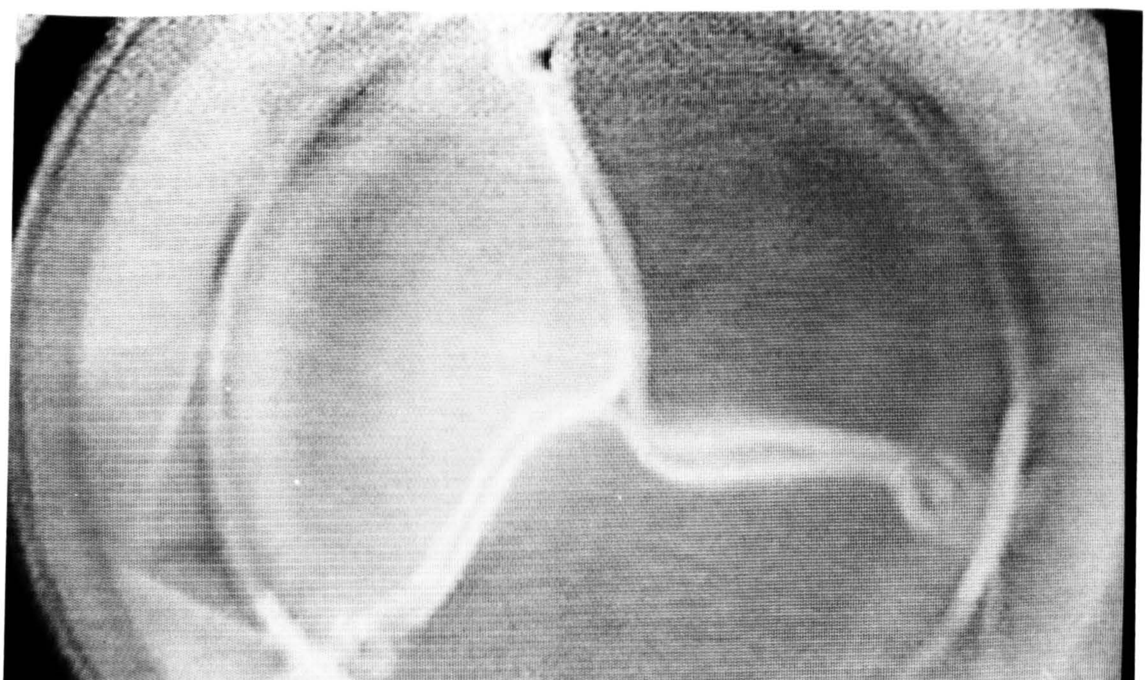

Figure 7.11 An open valve with stitches at the top of the posts in the function test apparatus

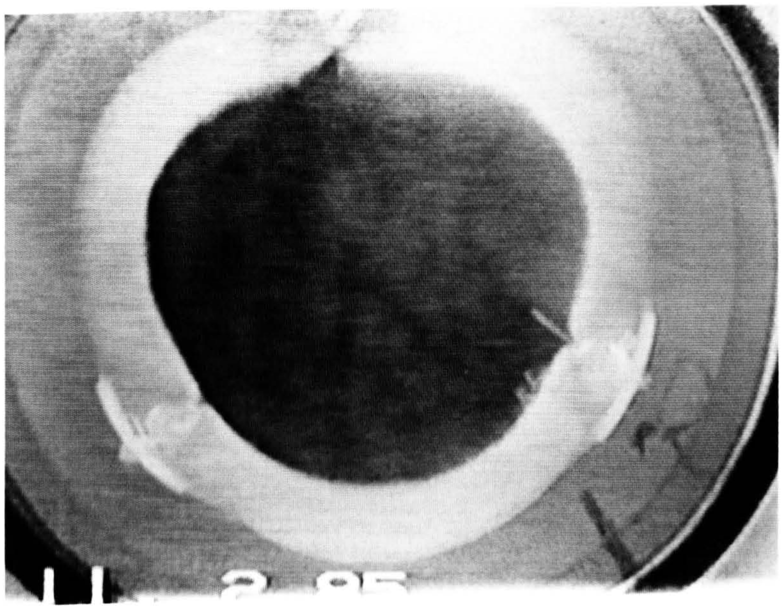

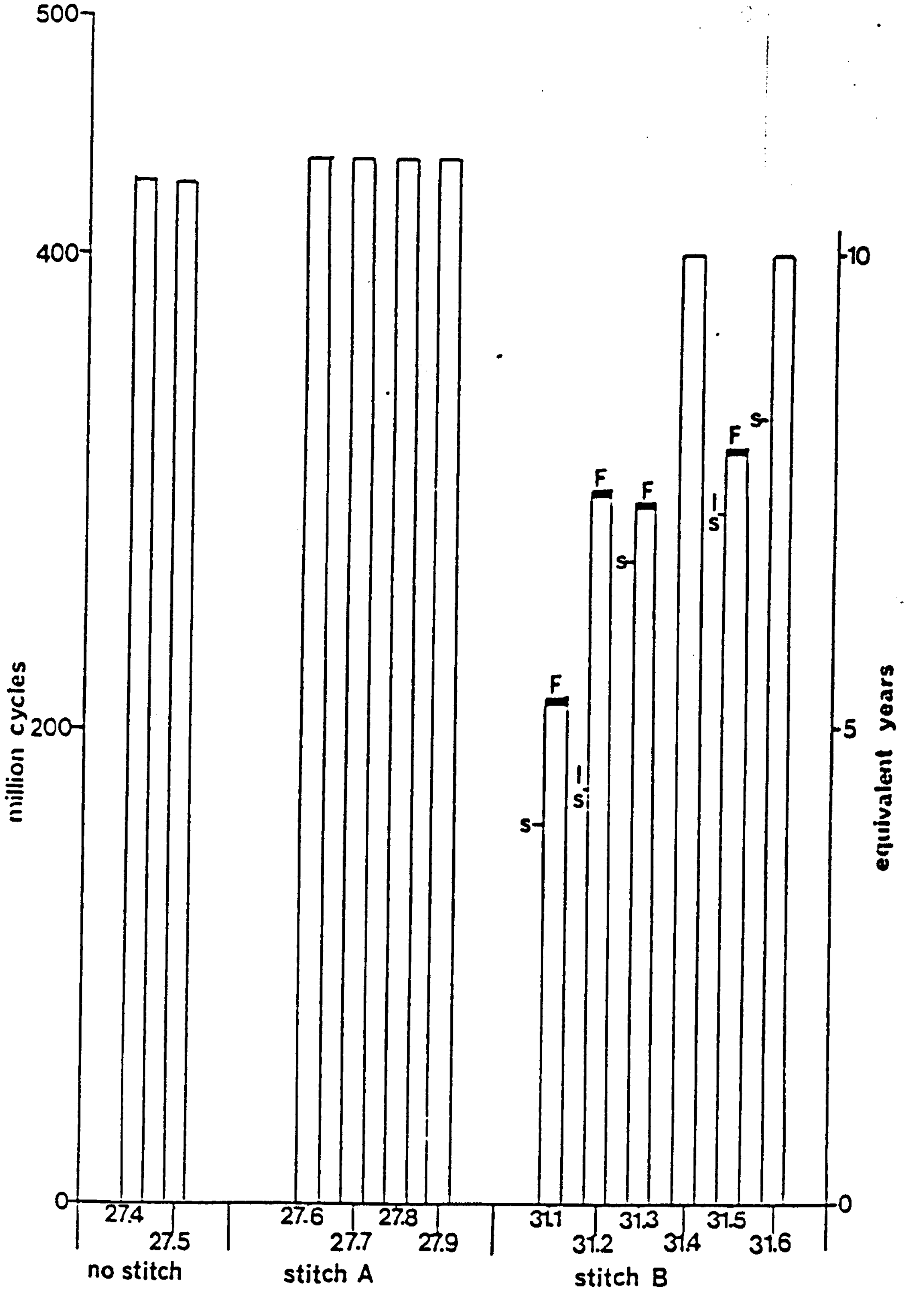

Figure 7.12 Results of accelerated fatigue tests on two valves without stitches, four valves with stitch configuration A and six valves with stitch configuration B.

Figure 7.13 Valves 27.6 to 27.9 (a to d) after 440 million cycles in the fatigue tester

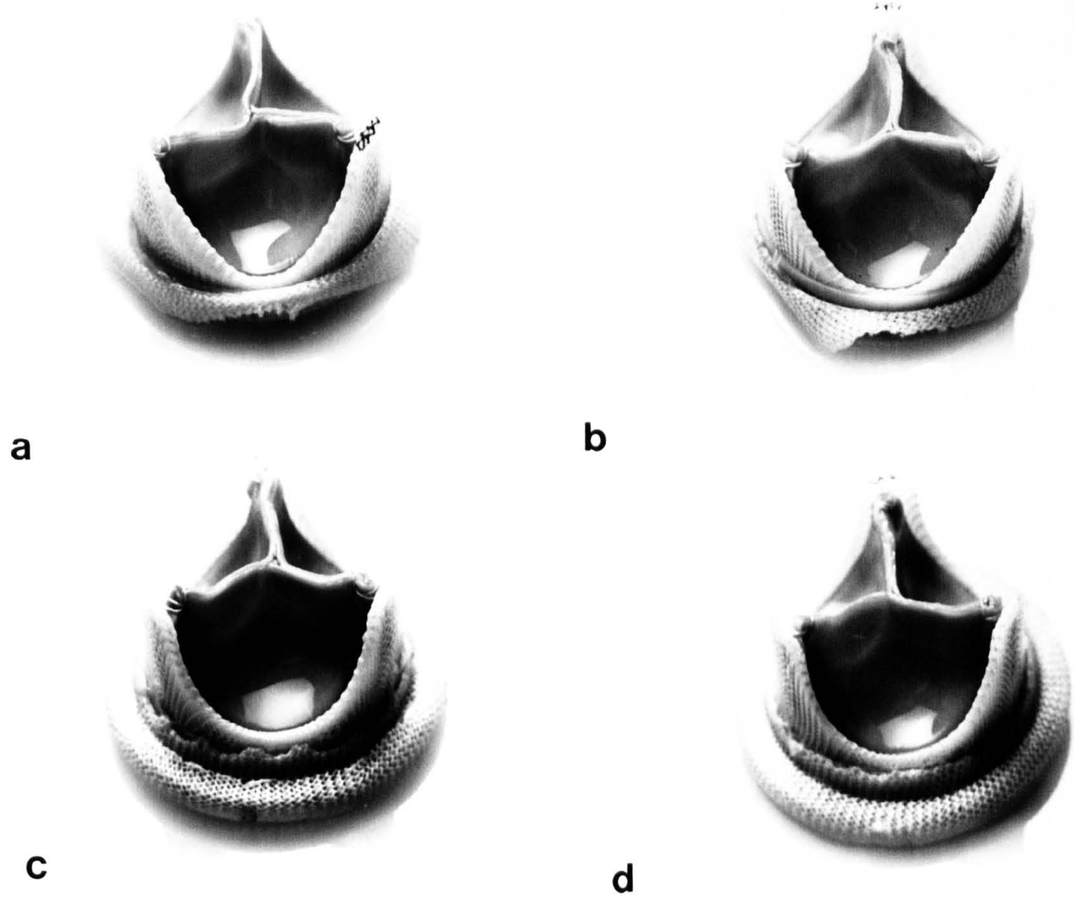
a
b
c
d

Figure 7.14 Valve 31.1 (above) and valve 31.3 (below) with stitch configuration B after 160 and 270 million cycles in the fatigue tester

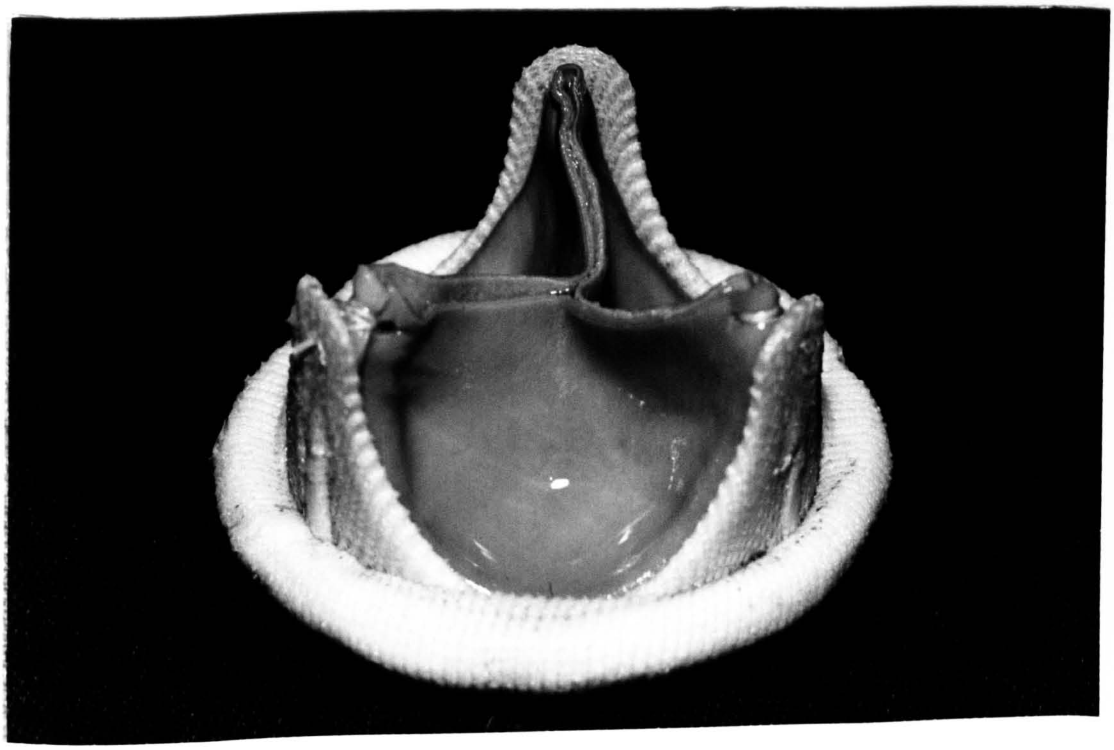

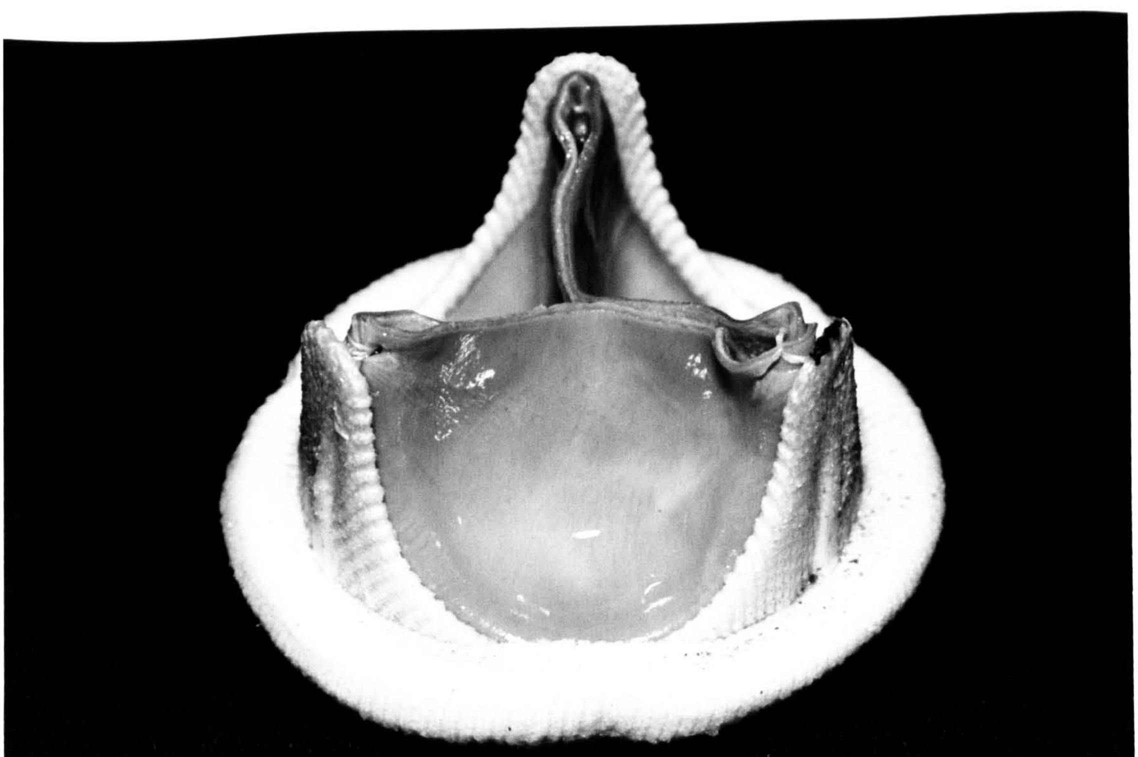

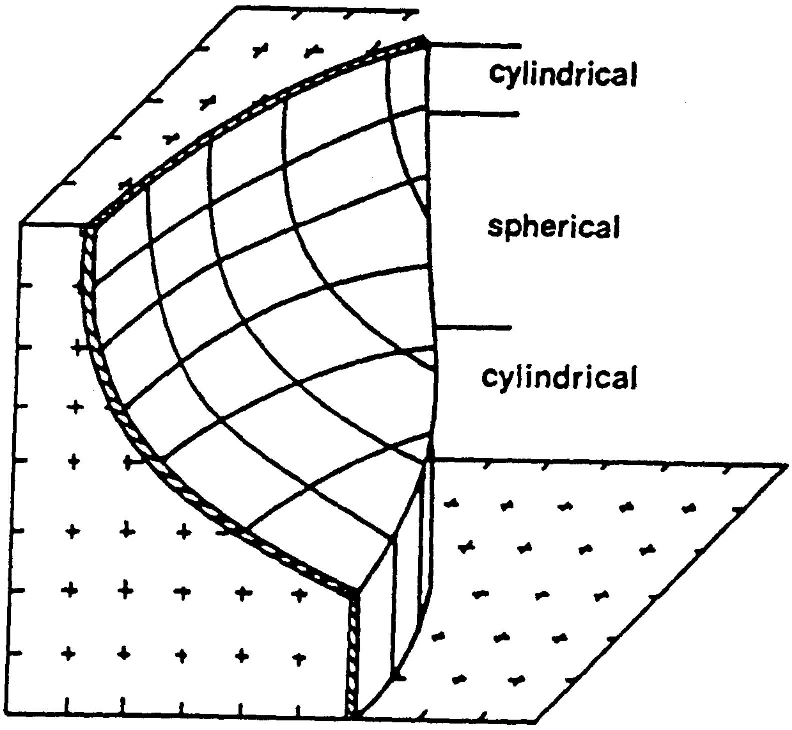

Figure 7.15 Three dimensional diagram through the centre line of the leaflet.

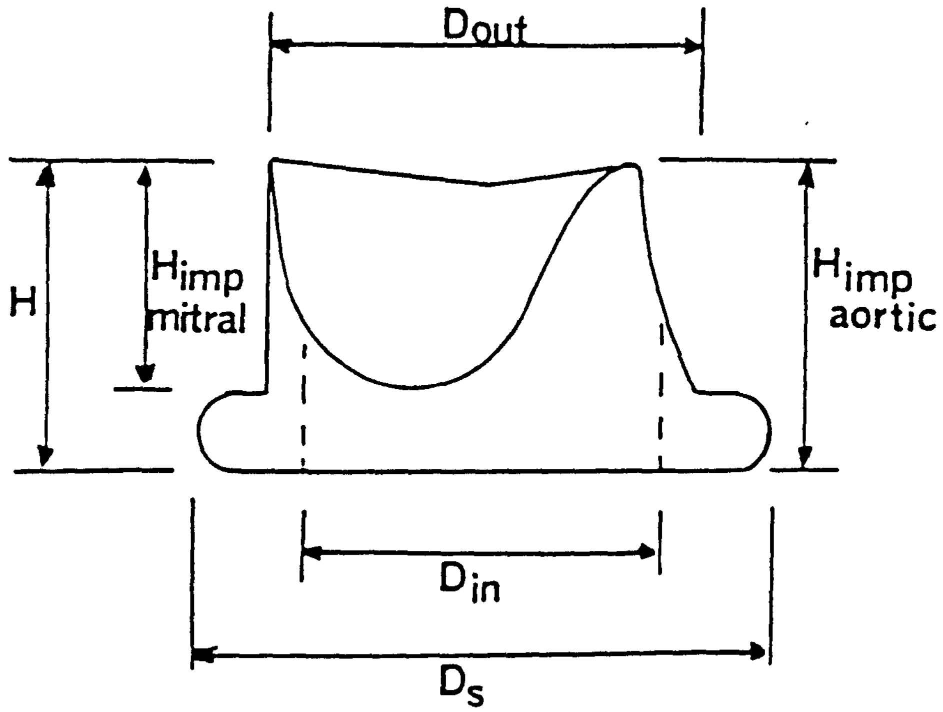

Figure 7.16 Diagram showing the critical dimensions for implantation of the valve.

TABLE 7.1

Key dimensions for the valves in mm

Size		Dout	Di	Ds	H	Himp
31	Mitral	31.5	25.6	41	22	17
29	Mitral	29.5	23.6	39	21	16
27	Mitral	27.5	21.8	37	20	15
25	Mitral	25.5	19.8	35	19	14
27	Aortic	27.5	21.8	33	19.5	19
25	Aortic	25.5	19.8	31	18.5	18
23	Aortic	23.5	18	29	17.5	17
21	Aortic	21.5	16	27	16.5	16
19	Aortic	19.5	14.2	25	15.5	15

Size		he	hf	Rc	w	d	Sab	q
31	Mitral	18	16	13	2	13	28.8	30.5
29	Mitral	17	15	12	2	12	26.7	28.5
27	Mitral	16	14	11	2	11	24.6	26.5
25	Mitral	15	13	10	2	10.3	22.8	24.5
27	Aortic	16	14	11	1.8	11	24.6	26.5
25	Aortic	15	13	10	1.8	10.3	22.8	24.5
23	Aortic	14	12	9	1.8	9.3	20.7	22.5
21	Aortic	13	11	8	1.8	8.3	18.6	20.5
19	Aortic	12	10	7	1.8	7.5	16.8	18.5

Figure 7.17 Views of a size 27 mm mitral valve showing the outflow and inflow aspects of the valve

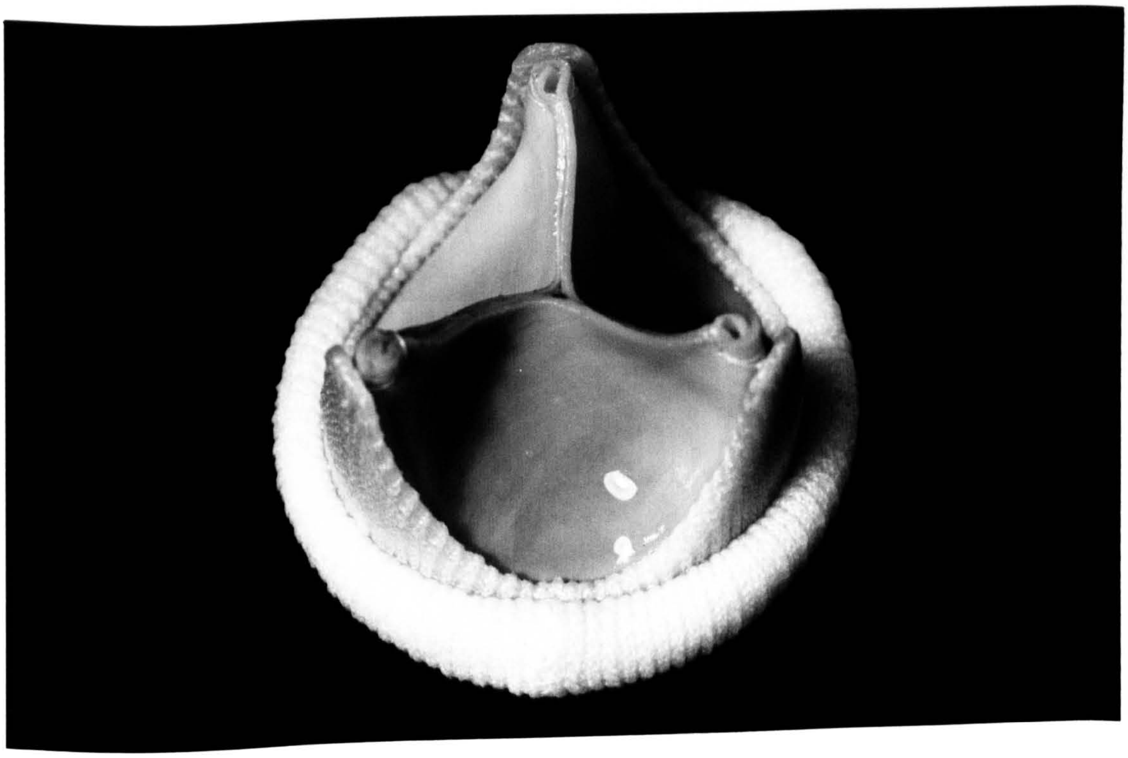

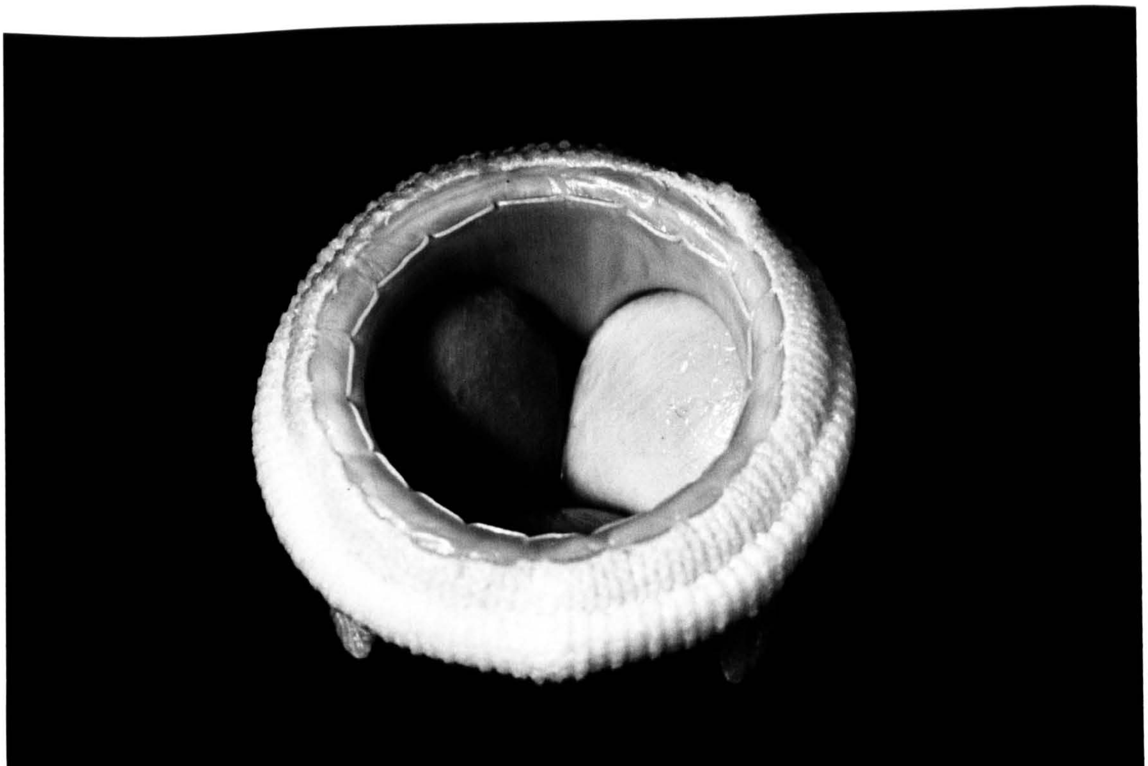

Figure 7.18 Views of a size 25mm aortic valve showing the outflow and inflow aspects of the valve

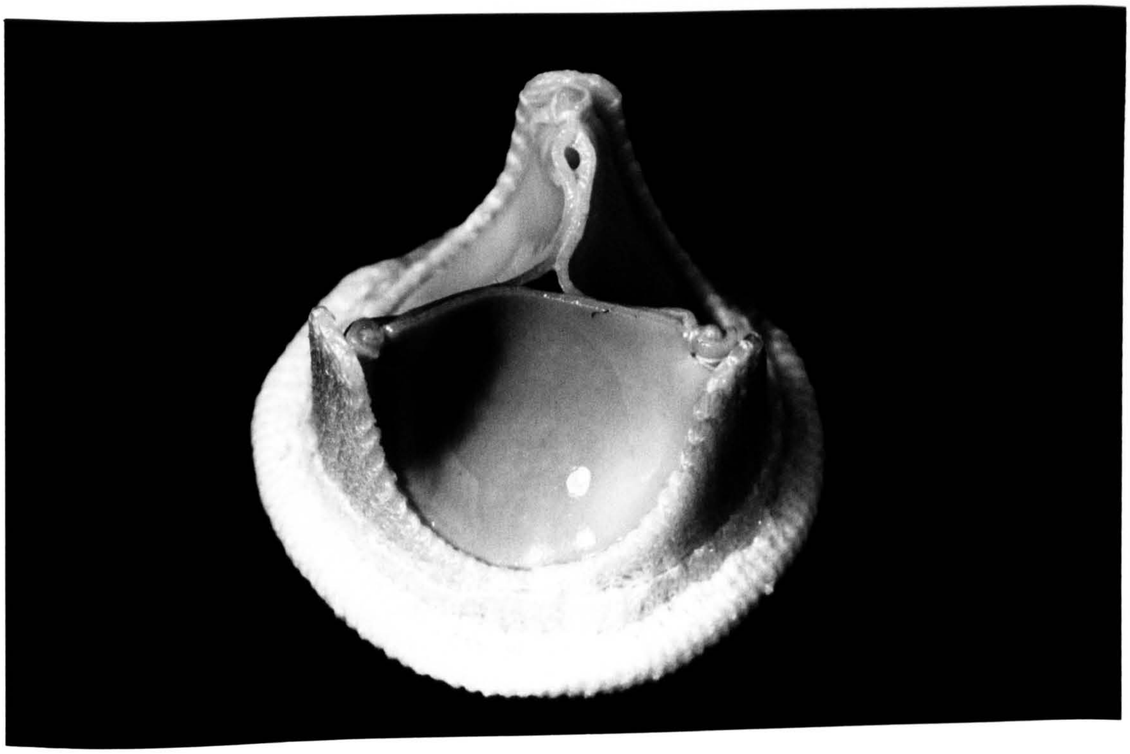

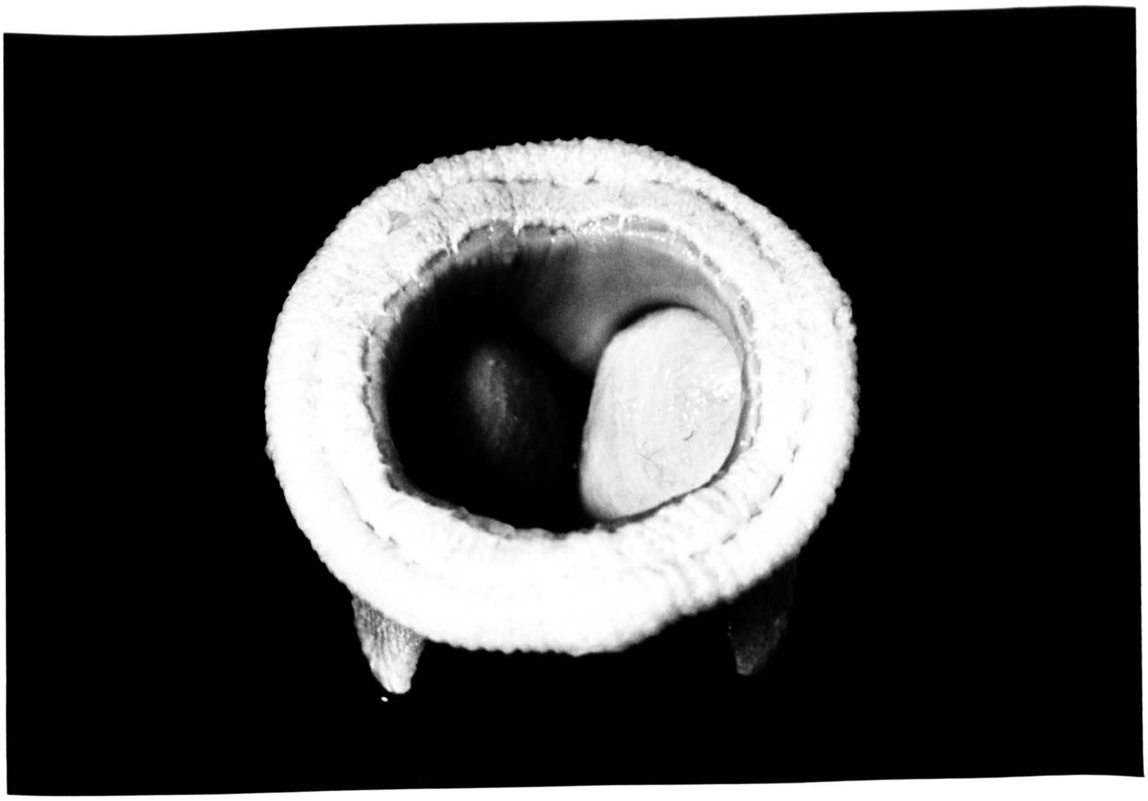

TABLE 8.1

Key dimensions for the Glasgow and other pericardial valves
(dimensions mm)

Valve size 29mm mitrals	Implant Diameter Dout	Internal Diameter Di	Sewing Diameter Ds	Implant Height Himp	Overall Height H
Glasgow	29.5	23.6	39	16	21
ISU	31	25	39	18	20
ISLP	31	24.5	40	17	19
HP	29	24	36	14	17
MM	29	24.5	41	14.5	16.5
Size 23mm aortic					
Glasgow	23.5	18	29	16.5	17.5
ISU	28/25	19.5	28	16	18.5
ISLP	26/25	19.5	27	14.5	17
HP	24	20	28	14	16
MM	22.5	19	26	14	15

Figure 8.1 Views of the valve in the function test apparatus showing the synchronised leaflet opening and closure at 10 ms intervals opening

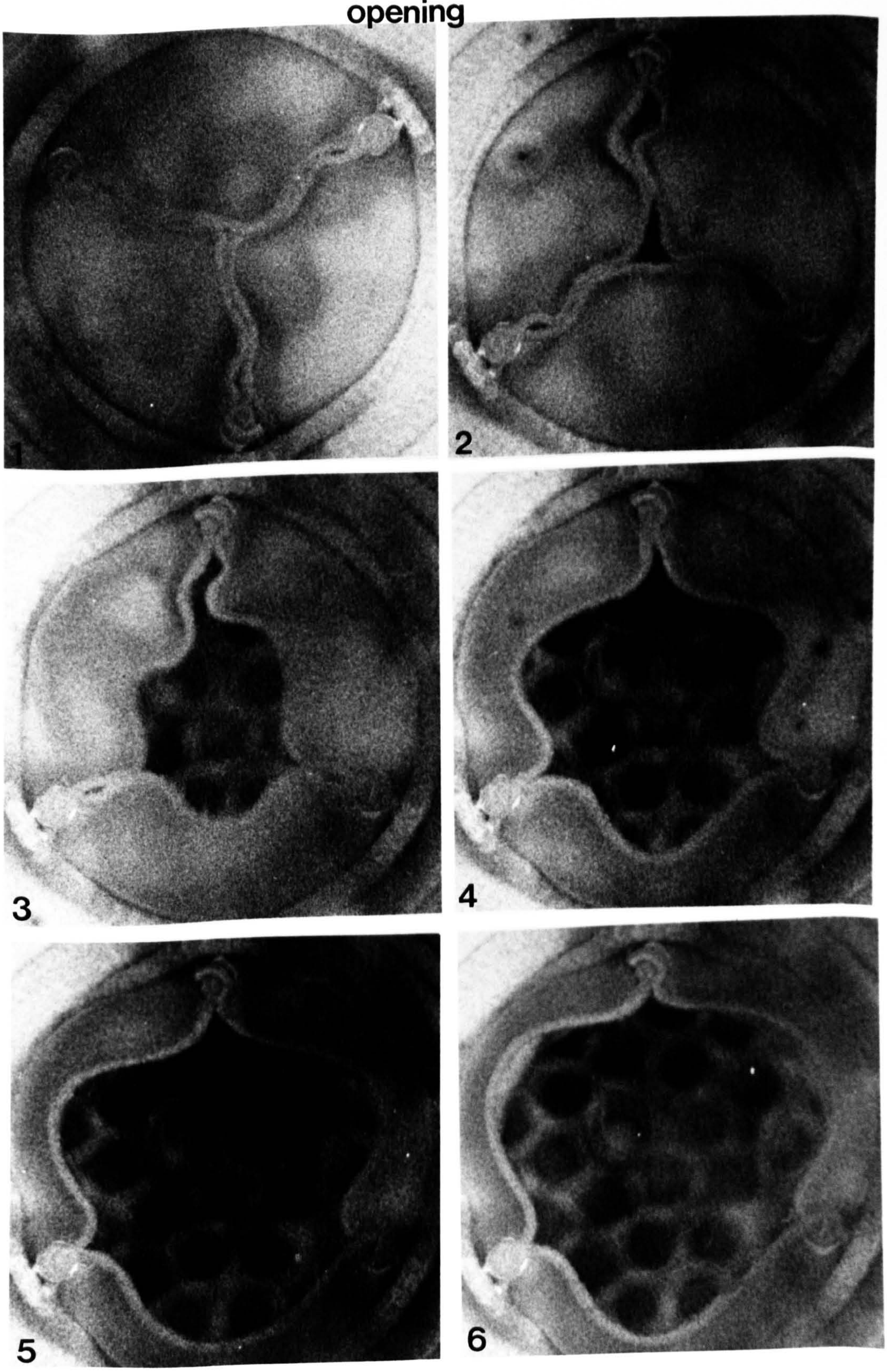

closure

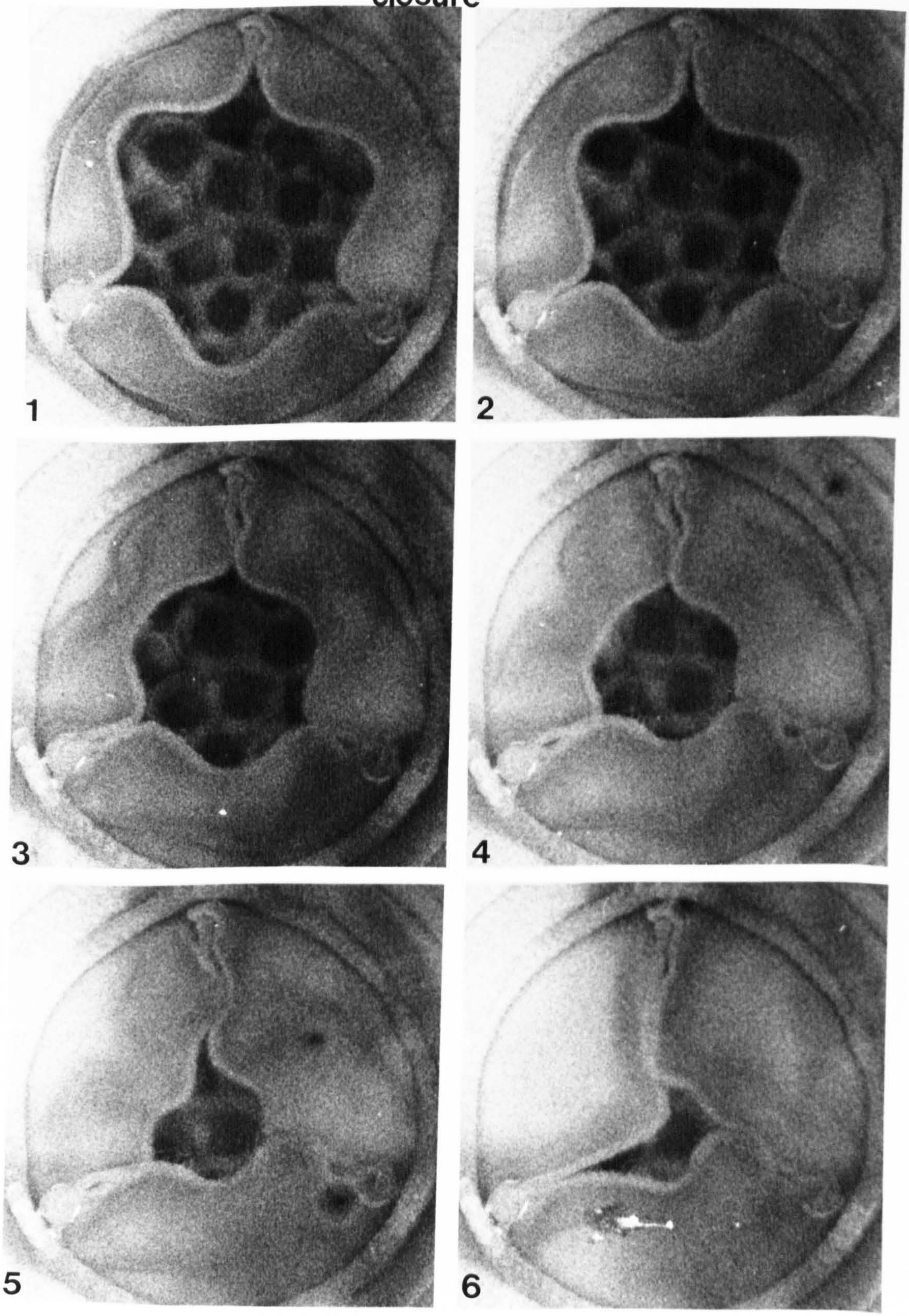

Figure 8.2a A size 25 mm valve in the function test apparatus at a steady flow of 40 ml s^{-1} with one leaflet closed

Figure 8.2b A size 25 mm valve in the function test apparatus at a steady flow of 40 ml s^{-1} with one leaflet only opening at the free edge

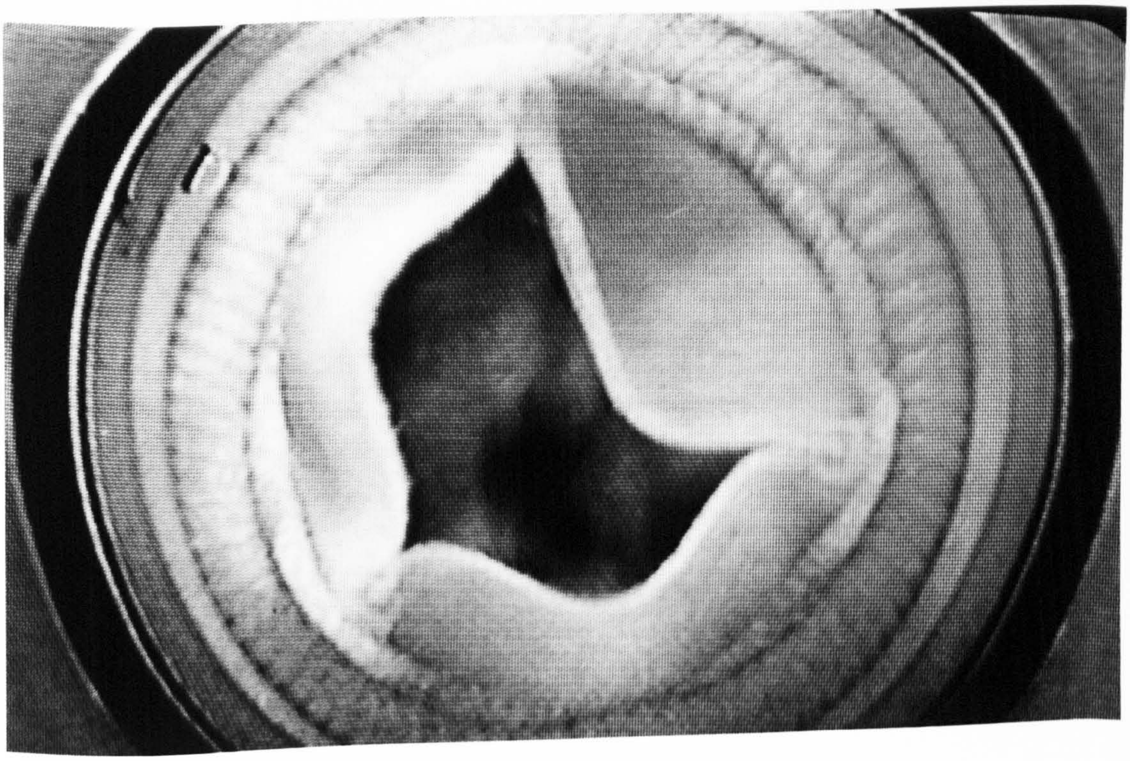

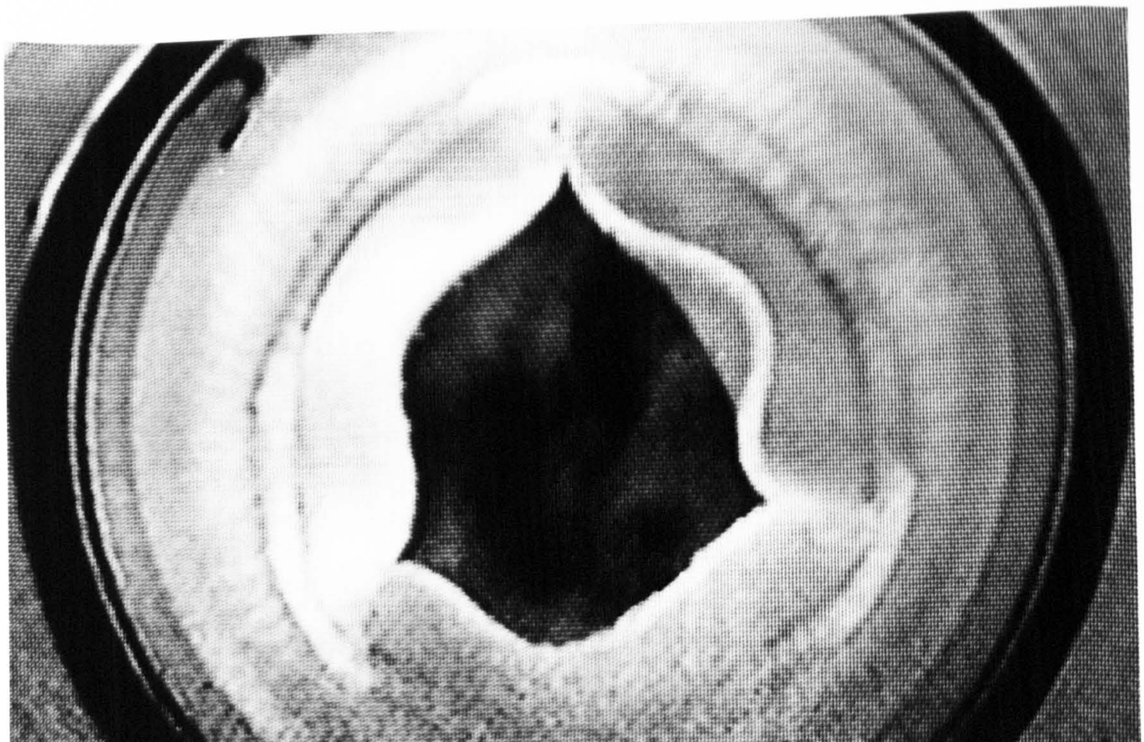

Figure 8.3 Size 25 mm mitral valve in the function test apparatus showing

a] The open position

b] The closed unloaded position

c] The closed position under back pressure

d] The closed position under back pressure (side view)

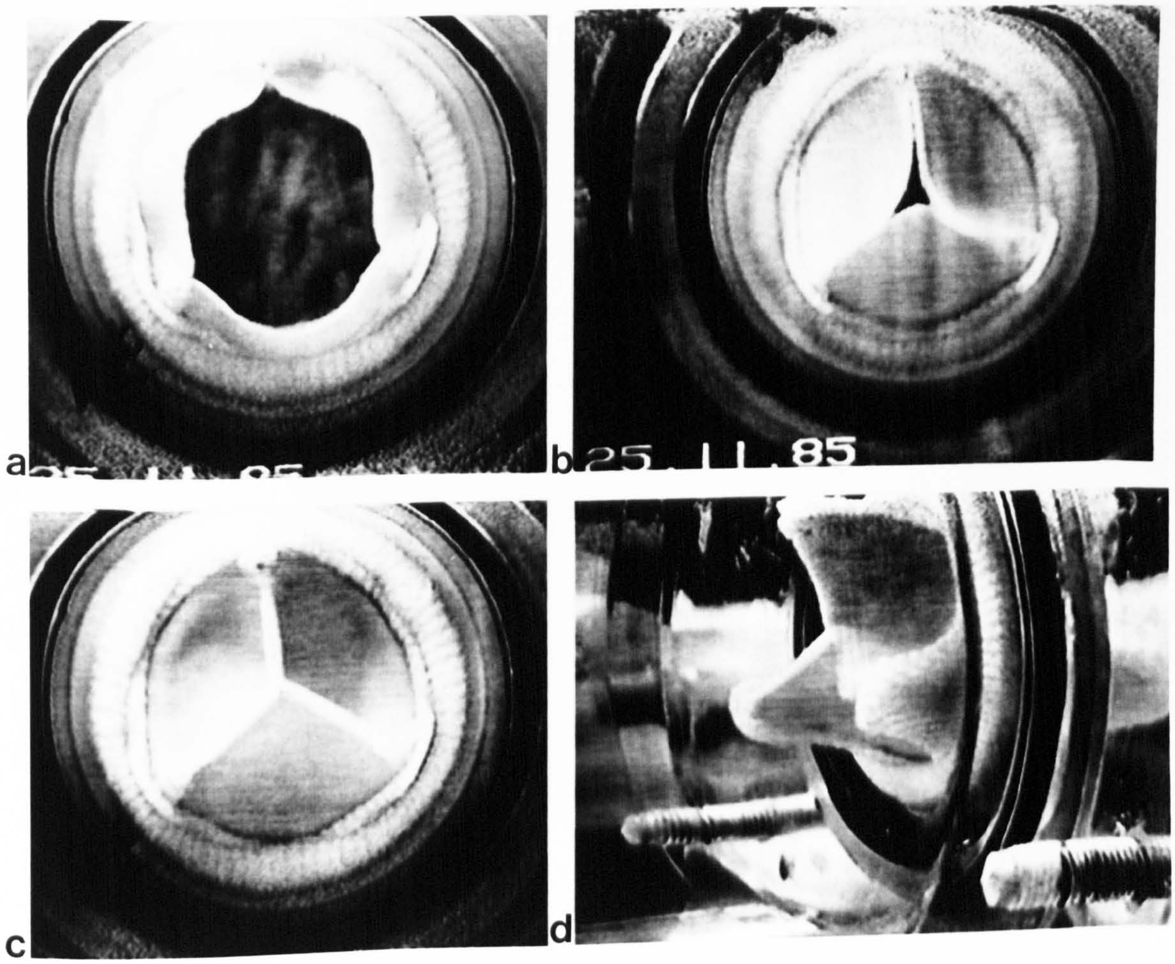
a
b
25 . 11 . 85
c
d

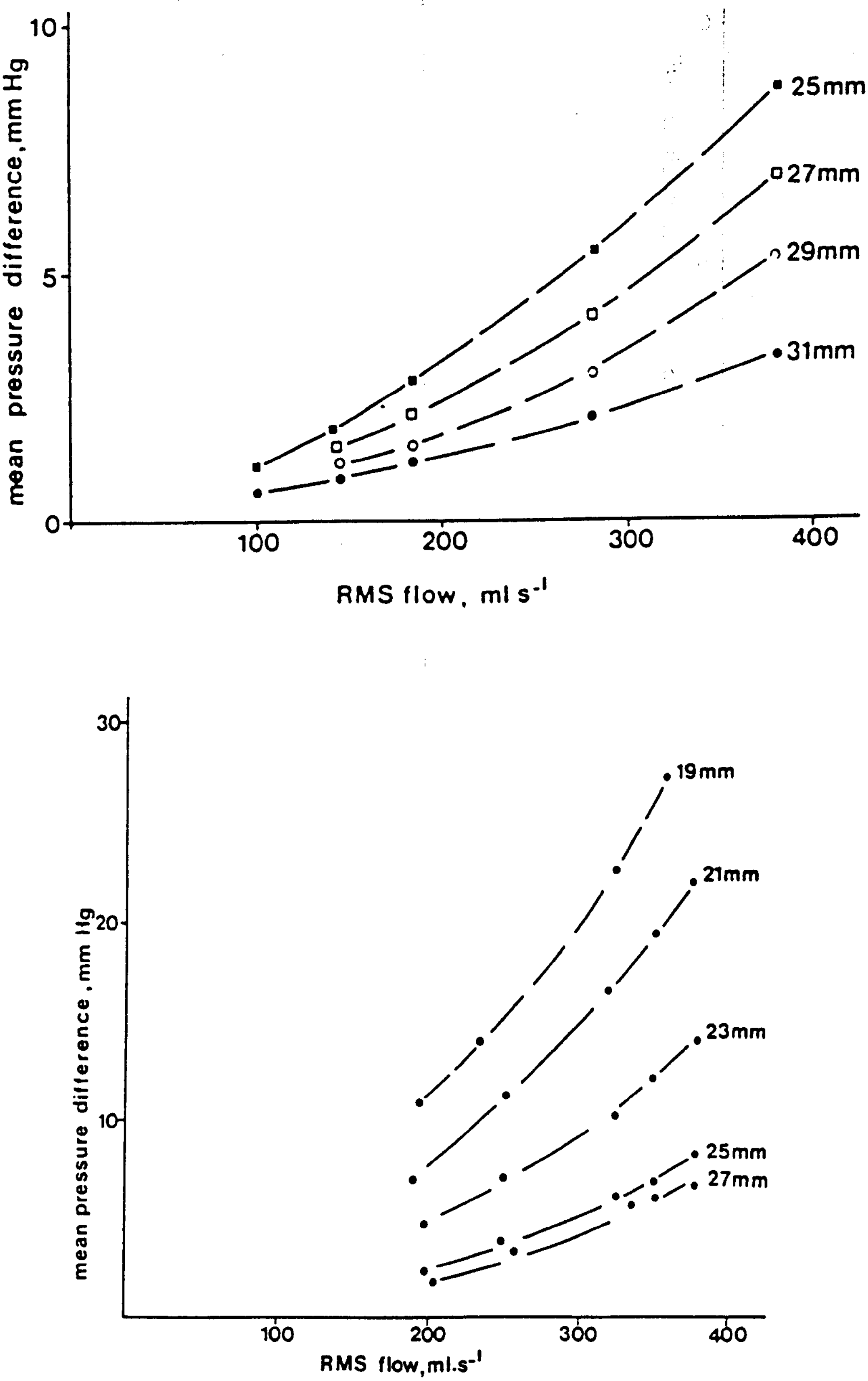

Figure 8.4 Mean pressure difference plotted against RMS flow for size 25 to 31 mm mitral valves and size 19 to 27 mm aortic valves.

TABLE 8.2

Variation in the effective orifice area (EOA) with flow for the size 29 mm mitral and 23 mm aortic valves

RMS flow ml s^{-1}	EOA cm^2	RMS flow ml s^{-1}	EOA cm^2
100	2.25	196	1.67
146	2.7	250	1.86
192	3.03	325	1.97
285	3.5	346	1.99
368	3.5	382	1.97

TABLE 8.3

Comparison of the calculated EOA of the valves with the actual orifice area of the valve frame

Size mm	Position	Actual orifice area of frame cm^2	EOA cm^2	Ratio
31	Mitral	5.1	4.0	0.78
29	Mitral	4.4	3.51	0.79
27	Mitral	3.7	2.79	0.76
25	Aortic	3.07	2.6	0.84
23	Aortic	2.43	1.99	0.81
21	Aortic	2.01	1.54	0.76
19	Aortic	1.58	1.29	0.82

TABLE 8.4

The variation in the mean pressure difference across size 25 mm mitral valves

RMS Flow ml s^{-1}	Mean pressure difference mmHg
186	3.21
186	3.07
184	2.7
185	3.52
186	3.28
186	2.8
185	3.5
185	2.78
183	3.5
180	3.02
mean ± 1SD	3.14 ± 0.31

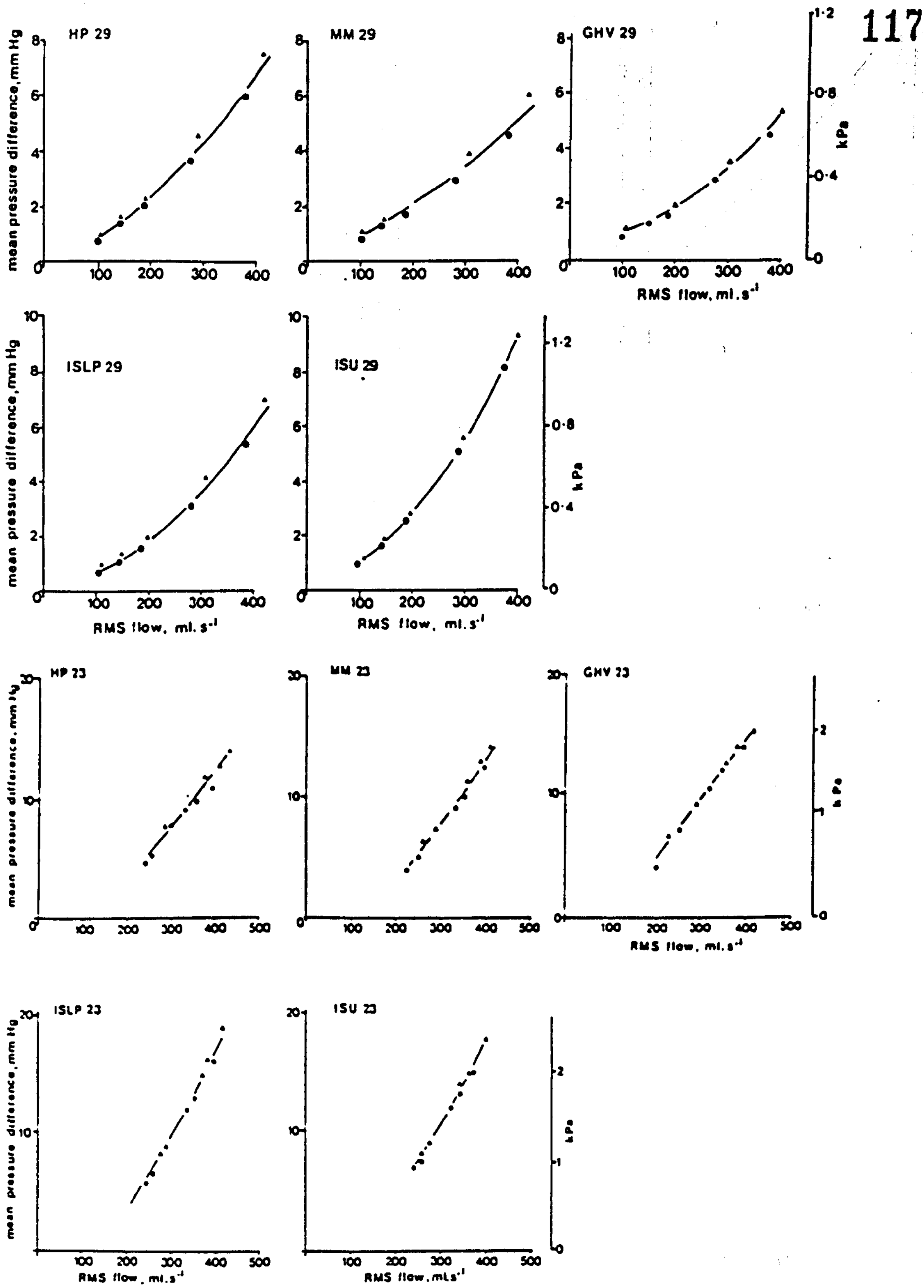

Figure 8.5 The mean pressure difference across the size 29 mm and size 23 mm Glasgow valves (GHV) compared to the Hancock pericardial (HP), Mitral Medical (MM), Ionescu Shiley Low Profile (ISLP) and Ionescu Shiley Standard (ISU) valves.

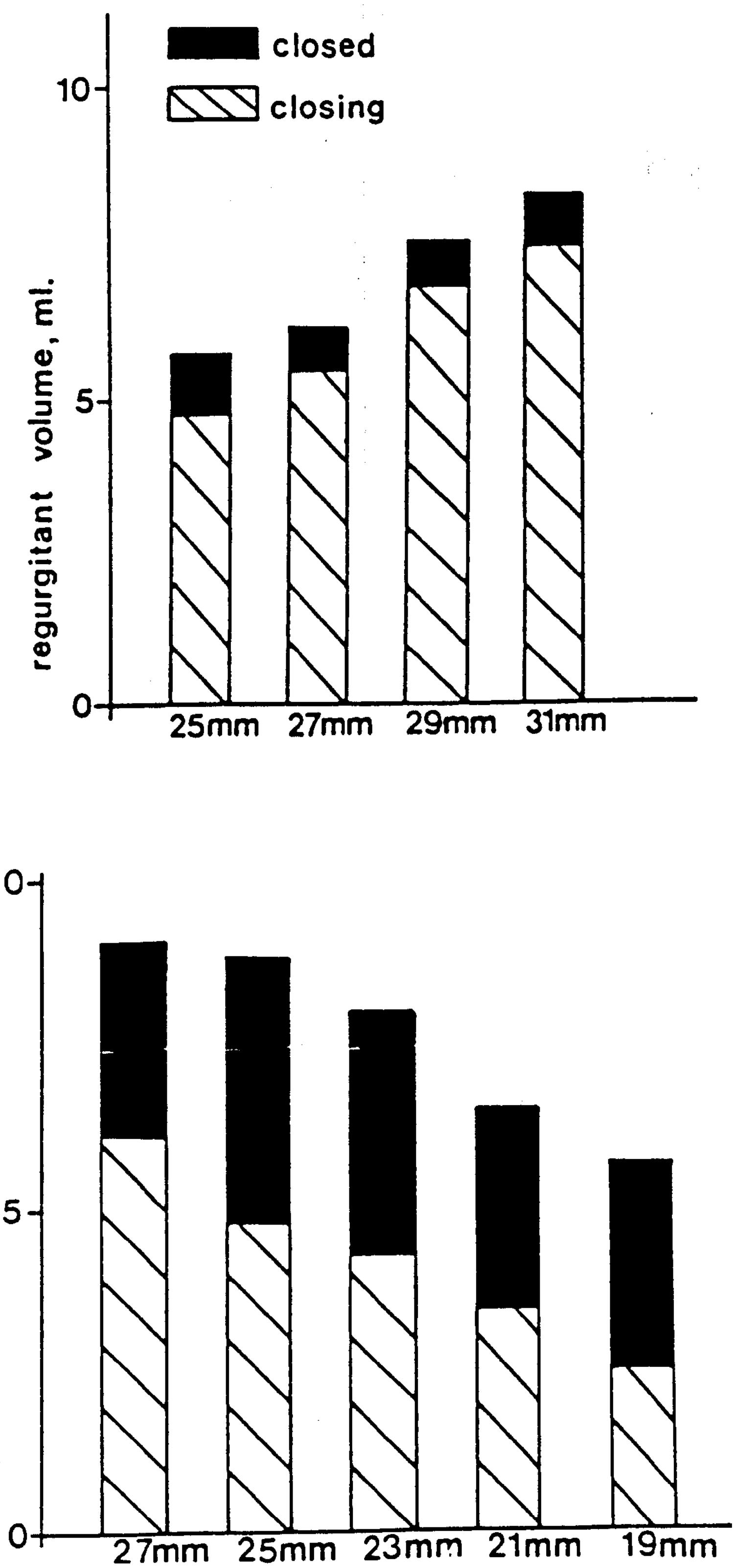

Figure 8.6 Regurgitant volumes for the size 25 mm to 31 mm mitral valves and size 19 to 27 mm aortic valves.

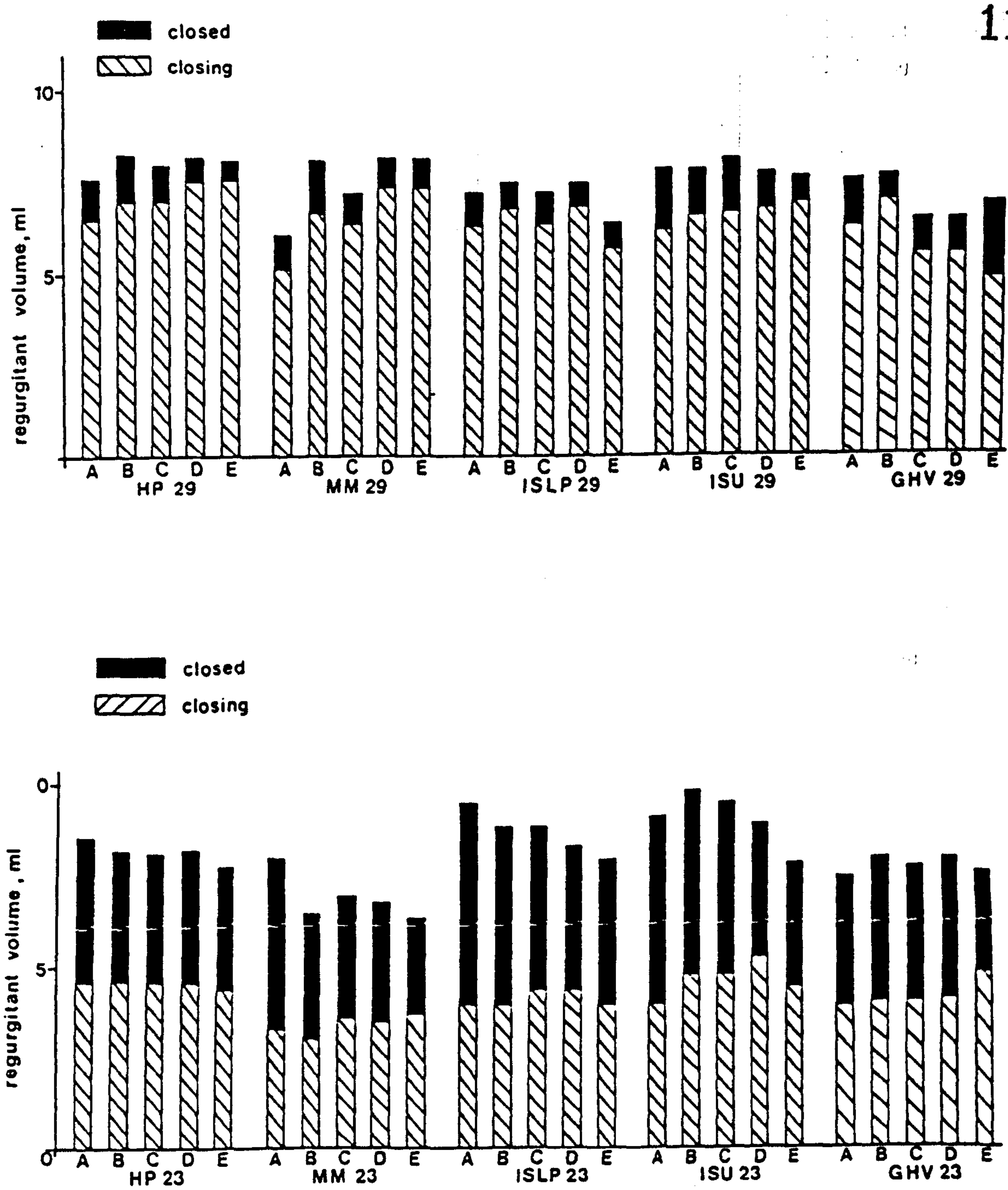

Figure 8.7 Regurgitant volumes for the size 29 and size 23 mm Glasgow valves (GHV) compared to the Hancock Pericardial (HP) Mitral Medical (MM), Ionescu Shiley Low Profile (ISLP) and Ionescu Shiley Standard (ISU) valves (ISLP) valves for the five flow conditions A to F.

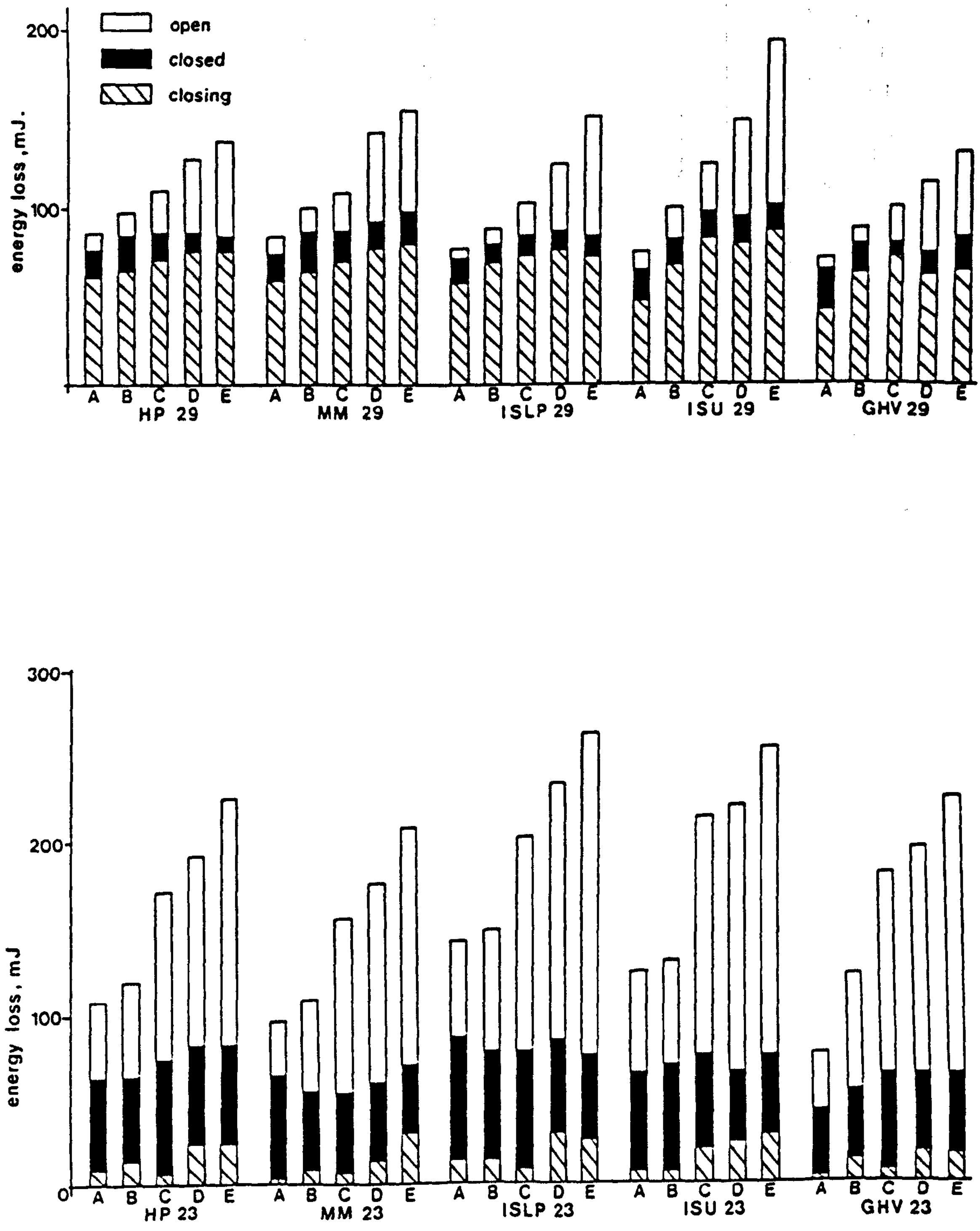

Figure 8.8 Energy losses across the Glasgow valves (GHV) (size 29 and 23 mm) compared to the HP, MM, ISLP and ISU pericardial valves for the five flow conditions A to F.

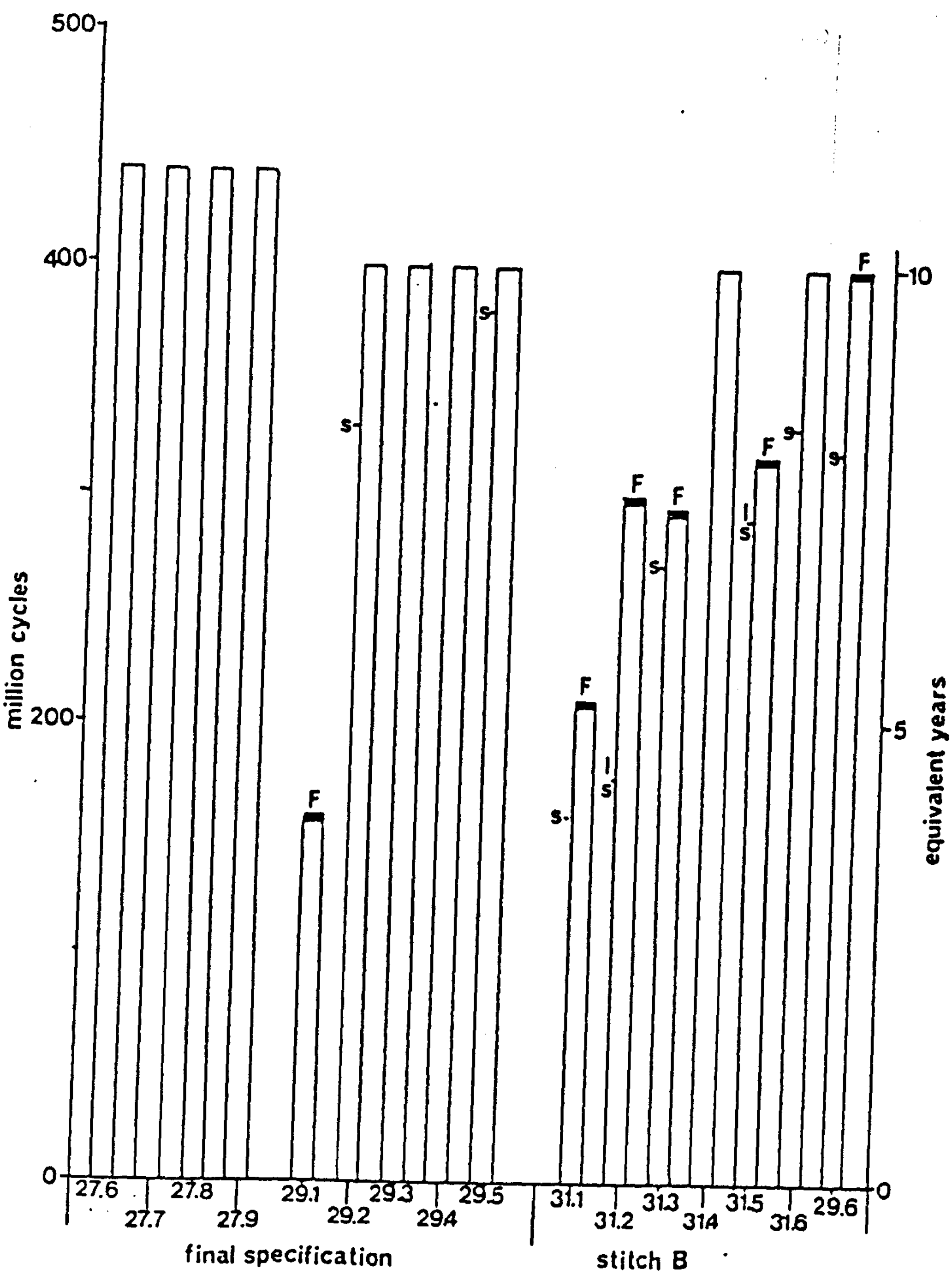

Figure 8.9 Fatigue test results for nine valves manufactured to the final specification and seven valves with stitch configuration B.

Figure 8.10 Valve 29.1 failed after 156 million cycles in the fatigue tester

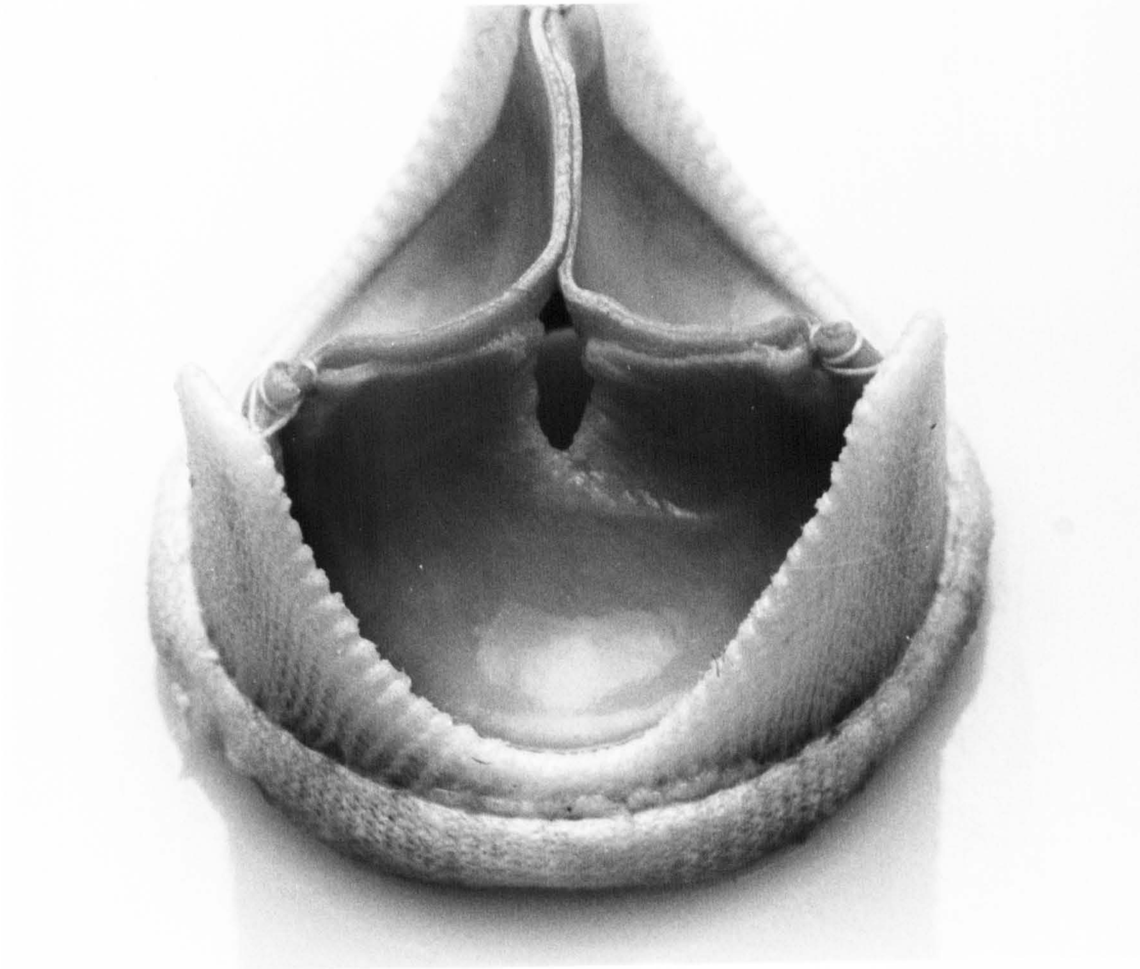

Figure 8.11 Valves 29.2 to 29.5 after 440 million cycles in the fatigue tester

a] Valve 29.2

b] Valve 29.3

c] Valve 29.6

d] Valve 29.5

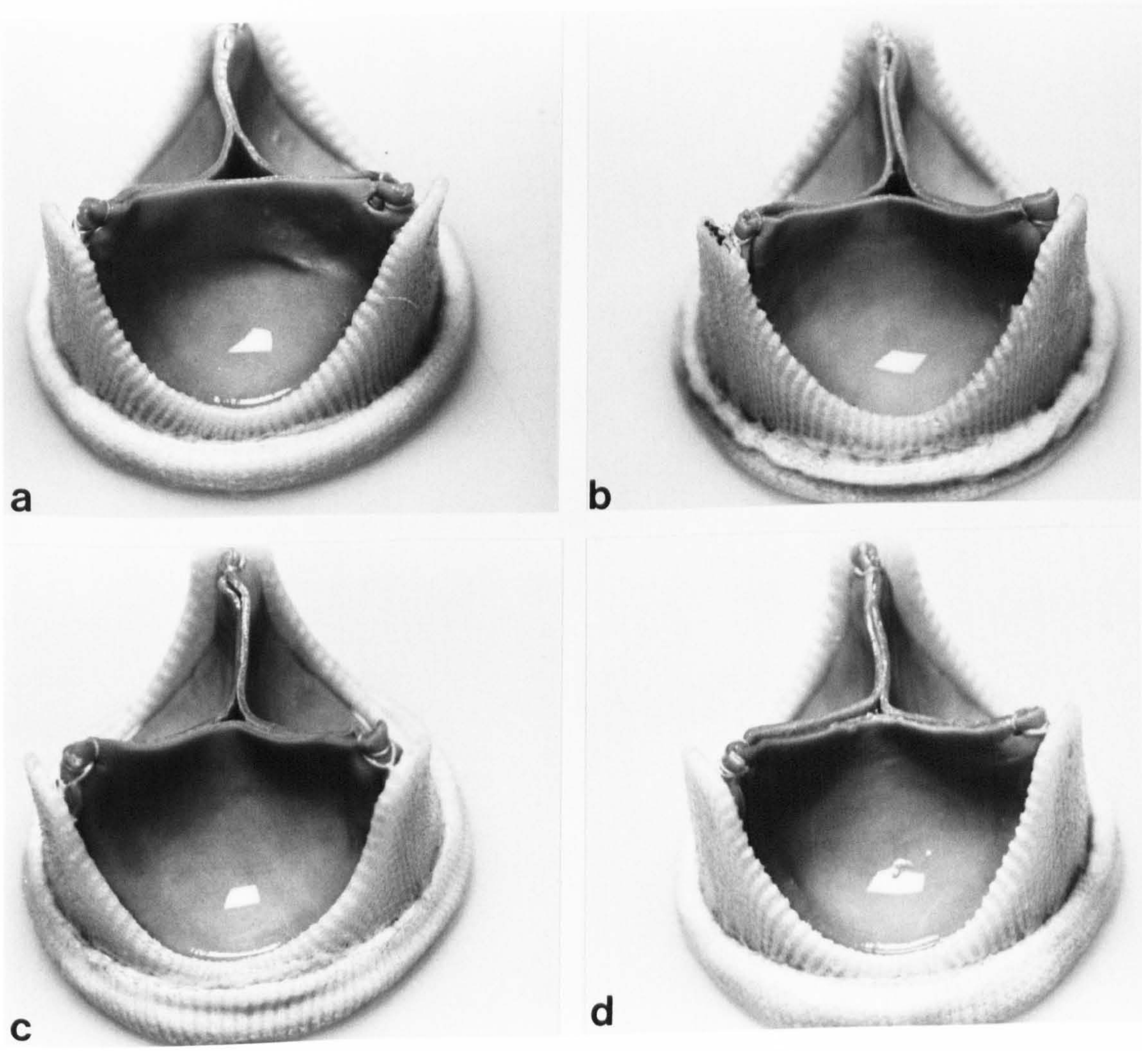
a
b
c
d

Figure 8.12 Valves 31.1 to 31.6 and valve 29.6 after the fatigue tests

a] Valve 31.1

b] Valve 31.2

c] Valve 31.3

d] Valve 31.4

e] Valve 31.5

f] Valve 31.6

g] Valve 29.6

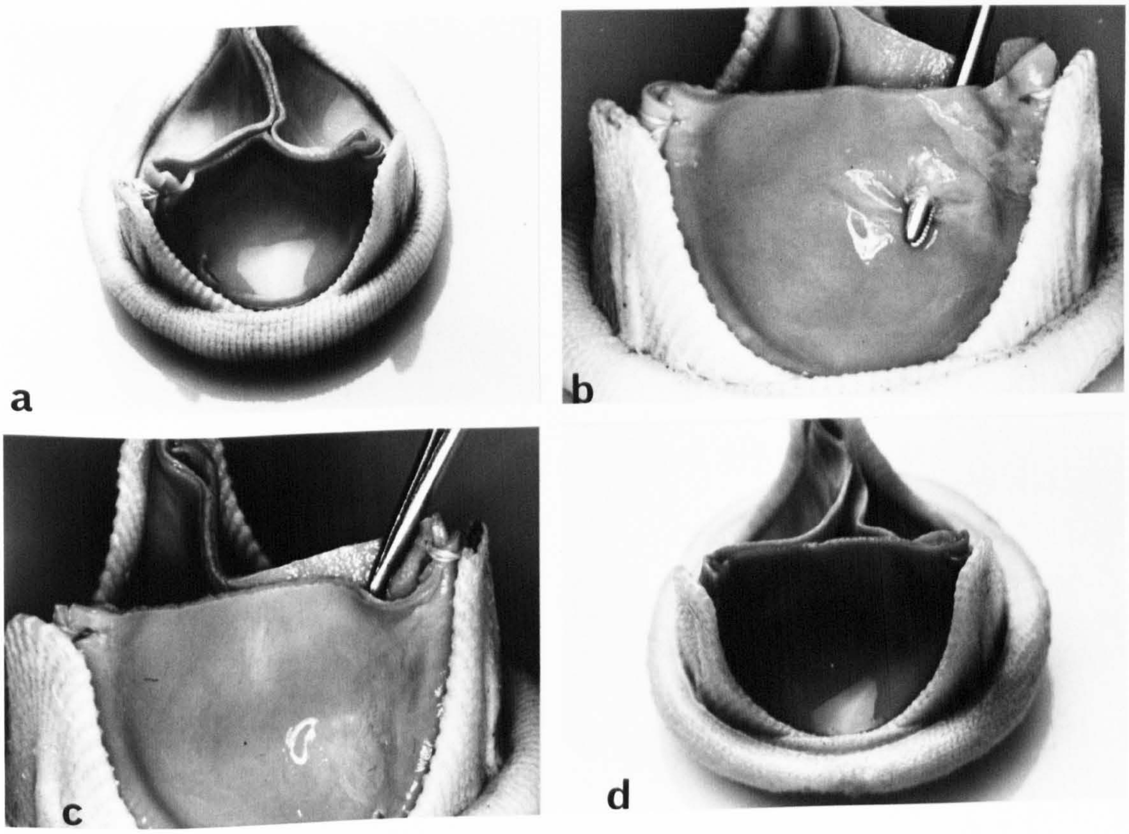
a
b
c
d

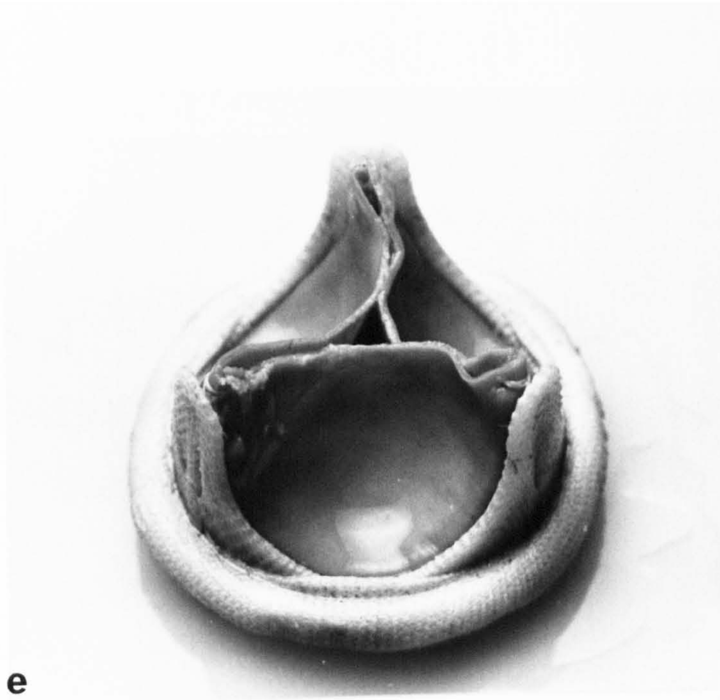

e

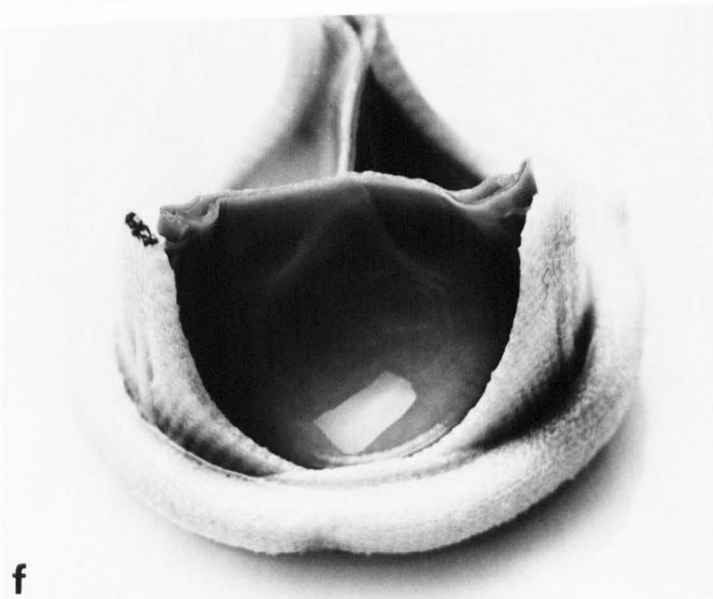

f

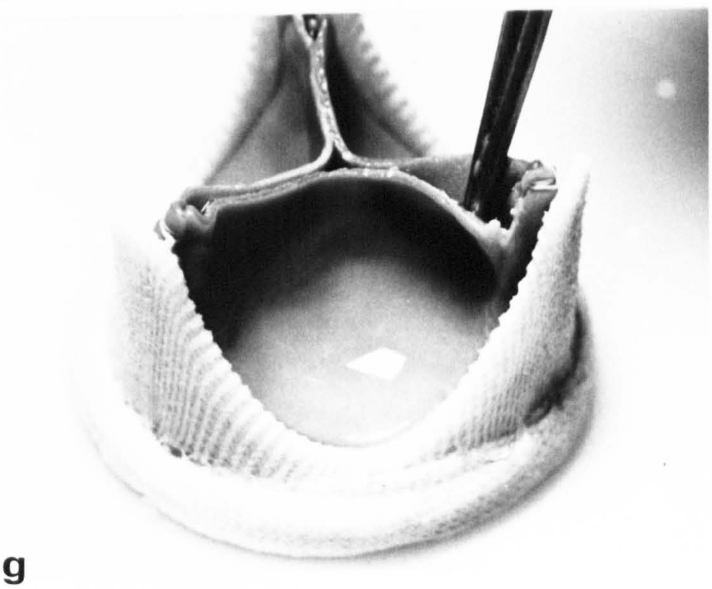

g

TABLE 8.5

Comparison of the hydrodynamic function of the valves
before and after the fatigue tests

Valve	RMS flow ml s^{-1}	Mean pressure difference mmHg before	Mean pressure difference mmHg after	Regurgitation ml closing before	Regurgitation ml closing after	Regurgitation ml closed before	Regurgitation ml closed after
27.6	192	2.2	2.4	5.9	6.1	0.7	1.1
27.7	194	2.6	2.1	4.0	5.0	0.8	0.5
27.8	192	3.4	2.9	5.9	6.6	1.0	0.3
27.9	190	2.9	2.4	5.1	5.7	0.8	0.1
29.1	146	1.2	1.8	7.5	8.8	1.2	23.8 F
29.2	142	1.2	1.3	7.0	6.6	1.1	0.9
29.3	143	1.0	1.0	5.9	5.3	1.1	0.8
29.4	141	1.1	1.2	7.0	5.6	0.7	0.4
29.5	143	1.2	1.1	7.0	6.8	0.5	0.1
31.1	190	1.3	1.6	7.9	8.3	0.8	0.3 F
31.2	191	1.2	1.0	7.5	8.4	0.3	4.9 F
31.3	186	1.0	0.8	7.6	7.8	1.3	1.4 F
31.4	190	1.2	1.0	7.8	7.8	1.0	0.8
31.5	193	1.0	1.1	7.9	4.8	1.1	24.5 F
31.6	186	1.3	1.2	7.3	7.5	0.8	0.5
29.6	145	1.1	0.9	6.6	7.0	0.8	2.6 F

Figure 9.1 Explanted valve 1

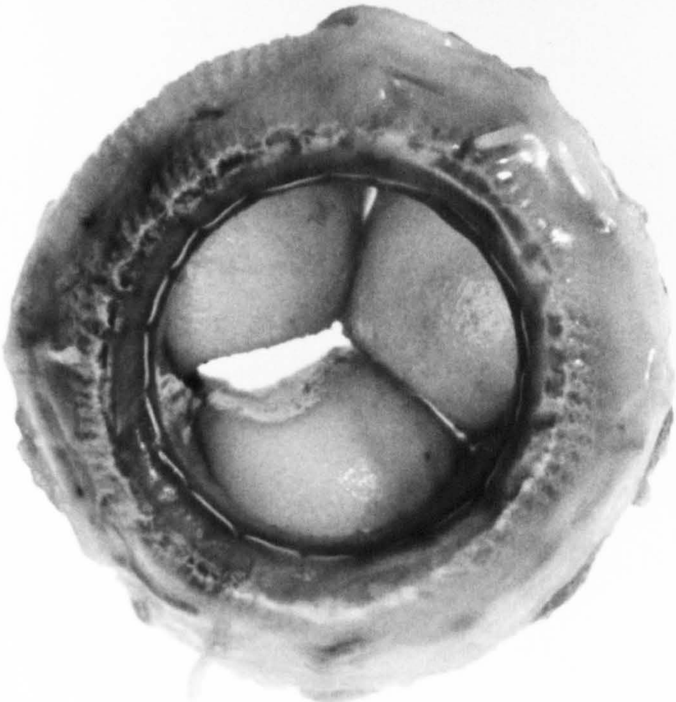

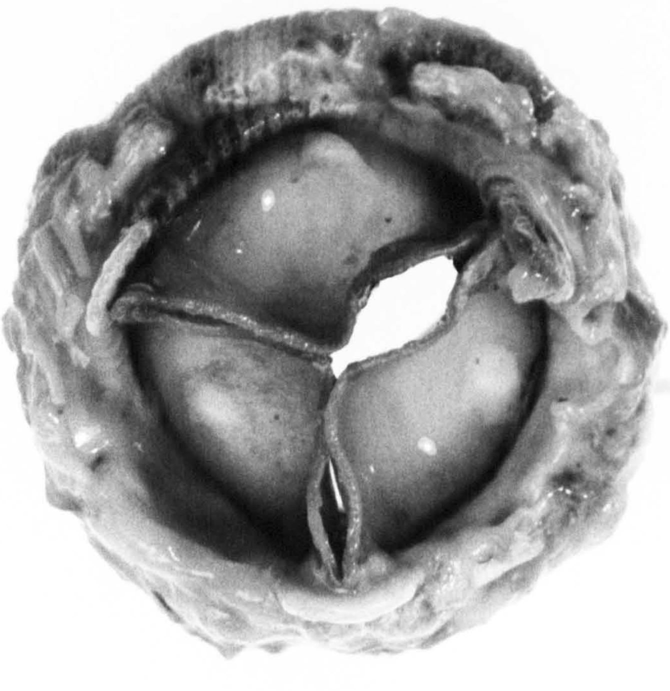

Figure 9.2 Explanted valve 2

Figure 9.3 Explanted valve 3

Figure 9.4 Explanted valve 4

Figure 9.5 Explanted valve 5

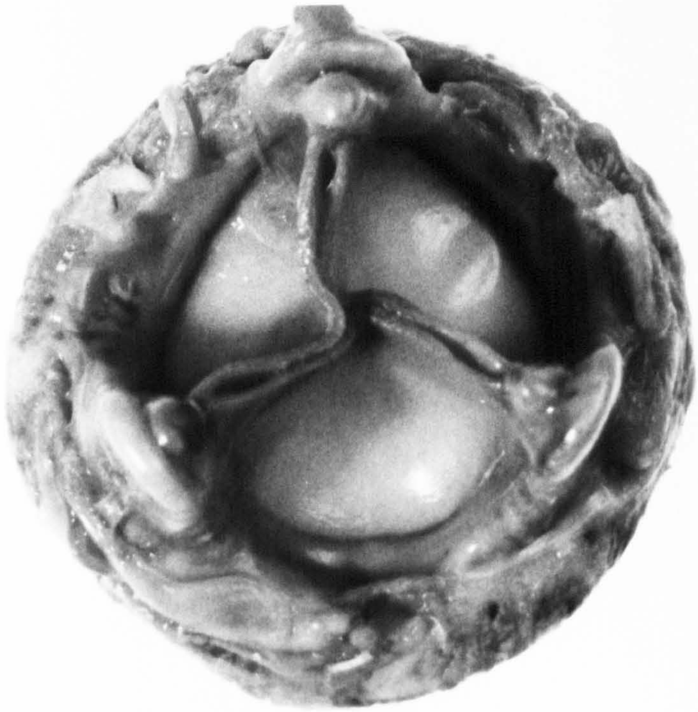

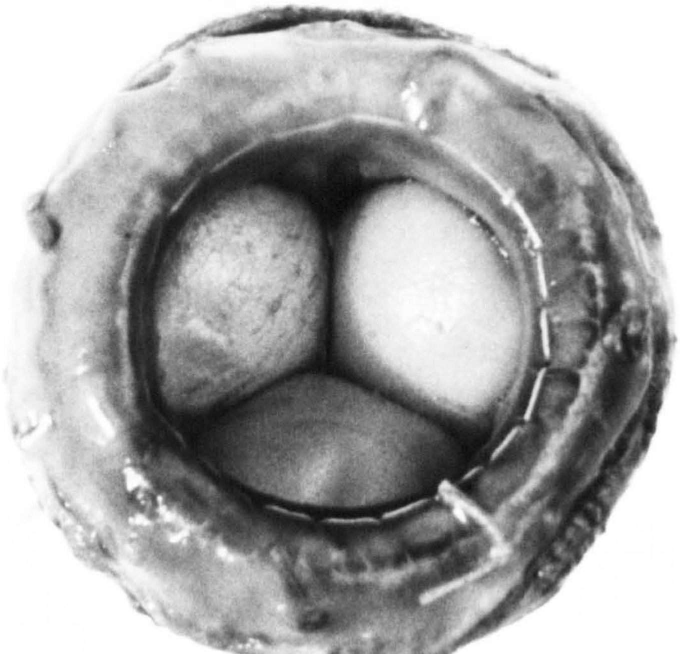

Figure 9.6 Explanted valve 6

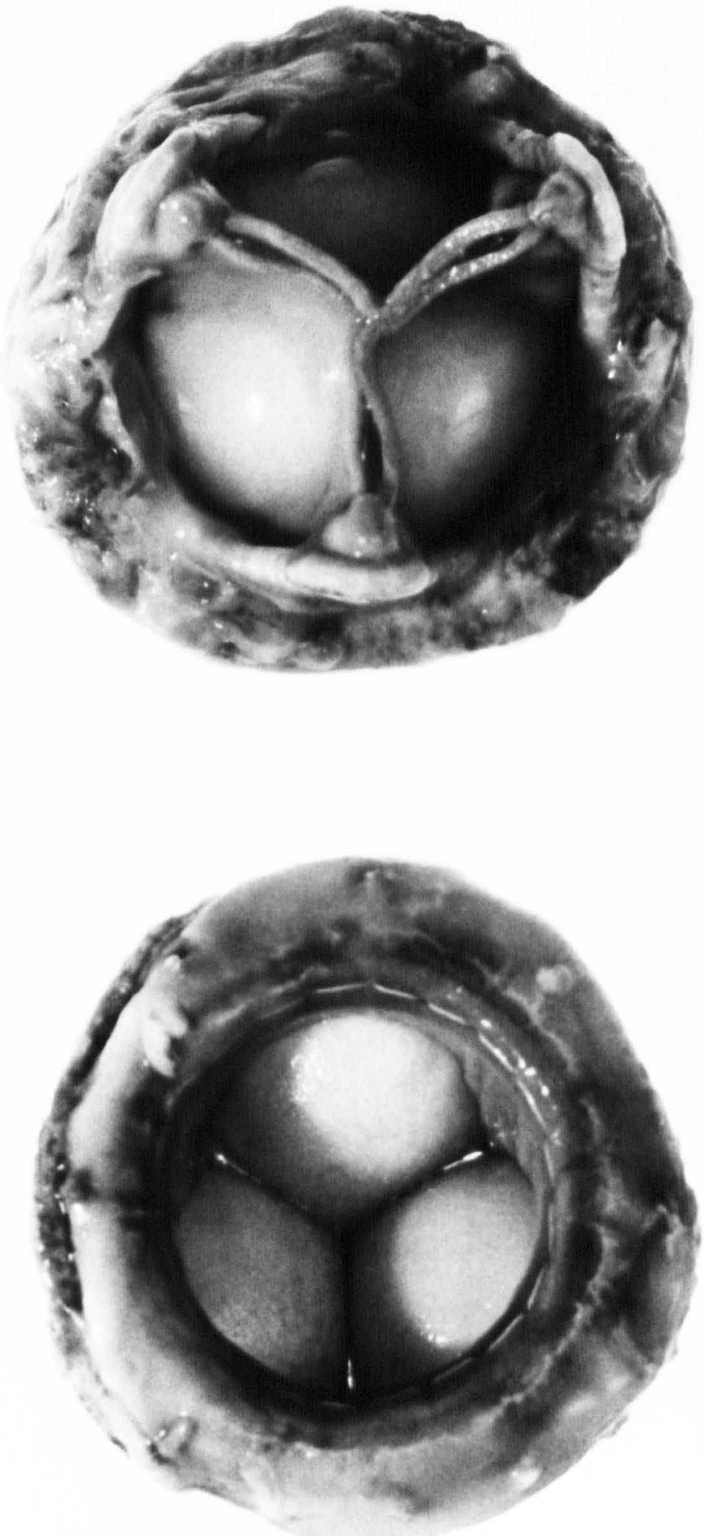

Figure 9.7 Explanted valve 7

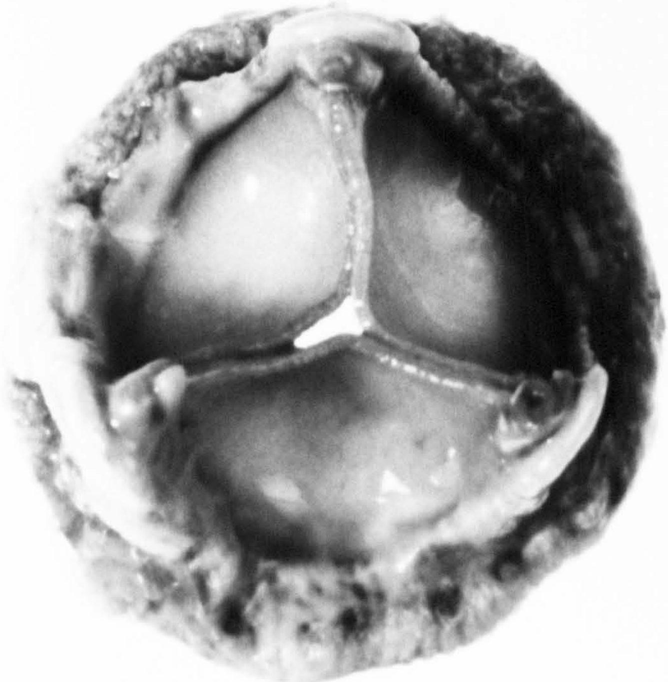

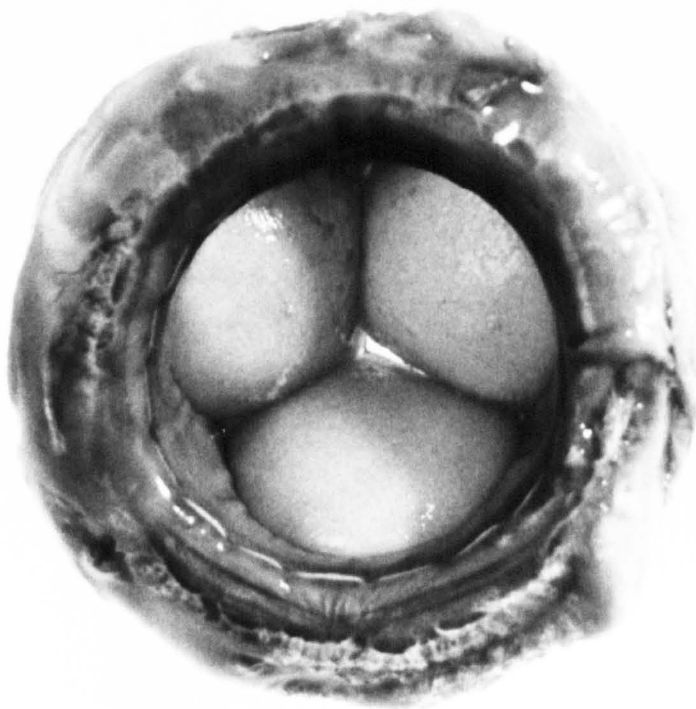

Figure 9.8 X-ray film of explanted valves 1 to 7 and a control valve prior to implant

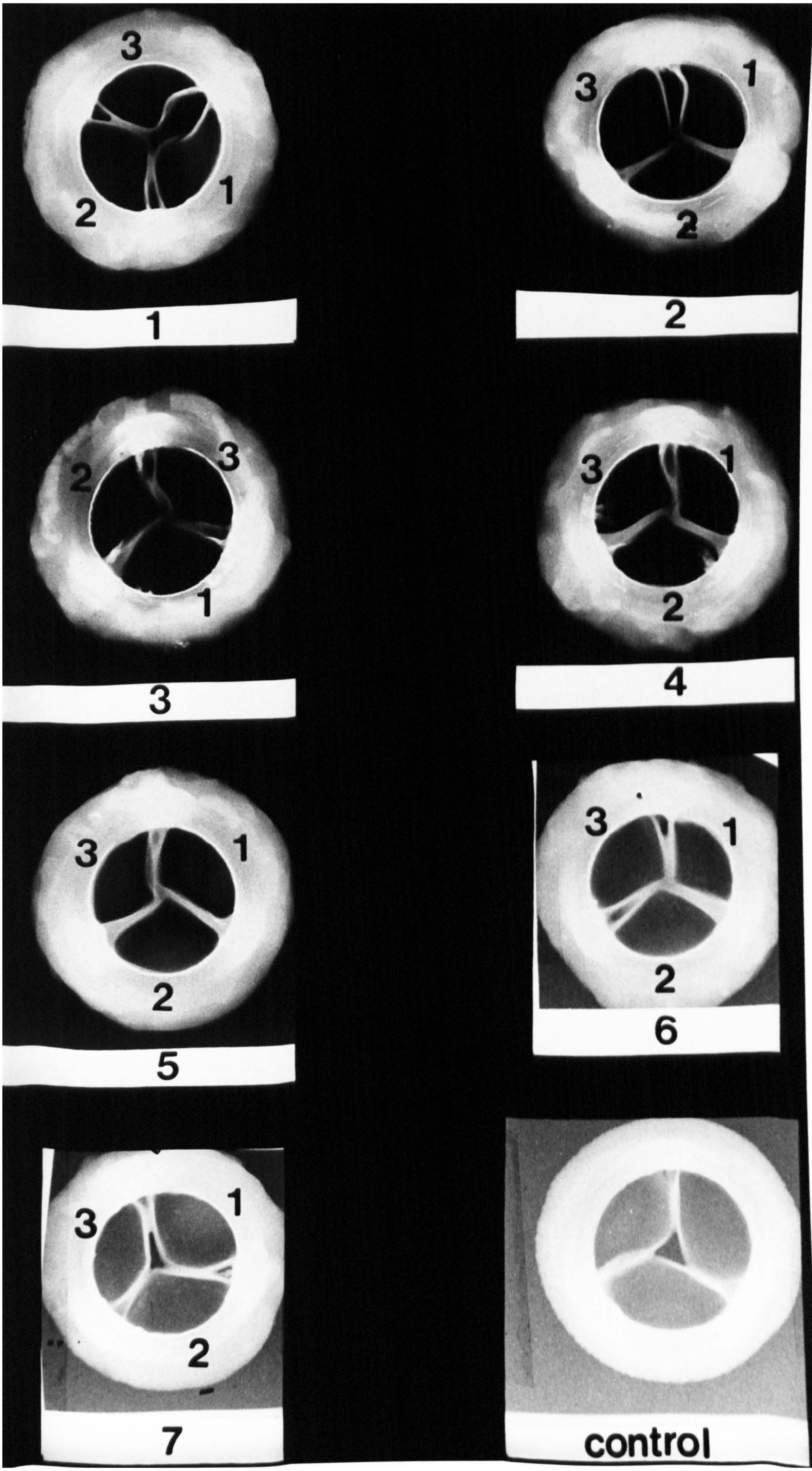

1
2
3
4
5
6
7
control

Figure 9.9 X-ray film of leaflets from explanted valves 1 to 5 and valve 7

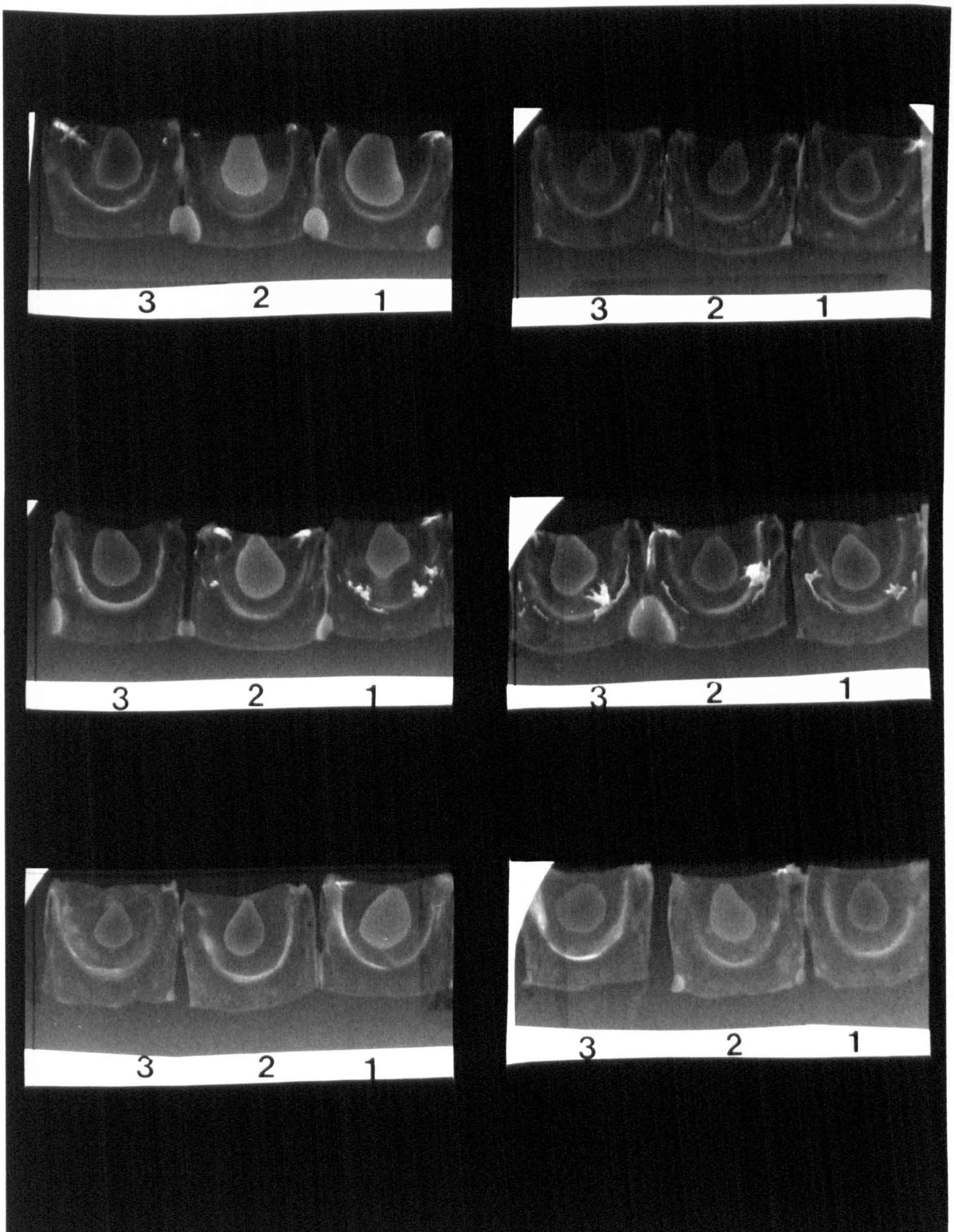
3 2 1
3 2 1
3 2 1
3 2 1
3 2 1
3 2 1

TABLE 9.1

Hydrodynamic function test results on

implanted I and explanted E valves

Valve No.	RMS Flow ml s^{-1}	Mean Pressure Difference mmHg		EOA cm^2		Regurgitation ml			
						Closing		Closed	
		I	E	I	E	I	E	I	E
1	100	1.2	1.8	1.8	1.5	4.8	5.4	2.9	2.8
1	180	2.7	4.3	2.2	1.7	4.5	5.5	2.9	2.9
2	104	1.5	2.0	1.7	1.4	4.8	4.2	2.5	1.7
2	187	3.3	4.3	2.0	1.7	4.4	4.4	1.9	1.2
3	102	1.2	2.9	1.9	1.2	4.3	6.7	2.1	1.2
3	183	3.8	7.1	1.8	1.3	5.2	5.2	2.5	1.3
4	100	1.5	3.8	1.6	1.0	5.3	4.1	2.1	0
4	173	3.4	8.3	1.9	1.3	5.4	3.7	2.0	0.3
5	101	1.5	2.1	1.6	1.4	5.0	4.8	2.7	1.4
5	182	3.6	4.6	1.9	1.6	5.0	4.6	2.3	1.2
6	105	1.8	2.6	1.5	1.3	5.0	7.0	2.0	1.9
6	184	3.9	5.2	1.7	1.5	4.8	6.7	2.0	1.4
7	100	1.5	2.4	1.6	1.2	5.1	4.4	2.4	1.6
7	181	3.0	5.4	2.0	1.5	4.7	4.2	3.2	1.0

Figure 9.10 Histological section of a pericardial valve leaflet, a] prior to implant, and b] after explant. a] is a transverse section through the leaflet and b] a section parallel to the surface of the leaflet (Mag x 100) haematoxylin and eosin stain)

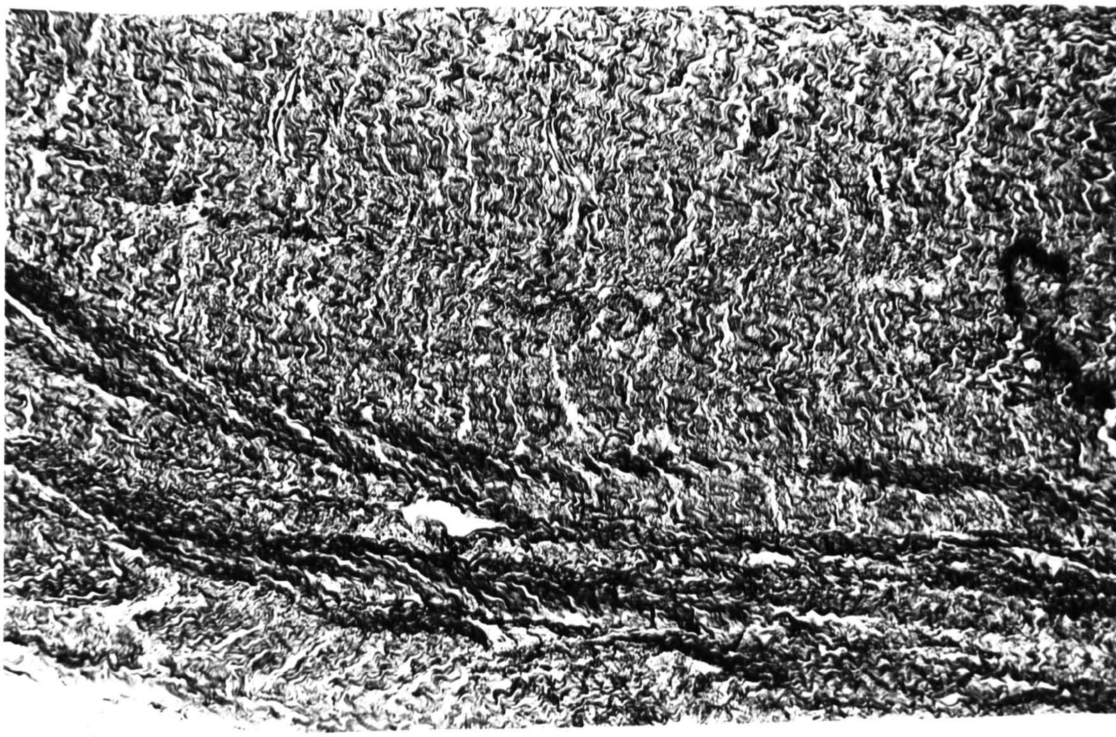
a


b

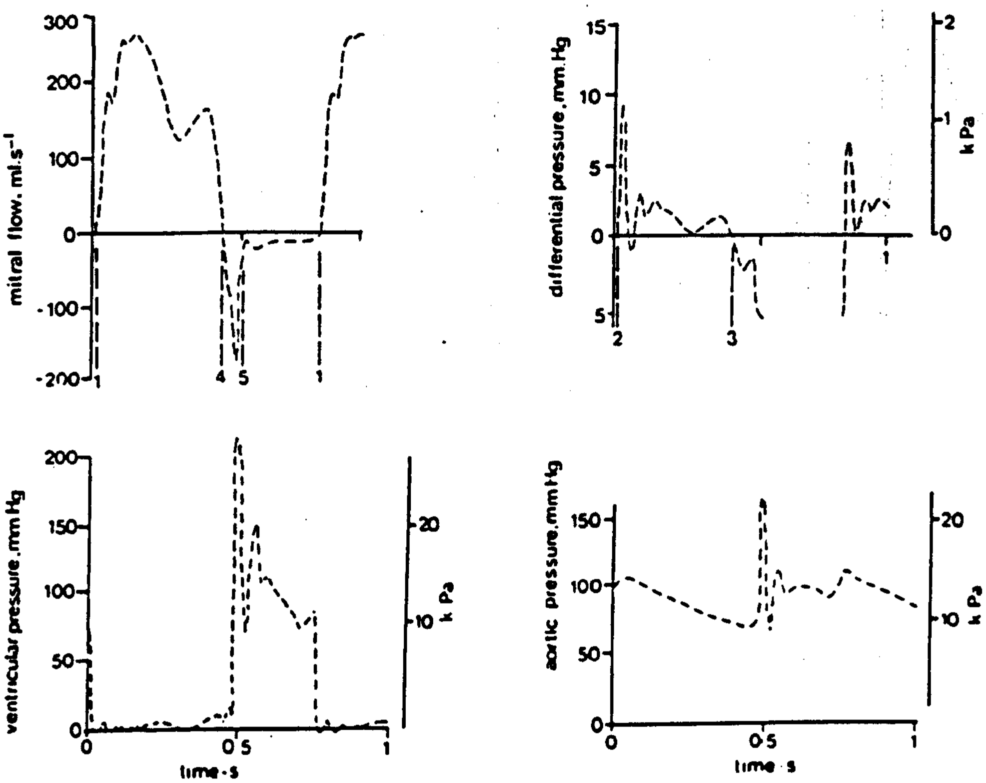

Figure A1.1 Pressure and flow waveforms for a Bjork-Shiley size 29 mm spherical disc valve in the mitral position, test conditions C, showing reference points 1 to 5.

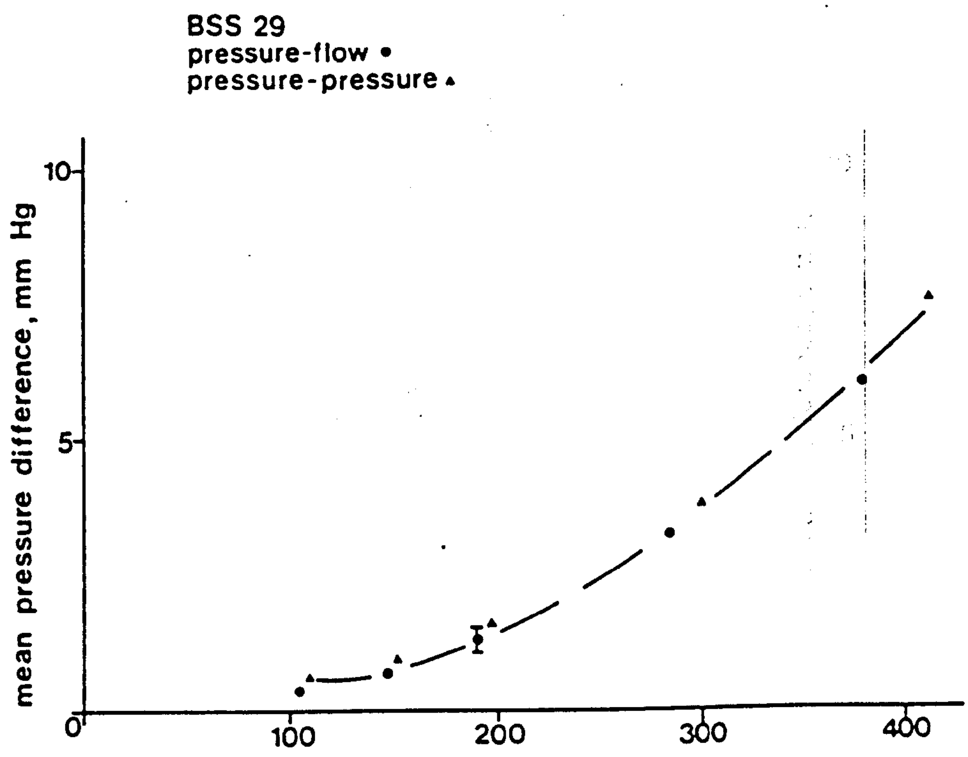

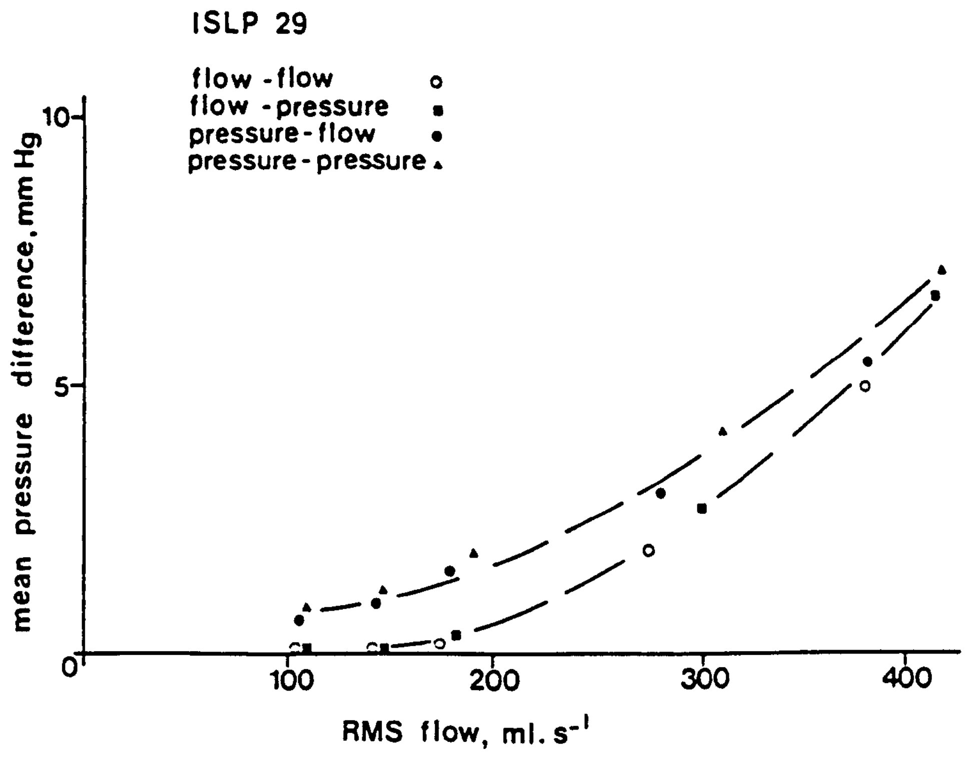

Figure A1.2 Mean pressure difference plotted against RMS forward flow for the size 29 mm Bjork-Shiley Tilting Disc valve BSS and the ISLP valves ● pressure flow, ▲ pressure-pressure, 0 flow-flow, ■ flow-pressure time intervals.

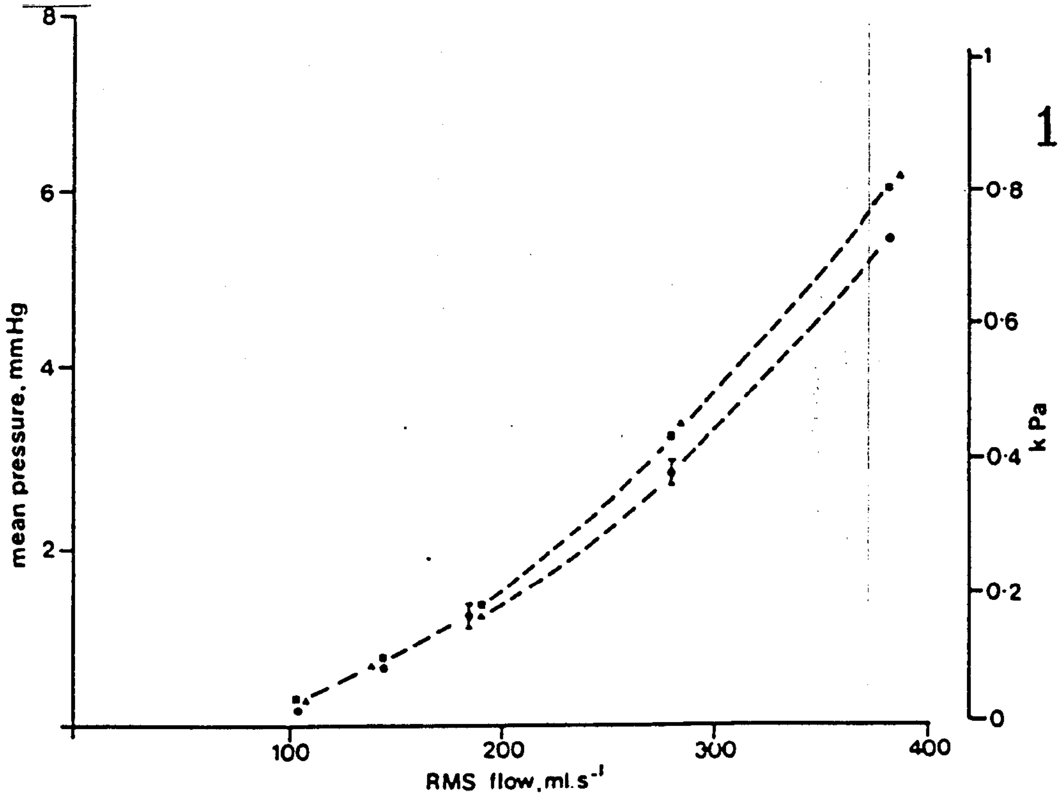

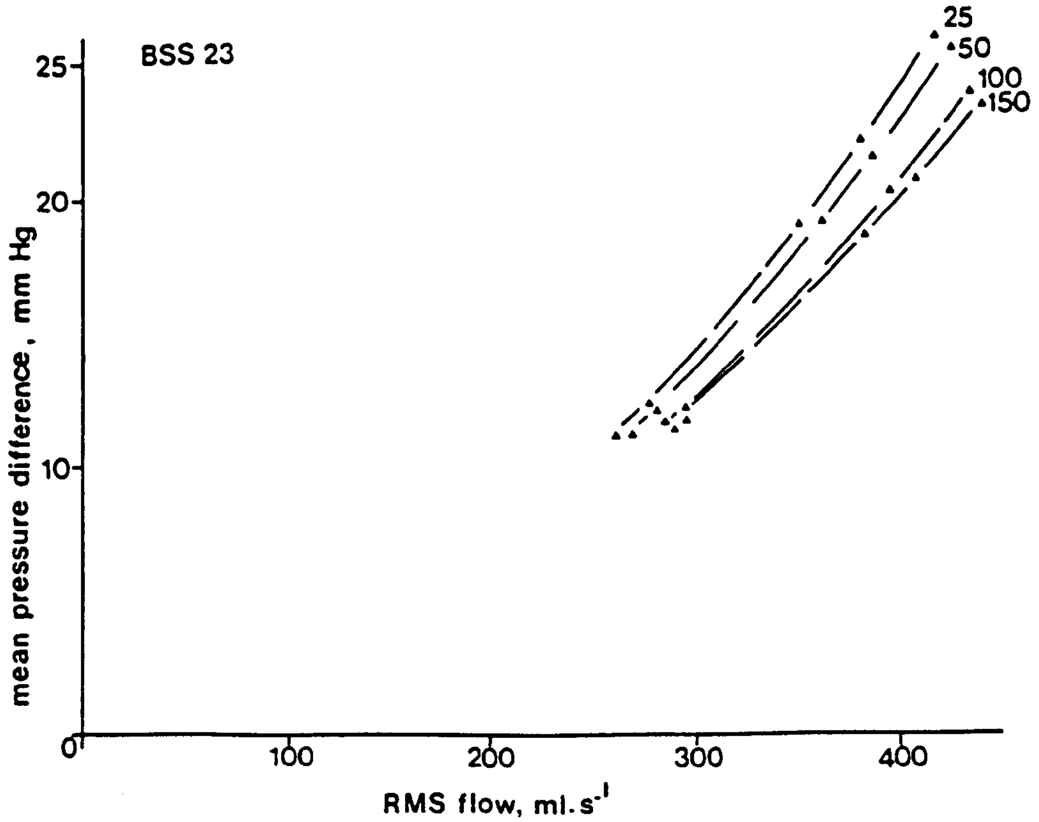

Figure A1.3 Mean pressure difference plotted against RMS forward flow for the BSS 29 mm mitral valves (above) and the BSS 23 mm aortic valve for varying downstream pressure measurement points. For the mitral valve 75 mm, 50 mm and 25 mm downstream of the valve.

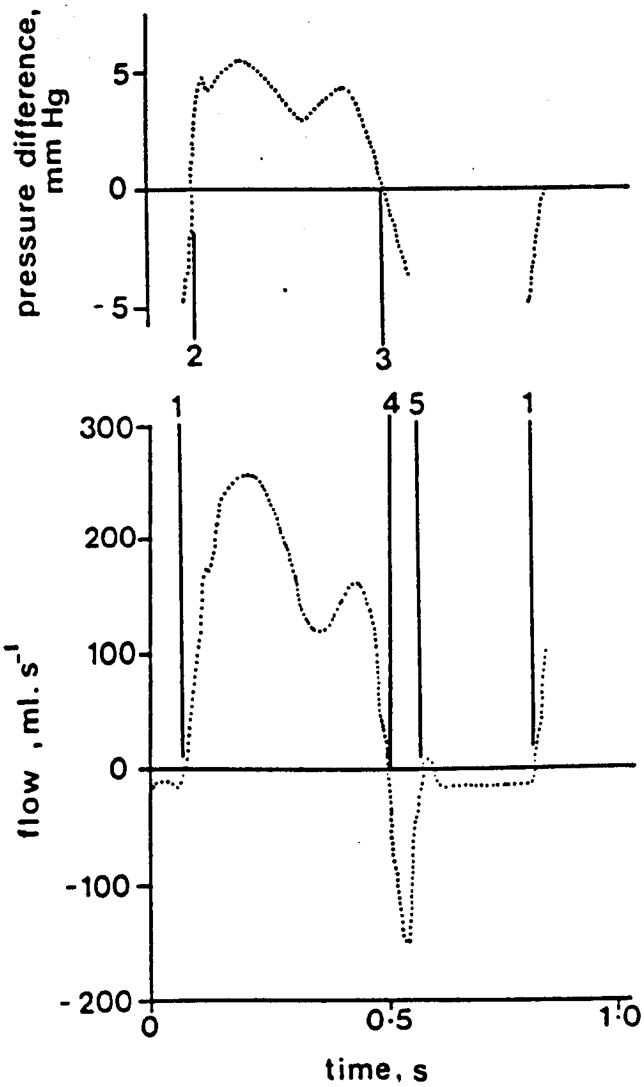

Figure A1.4 Flow and differential pressure waveforms showing the reference points and reverse flow time intervals.

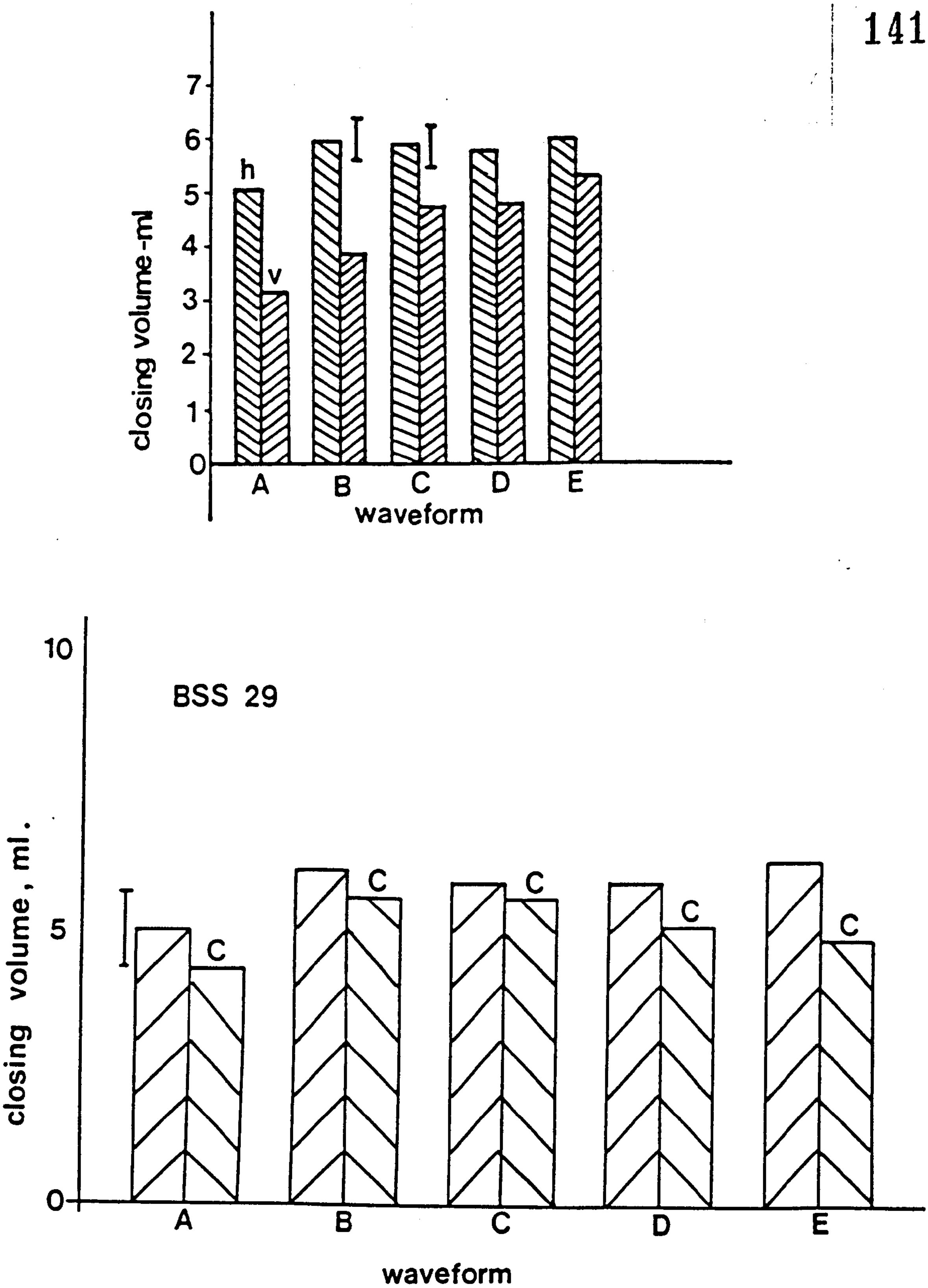

Figure A1.5 Dynamic regurgitation closing volume for the size 29 mm BSS valve positioned in the horizontal (h) and vertical plane (v) above and with compliance (c) in the pump chamber (below).

Error bars are ± 2SD.